



Multinuclear association of tetraethylisocyanideplatinum (II) tetracyanoplatinate (II) and the oxidized solutions of tetracyanoplatinate (II)  
by Phillip John Martellaro

A thesis submitted in partial fulfillment of the requirements for the degree of Doctor of Philosophy in Chemistry  
Montana State University  
© Copyright by Phillip John Martellaro (1998)

Abstract:

The colors exhibited in the solid phase of the tetracyanoplatinate salts do not always exist into the solution state. The color of the solid complex is attributed to the metal-metal interaction distance. The closer the metal-metal interaction is the lower in energy the corresponding absorption band will be.

Oxidation of the tetracyanoplatinates gives numerous species in solution. Oxidized solutions result in six species that have been characterized using  $^{195}\text{Pt}$  nmr. These are the (Formula not captured by OCR), (Formula not captured by OCR) and (Formula not captured by OCR). Initial reaction solutions are a faint yellow color but when they are allowed to stand idle for at least one week a purple colored solution exists. During this time all the  $^{195}\text{Pt}$  nmr resonances are still present but in different proportions. The purple solutions are attributed to paramagnetic multi-nuclear associated species.

The double complex salt tetraethylisocyanideplatinum(II) tetracyanoplatinate(II) gives brilliant red colored solutions when concentrations are at least  $1 \times 10^{-3}\text{M}$ . The color is the result of multi-nuclear association. The species in solution at (Formula not captured by OCR) are the di-nuclear (Formula not captured by OCR) two tri-nuclear species (Formula not captured by OCR) and the tetra-nuclear (Formula not captured by OCR). The thermodynamics of the solution reveals the greater enthalpy of formation for the dinuclear and tetranuclear species. The even numbered associated species have  $C_{4v}$  symmetry and thus have a dipole moment. The net dipole results in the greater ordering of solvent. The odd numbered associated platinum species are  $D_{4h}$  and have no net dipole moment. The greater ordering in the even numbered species results in the more exothermic values of enthalpy due to bond formation with the solvent. The greater ordering of solvent for the di-nuclear and tetra-nuclear species also explains the corresponding more negative values of entropy for the even numbered species compared with the more positive entropic values of the odd numbered species.

The complexes cis-bisethylisocyanidedicyanoplatinum(II), cis-bismethyldicyanoplatinum(II) and tetra-n-butylammoniummonomethylisocyanidetricyanoplatinum(II) were structured. All three complexes contained shorter platinum-carbon bond lengths for the isocyanide compared to the cyanide. This reveals the greater  $\pi$ -acidity of the isocyanide ligand.

MULTINUCLEAR ASSOCIATION OF TETRAETHYLISOCYANIDEPLATINUM(II)  
TETRACYANOPLATINATE(II) AND THE OXIDIZED SOLUTIONS OF  
TETRACYANOPLATINATE(II)

By

Phillip John Martellaro

A thesis submitted in partial fulfillment  
of the requirements for the degree

of

Doctor of Philosophy

in

Chemistry

MONTANA STATE UNIVERSITY-BOZEMAN  
Bozeman, Montana

December 1998

D378  
M 3614

APPROVAL

of a thesis submitted by

Phillip John Martellaro

This thesis has been read by each member of the thesis committee and has been found to be satisfactory regarding content, English usage, format, citations, bibliographic style, and consistency, and is ready for submission to the College of Graduate Studies.

Edwin H. Abbott Edwin H. Abbott 12/14/98  
(Signature) Date

Approved for the Department of Chemistry

David M. Dooley David M. Dooley 12/17/98  
(Signature) Date

Approved for the College of Graduate Studies

Joseph J. Fedock Joseph J. Fedock 12/31/98  
(Signature) Date

## STATEMENT OF PERMISSION TO USE

In presenting this thesis in partial fulfillment of the requirements for a doctoral degree at Montana State University-Bozeman, I agree that the Library shall make it available to borrowers under the rules of the Library. I further agree that copying of this thesis is allowable only for scholarly purposes, consistent with "fair use" as prescribed in the U.S. Copyright Law. Requests for extensive copying or reproduction of this thesis should be referred to University Microfilms International, 300 North Zeeb Road, Ann Arbor, Michigan 48106, to whom I have granted "the exclusive right to reproduce and distribute my dissertation in and from microform along with the non-exclusive right to reproduce and distribute my abstract in any format in whole or in part."

Signature: 

Date: 1-5-99

## TABLE OF CONTENTS

|  |     |
|--|-----|
| LIST OF TABLES.....  | vii |
| LIST OF FIGURES .....  | x   |
| ABSTRACT.....  | xiv |
| INTRODUCTION .....   | 1   |
| Complexes With Platinum-Platinum Interactions.....   | 1   |
| The Tetracyanoplatinate Salts (TCP's).....   | 7   |
| Tetracyanoplatinate(II) in the Solid State.....  | 7   |
| Tetracyanoplatinate(II) in the Solution State.....   | 9   |
| Double Salt Complexes (DS).....  | 10  |
| Partially Oxidized Tetracyanoplatinate (POTCP).....  | 12  |
| Solid State Properties of the Partially Oxidized Tetracyanoplatinate(II)<br>Complexes.....   | 12  |
| Two Different Types of PO Compounds .....  | 14  |
| Solution Studies on the Partially Oxidized Compounds.....  | 17  |
| Partially Oxidized Bisoxalatoplatinate Solution Chemistry .....  | 18  |
| Anion-Deficient Partially Oxidized Tetracyanoplatinate(II) Solution<br>Chemistry.....  | 19  |
| Cation-Deficient Partially Oxidized Tetracyanoplatinate(II) Solution<br>Chemistry.....   | 20  |
| Platinum(II) Isocyanide Complexes .....  | 22  |
| Chemistry Effects on Platinum Atom From the Isocyanide Ligand .....  | 22  |
| Vapochromic Double Salts .....   | 26  |
| Solid State Properties of the Vapochromic Double Salts .....   | 26  |
| Solution State Properties of the Double Complex Salts .....  | 28  |
| Mixed Cyanide/Isocyanide Platinum(II) Complexes.....   | 29  |
| Bonding Descriptions for the Platinum-Platinum Complexes.....  | 30  |
| <sup>195</sup> Pt Nuclear Magnetic Resonance .....   | 36  |
| EXPERIMENTAL METHODS .....   | 39  |
| Preparation of Compounds.....  | 39  |
| Starting Materials.....  | 39  |
| Preparation of MPt(CN) <sub>4</sub> M=K <sub>2</sub> ,Ba,Na <sub>2</sub> ,Cs <sub>2</sub> and [t-n-butylN] <sub>2</sub> ( <b>8A-8D</b> ).... | 39  |
| Preparation of K <sub>2</sub> Pt(ox) <sub>2</sub> ( <b>16</b> ).....   | 41  |
| Preparation of K <sub>2</sub> Pt(ox)(CN) <sub>2</sub> ( <b>17</b> ).....   | 41  |

|  |    |
|--|----|
| Preparation of $K_2Pt(CN)_4(OH)_2$ ( <b>11A</b> ) .....  | 42 |
| Preparation of $BaPt(CN)_4(OH)_2 \cdot 7H_2O$ ( <b>11B</b> ) .....   | 43 |
| Partial Oxidation of $K_2Pt(CN)_4 \cdot 3H_2O$ .....   | 43 |
| Partial Oxidation of $Cs_2Pt(CN)_4 \cdot H_2O$ with $H_2O_2$ .....   | 44 |
| Partial Oxidation of $Cs_2Pt(CN)_4$ with $HNO_3$ .....   | 44 |
| Oxidation of ( <b>8A</b> ) with Oxone .....  | 45 |
| Oxidation of ( <b>8A</b> ) with $HNO_3$ .....  | 45 |
| Oxidation of ( <b>8A</b> ) with $Ce^{4+}$ .....  | 45 |
| Oxidation of ( <b>8B</b> ) with $H_2O_2$ .....   | 45 |
| Preparation of $[Pt(CNR)_4][BF_4]$ (R = $CH_3$ ( <b>19A</b> ) and $CH_2CH_3$ ( <b>20A</b> )) .....                     | 46 |
| Preparation of $Pt(CNCH_2CH_3)_2(CN)_2$ ( <b>21</b> ) .....  | 46 |
| Preparation of $Pt(CNCH_3)_2(CN)_2$ ( <b>22</b> ) .....  | 47 |
| Preparation of [tetra-n-butylN][ $Pt(CNCH_3)(CN)_3$ ] ( <b>23</b> ) .....  | 47 |
| Preparation of the Double Salts $[Pt(CNR)_4][Pt(CN)_4]$ (R= $CH_3$ ( <b>24</b> ))<br>R= $CH_2CH_3$ ( <b>5</b> )) ..... | 48 |
| Preparation of the Platinum(I) $[Pt(CNC_2H_5)_3]_2[BF_4]_2$ ( <b>13</b> ) .....  | 48 |
| Preparation of the Continuous Variations Method (CV) Solutions .....   | 48 |
| Instrumentation and Techniques .....   | 49 |
| Nuclear Magnetic Resonance (NMR) .....   | 49 |
| Ultraviolet and Visible Spectroscopy .....   | 50 |
| X-ray Crystallography .....  | 50 |
| pH Measurements .....  | 50 |
| Equilibrium Calculations .....   | 50 |
| Labeling of Multinuclear Species .....   | 51 |
| Numbering of Compounds .....   | 51 |
| RESULTS AND DISCUSSION .....   | 52 |
| Solution Studies of the Pt(II) Cyanoplatinates .....   | 52 |
| Unoxidized Pt(II) Cyanoplatinates .....  | 52 |
| Solution Chemistry of ( <b>8</b> ) .....   | 52 |
| Formation of the Mixed Complex ( <b>17A</b> ) .....  | 55 |
| Solution Studies of the Oxidized Pt(II) Cyanoplatinates .....  | 58 |
| Oxidation Reactions using Hydrogen Peroxide .....  | 58 |
| Oxidation of ( <b>17A</b> ) with $H_2O_2$ .....  | 58 |
| Oxidation of ( <b>8A</b> ) with $H_2O_2$ .....   | 59 |
| Oxidation of ( <b>8B</b> ) with $H_2O_2$ .....   | 66 |
| Oxidation of ( <b>8D</b> ) with $H_2O_2$ .....   | 67 |
| Oxidation using the Monopersulfate Compound Oxone .....  | 69 |
| Oxidation of ( <b>8A</b> ) with Oxone .....  | 69 |
| Characterization of the Dinuclear Species at -1776ppm .....  | 82 |
| Solution Studies of the Partially Oxidized Tetracyanoplatinates .....  | 85 |

|  |     |
|--|-----|
| Oxidation Reactions Using HNO <sub>3</sub> .....                                     | 85  |
| Oxidation of <b>(8A)</b> with HNO <sub>3</sub> .....                                 | 85  |
| Oxidation of <b>(8B)</b> with HNO <sub>3</sub> .....                                 | 88  |
| Oxidation of <b>(8D)</b> with HNO <sub>3</sub> .....                                 | 89  |
| Oxidation of <b>(8A)</b> with Ce <sup>4+</sup> .....                                 | 91  |
| Oxidation of <b>(8A)</b> with <b>(11A)</b> .....                                     | 92  |
| Species Responsible for POTCP Formation .....  | 97  |
| Comparisons of the dianions <b>(8)</b> and Pt(ox) <sup>2-</sup> <b>(16)</b> .....    | 98  |
| Investigation of the Pt(IV) <b>(11)</b> .....  | 100 |
| Titration of <b>(11)</b> .....   | 100 |
| Formation of <b>(11)</b> .....   | 103 |
| Crystal Structure of <b>(11B)</b> .....  | 105 |
| Solution Studies of the Double Complex Salt <b>(5)</b> .....                         | 112 |
| Visible Absorption Evidence of Multi-Nuclear complexes in Solution .....             | 112 |
| Modeling the Solution Equilibrium Using Continuous Variations                        |     |
| Method .....   | 119 |
| Determination of the Stoichiometry of the Solution Species .....                     | 119 |
| Trimer Formation .....   | 125 |
| Equilibrium Model Selection .....  | 133 |
| Double Salt Solution Preparations .....  | 135 |
| Solving of the Equilibrium Constants .....   | 136 |
| Determination of K <sub>1</sub> .....  | 140 |
| Determination of K <sub>2</sub> , K <sub>3</sub> and K <sub>4</sub> .....            | 141 |
| Accuracy of the Equilibrium Constants .....  | 149 |
| Thermodynamic Studies of the Multi-nuclear Species .....                             | 151 |
| Bonding Interpretation of the Thermodynamic Studies .....                            | 155 |
| Accuracy of the Thermodynamic Values .....   | 157 |
| <sup>195</sup> Pt NMR of the Double Salt Solutions .....                             | 158 |
| Studies on the mixed cyano/isocyanoplatinum Complexes .....                          | 161 |
| Crystal Structures of the mixed cyanide and isocyanide complexes .....               | 162 |
| Crystal Structure of <b>(21)</b> .....   | 162 |
| Crystal Structure of <b>(22)</b> .....   | 170 |
| Crystal Structure of <b>(23)</b> .....   | 170 |
| <sup>195</sup> Pt NMR of the Reaction Solutions leading to the Mixed Complexes ..... | 186 |
| Platinum-Platinum Bond Distance in the Pt(I) <b>(13)</b> .....                       | 187 |
| <sup>195</sup> Pt NMR chemical shifts .....  | 189 |
| Trends for the Determination of <sup>195</sup> Pt NMR Chemical Shifts .....          | 189 |
| Predicting Platinum Chemical Shifts .....  | 193 |
| Hard Acid/Soft Base Effects on the Platinum Chemical Shift .....                     | 193 |
| Applying Comparative Methods for Predicting Platinum Chemical                        |     |
| Shifts .....   | 195 |
| Oxidation State Effect on the Platinum Chemical Shift .....                          | 197 |

|  |     |
|--|-----|
| <sup>195</sup> Pt nmr and <sup>1</sup> H nmr Studies of the Mixed Cyanide and Isocyanide<br>Complexes.....                       | 200 |
| Trends in the Chemical Shift with Alkylation of the Cyanide .....  | 200 |
| Coupling in the Mixed Complexes .....  | 201 |
| Crystal Structure of the Pt(IV) Complex Pt(CN) <sub>4</sub> {S(CH <sub>3</sub> ) <sub>2</sub> } <sub>2</sub> ( <b>33</b> ) ..... | 207 |
| SUMMARY AND CONCLUSIONS.....   | 214 |
| REFERENCES .....   | 222 |

## LIST OF TABLES

| Table   | Page |
|---|------|
| Table 1. Pt-Pt Distances and Colors of the Tetracyanoplatinate salts .....  | 8    |
| Table 2. Bond Distance of POTCP. ....   | 13   |
| Table 3. Absorption Shifts for a Vapochromic Solid State Film.....  | 27   |
| Table 4. $^{195}\text{Pt}$ and $^{13}\text{C}$ nmr Chemical Shifts of the Oxidized Products .....   | 81   |
| Table 5. Crystallographic Data for Bariumdiaquotetracyanoplatinate(IV) <b>11B</b> .   | 107  |
| Table 6. Data collection and Structure Refinement Data for <b>11B</b> .....   | 108  |
| Table 7. Atomic Coordinates and equivalent isotropic displacement coefficients for <b>11B</b> .....   | 109  |
| Table 8. Bond lengths (Å) for <b>11B</b> .....  | 110  |
| Table 9. Bond angles ( $^{\circ}$ ) for <b>11B</b> .....  | 110  |
| Table 10. Anisotropic displacement coefficients for <b>11B</b> .....  | 111  |
| Table 11. Overall Formation Constants in the Multi-Nuclear Association of the Double Complex Salt <b>(5)</b> .....  | 146  |
| Table 12. Molar absorptivities of <b>(5)</b> , <b>(25)</b> , <b>(27)</b> and <b>(30)</b> .....  | 146  |
| Table 13. Molar absorptivities of <b>(8)</b> , <b>(20)</b> , .....  | 148  |
| Table 14. Stepwise Equilibrium Constants for <b>(5)</b> , <b>(25)</b> , <b>(27)</b> and <b>(30)</b> at $7^{\circ}\text{C}$ , $12^{\circ}\text{C}$ , $17^{\circ}\text{C}$ and $22^{\circ}\text{C}$ ..... | 149  |
| Table 15. Thermodynamic Parameters for the Stepwise Formation Constants of <b>(5)</b> , <b>(25)</b> , <b>(27)</b> and <b>(30)</b> .....   | 154  |
| Table 16. Crystallographic Data for dicyanobisethylisocyanideplatinum(II) <b>21</b> .   | 165  |
| Table 17. Data collection and Structure Refinement Data for <b>21</b> .....   | 166  |

|  |     |
|--|-----|
| Table 18. Atomic Coordinates and equivalent isotropic displacement coefficients for <b>21</b> .....        | 167 |
| Table 19. Bond lengths (Å) for <b>21</b> .....   | 168 |
| Table 20. Bond angles (°) for <b>21</b> .....  | 168 |
| Table 21. Anisotropic displacement coefficients (Å <sup>2</sup> ) for <b>21</b> .....                      | 169 |
| Table 22. Crystallographic Data for dicyanobismethylisocyanideplatinum(II) <b>22</b> .....                 | 173 |
| Table 23. Data collection and structure refinement data for <b>22</b> .....                                | 174 |
| Table 24. Atomic Coordinates and equivalent isotropic displacement coefficients for <b>22</b> .....        | 175 |
| Table 25. Bond lengths (Å) for <b>22</b> .....   | 176 |
| Table 26. Bond angles (°) for <b>22</b> .....  | 176 |
| Table 27. Anisotropic displacement coefficients (Å <sup>2</sup> ) for <b>22</b> .....                      | 177 |
| Table 28. Crystallographic data for tricyanomonomethylisocyanideplatinum(II) <b>23</b> .....               | 180 |
| Table 29. Data collection and structure refinement data for <b>23</b> .....                                | 181 |
| Table 30. Atomic Coordinates and equivalent isotropic displacement coefficients for <b>23</b> .....        | 182 |
| Table 31. Bond lengths (Å) for <b>23</b> .....   | 183 |
| Table 32. Bond angles (°) for <b>23</b> .....  | 184 |
| Table 33. Anisotropic displacement coefficients (Å <sup>2</sup> ) for <b>22</b> .....                      | 185 |
| Table 34. <sup>195</sup> Pt NMR resonance shifts of ( <b>8</b> ) with different solvents.....              | 190 |
| Table 35. Chemical shift dependence of different ligands through the periodic table with platinum(II)..... | 194 |

|  |     |
|--|-----|
| Table 36. Chemical shift dependence of substituted thiocyanides.....   | 194 |
| Table 37. Change in chemical shift for Pt(II) and Pt(IV) Complexes with<br>some common ligands.....            | 198 |
| Table 38. $^{195}\text{Pt}$ NMR chemical shifts of <b>(19)</b> and <b>(20)</b> in $\text{CD}_3\text{CN}$ ..... | 200 |
| Table 39. Couplings observed for the platinum methylisocyanide complexes .                                     | 206 |
| Table 40. Couplings observed for the platinum ethylisocyanide complexes. ....                                  | 206 |
| Table 41. $^1\text{H}$ NMR data for the methylisocyanides.....   | 206 |
| Table 42. $^1\text{H}$ NMR data for the ethylisocyanides.....  | 206 |
| Table 43. Crystallographic data for<br>tetracyanobis(di-methylsulfide)platinum(IV) <b>33</b> .....             | 209 |
| Table 44. Data collection and structure refinement data for <b>23</b> .....                                    | 210 |
| Table 45. Atomic Coordinates and equivalent isotropic displacement<br>coefficients for <b>33</b> .....         | 211 |
| Table 46. Bond lengths ( $\text{\AA}$ ) for <b>33</b> .....  | 212 |
| Table 47. Bond angles ( $^\circ$ ) for <b>33</b> .....   | 212 |
| Table 48. Anisotropic displacement coefficients ( $\text{\AA}^2$ ) for <b>33</b> .....                         | 213 |

## LIST OF FIGURES

| Figure   | Page |
|--|------|
| Figure 1. Depiction of the $\alpha$ -pyridone blue.....  | 2    |
| Figure 2. Depiction of the platinum atom arrangement in the tetracyanoplatinate(II), Partially Oxidized tetracyanplatinate and the Double Complex platinum salts. ....   | 3    |
| Figure 3. a) Structures of the Pt(II) carboxylato dimer b) Structure of the Pt(II) methyl complex.....   | 5    |
| Figure 4. Structure of the Pt(III) complex $[Pt_2(\mu-SO_4)_4(H_2O)_2]$ .....  | 6    |
| Figure 5. a) Depiction of the Magnus green salt and b) the ethylisocyanideplatinum(II) cyano double salt. ....   | 11   |
| Figure 6. Structure of the Pt(I) $[Pt(CNC_2H_5)_3]_2[BF_4]_2$ .....  | 24   |
| Figure 7. Arylisocyanidplatinum(II)tetracyanoplatinate(II) vapo-chromic salt.....  | 27   |
| Figure 8. Simplified MO sketch of two interacting square planar platinum complexes. ....   | 31   |
| Figure 9. a) Two platinum atoms interacting giving no net bonding interaction b) two platinum atoms interacting with a "configuration interaction" resulting in a net bonding interaction for two $d^8$ square planar platinum atoms. .... | 32   |
| Figure 10. Band model for the POTCP chain compounds. ....  | 34   |
| Figure 11. Band model of a chain of platinum(II) compounds.....  | 35   |
| Figure 12. Concentration study of (8) using $^{195}Pt$ nmr to determine if association of the dianion occurs in solution.....  | 54   |
| Figure 13. a) $^{195}Pt$ NMR of (17) with labeled $^{13}CN$ b) $^{13}C$ NMR of reaction 6. ...   | 57   |

|   |     |
|---|-----|
| Figure 14. $^{195}\text{Pt}$ NMR for reaction 3 at solution concentrations near the solubility limit of crystallization of <b>(6)</b> .....   | 60  |
| Figure 15. $^{195}\text{Pt}$ NMR for reaction 3 near the solubility limit of crystallization of <b>(6)</b> using labeled $^{13}\text{CN}$ .....   | 61  |
| Figure 16. Structural representations of <b>(8)</b> , <b>(11)</b> , <b>(25)</b> and <b>(27)</b> . ....  | 65  |
| Figure 17. $^{13}\text{C}$ NMR of the oxone oxidaitons using labeled $^{13}\text{CN}$ .....   | 73  |
| Figure 18. Time study of the oxone oxidaiton of <b>(8)</b> . Over a seven day period the emergence of <b>(25)</b> can be seen with a decrease in the S/N of <b>(8)</b> and <b>(11)</b> . ....   | 77  |
| Figure 19. Structural representation of the multinuclear complex <b>(32)</b> .....  | 79  |
| Figure 20. $^{12}\text{C}$ NMR of the oxone oxidaiton of <b>(8)</b> with the natural abundance of $^{13}\text{CN}$ .....  | 80  |
| Figure 21. a) $^{195}\text{Pt}$ NMR of <b>(8)</b> and <b>(11)</b> combined in water b) $^{195}\text{Pt}$ NMR of reaction 8 after it was dried and brought back up in $\text{D}_2\text{O}$ ..... | 95  |
| Figure 22. $^{195}\text{Pt}$ NMR of reaction 9.....   | 96  |
| Figure 23. $^{195}\text{Pt}$ NMR monitored base titration of <b>(11)</b> .....  | 102 |
| Figure 24. Thermal ellipsoid plot of <b>(11B)</b> .....   | 106 |
| Figure 25. UV-Visible absorption spectra of separate equally concentrated solutions of <b>(8)</b> and <b>(20)</b> and the spectrum of the two solutions mixed together.....                     | 114 |
| Figure 26. UV-Visible absorption spectrum of a $1.0 \times 10^{-2}\text{M}$ solution of the DS <b>(5)</b> .....   | 115 |
| Figure 27. The DS <b>(5)</b> diluted over a ten fold concentration range of $1.0 \times 10^{-3}\text{M}$ to $1.0 \times 10^{-4}\text{M}$ .....  | 116 |
| Figure 28. Continuous Variations (CV) plot of the 319nm band at $1.0 \times 10^{-3}\text{M}$ in total platinum concentration of <b>(8)</b> and <b>(20)</b> . ....                               | 120 |
| Figure 29. CV experiment of the 363nm band at $1.0 \times 10^{-4}\text{M}$ in total platinum concentration of <b>(8)</b> and <b>(20)</b> .....  | 121 |

|   |     |
|---|-----|
| Figure 30. CV experiments for the determination of stoichiometry for <b>(5)</b> , <b>(28)</b> and <b>(29)</b> at $1.0 \times 10^{-5}M$ , $1.0 \times 10^{-4}M$ and $1.0 \times 10^{-3}M$ respectively ..... | 122 |
| Figure 31. Structural representations of the three multinuclear species that result in absorption maxima at 319nm, 363nm and 420nm. ....  | 123 |
| Figure 32. Visible region of the spectrum for solution ratios of <b>(20)</b> : <b>(8)</b> revealing the 363nm absorption maxima for <b>(28)</b> and the false maxima for <b>(30)</b> at 385nm.....          | 126 |
| Figure 33. A 1:9 solution ratio of <b>(20)</b> to <b>(8)</b> at four different temperatures. The multi-temperature experiment reveals the absorption maxima at 350nm for <b>(30)</b> .....                  | 127 |
| Figure 34. Structural representation for the tri-nuclear species <b>(30)</b> .....  | 130 |
| Figure 35. Comparison of UV bands for <b>(8)</b> and <b>(20)</b> and their 1:7 and 7:1 mixtures .....   | 132 |
| Figure 36. Overlay of two $1.0 \times 10^{-3}M$ solutions in pure water and the other in .1M $Al_2SO_4$ .....   | 137 |
| Figure 37. Overlay of the entire UV-Visible spectrum of the two parent ions of <b>(8)</b> and <b>(20)</b> and the spectrum of the two ions mixed together .....   | 139 |
| Figure 38. Pictorial representation of the equilibrium of <b>(5)</b> .....  | 143 |
| Figure 39. Temperature effect on the equilibrium of the DS in water.....  | 153 |
| Figure 40. $^{195}Pt$ NMR of <b>(5)</b> in water. ....  | 160 |
| Figure 41. Thermal ellipsoid plot of <b>(21)</b> .....  | 164 |
| Figure 42. Thermal ellipsoid plot of <b>(22)</b> .....  | 172 |
| Figure 43. Thermal ellipsoid plot of <b>(23)</b> .....  | 178 |
| Figure 44. Thermal ellipsoid plot of <b>(23)</b> and its counteranion.....  | 179 |
| Figure 45. $^{195}Pt$ NMR of the cis and trans forms of <b>(23)</b> .....   | 188 |

|  |     |
|--|-----|
| Figure 46. $^{15}\text{N}$ NMR Chemical shift comparison.....  | 192 |
| Figure 47. a) $^{195}\text{Pt}$ NMR of <b>(20)</b> in $\text{CD}_3\text{CN}$ b) of <b>(21)</b> c) <b>(23)</b> . .... | 203 |
| Figure 48. $^1\text{H}$ NMR spectrum of the tetramethylisocyanide <b>(19)</b> .....                                  | 204 |
| Figure 49. $^1\text{H}$ NMR of the bisethylisocyanide <b>(21)</b> b) the bismethylisocyanide <b>(22)</b> .....       | 205 |
| Figure 50. Thermal ellipsoid plot of <b>(33)</b> .....   | 208 |

## ABSTRACT

The colors exhibited in the solid phase of the tetracyanoplatinate salts do not always exist into the solution state. The color of the solid complex is attributed to the metal-metal interaction distance. The closer the metal-metal interaction is the lower in energy the corresponding absorption band will be.

Oxidation of the tetracyanoplatinates gives numerous species in solution. Oxidized solutions result in six species that have been characterized using  $^{195}\text{Pt}$  nmr. These are the  $\text{Pt}_3(\text{CN})_8^{2-}$ ,  $\text{Pt}_2(\text{CN})_6$ ,  $\text{Pt}_2(\text{CN})_8^{2-}$ ,  $\text{Pt}_2(\text{CN})_8(\text{H}_2\text{O})_2^{2-}$ ,  $\text{Pt}(\text{CN})_4(\text{H}_2\text{O})_2^{2-}$  and  $\text{Pt}(\text{CN})_2(\text{H}_2\text{O})_4^{2-}$ . Initial reaction solutions are a faint yellow color but when they are allowed to stand idle for at least one week a purple colored solution exists. During this time all the  $^{195}\text{Pt}$  nmr resonances are still present but in different proportions. The purple solutions are attributed to paramagnetic multi-nuclear associated species.

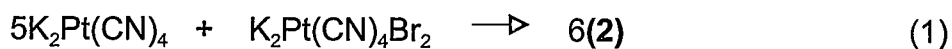
The double complex salt tetraethylisocyanideplatinum(II) tetracyanoplatinate(II) gives brilliant red colored solutions when concentrations are at least  $1 \times 10^{-3}\text{M}$ . The color is the result of multi-nuclear association. The species in solution at  $1 \times 10^{-3}\text{M}$  are the di-nuclear  $\text{Pt}(\text{CNC}_2\text{H}_5)_4[\text{Pt}(\text{CN})_4]$ , two tri-nuclear species  $[\text{Pt}(\text{CNC}_2\text{H}_5)_4]_2[\text{Pt}(\text{CN})_4]^{2+}$ ,  $[\text{Pt}(\text{CNC}_2\text{H}_5)_4][\text{Pt}(\text{CN})_4]_2^{2-}$  and the tetra-nuclear  $[\text{Pt}(\text{CNC}_2\text{H}_5)_4]_2[\text{Pt}(\text{CN})_4]_2$ . The thermodynamics of the solution reveals the greater enthalpy of formation for the dinuclear and tetranuclear species. The even numbered associated species have  $C_{4v}$  symmetry and thus have a dipole moment. The net dipole results in the greater ordering of solvent. The odd numbered associated platinum species are  $D_{4h}$  and have no net dipole moment. The greater ordering in the even numbered species results in the more exothermic values of enthalpy due to bond formation with the solvent. The greater ordering of solvent for the di-nuclear and tetra-nuclear species also explains the corresponding more negative values of entropy for the even numbered species compared with the more positive entropic values of the odd numbered species.

The complexes cis-bisethylisocyanidedicyanoplatinum(II), cis-bismethyldicyanoplatinum(II) and tetra-n-butylammoniummonomethylisocyanidetricyanoplatinum(II) were structured. All three complexes contained shorter platinum-carbon bond lengths for the isocyanide compared to the cyanide. This reveals the greater  $\pi$ -acidity of the isocyanide ligand.

## INTRODUCTION

Complexes with Pt-Pt Interactions

The interest and appreciation of the chemistry of metal-metal bonding originated during the middle part of this century (1 and references therein). Platinum, like other metals, exhibits two different classes of metal-metal bonding. The first class consists of molecules that contain metal atoms that are bonded directly with one another. These complexes contain no ligands that bridge between the two metal atoms. For platinum complexes this is seen in the partially oxidized tetracyanoplatinates (POTCP) as well as the platinum blues. A representation of the structural characteristics of the platinum blue complex  $\alpha$ -pyridone blue which is a dimer of the binuclear  $[(\text{NH}_3)_2\text{Pt}(\text{pyr})_2\text{Pt}(\text{HN}_3)_2]$  (**1**) and the POTCP  $\text{K}_2\text{Pt}(\text{CN})_4\text{X}_{.3}\cdot 3\text{H}_2\text{O}$  where X is Br (**2**) or Cl (**3**) is seen in figure 1 and 2 respectively. The POTCP is an infinite platinum-platinum bonded species whereas the platinum blues are tetraplatinum and considered finite platinum-platinum bonds. The platinum blues have been extensively studied because of their anti-tumor activity (2,3,4). Both (**1**) and (**2**) have drawn significant interest for different reasons and are formed according to equation 1.



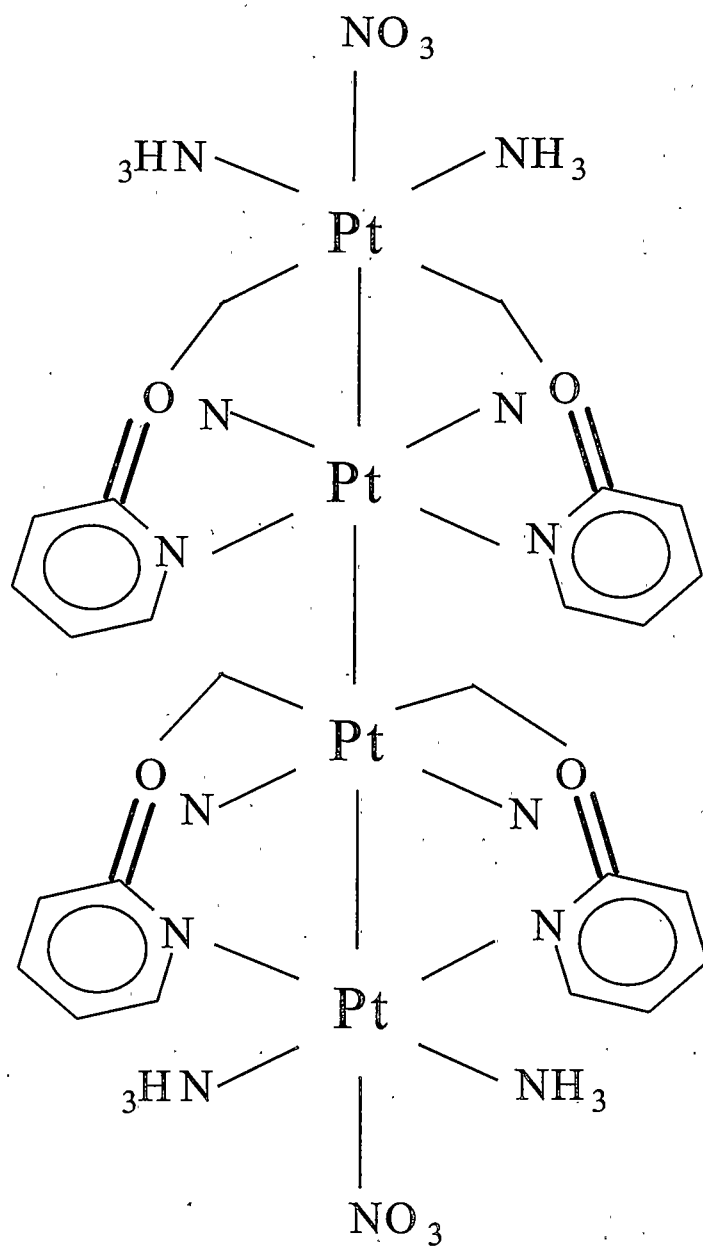
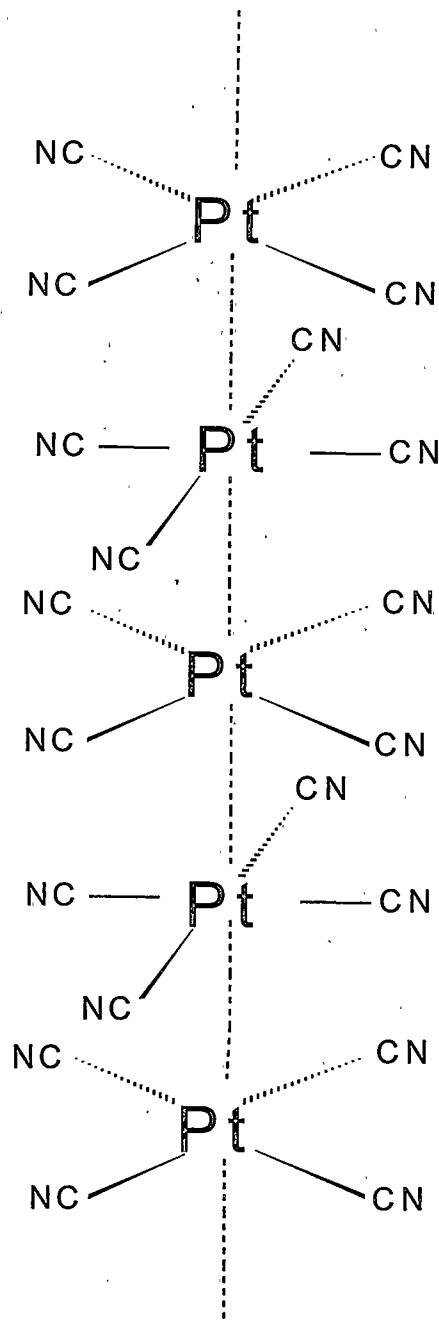


Figure 1. Depiction of the tetrameric  $\alpha$ -pyridone blue.



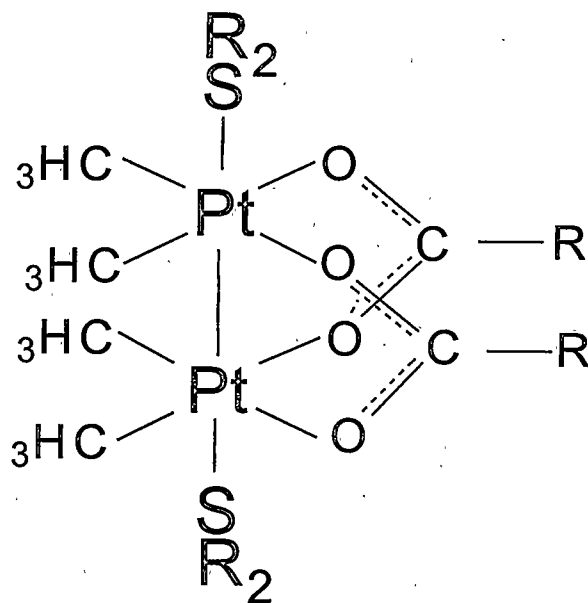
**Figure 2.** Depiction of the stacked platinum atoms in the TCP's, POTCP and DS.

The POTCP complexes have been studied for the most part because of their 1-D anisotropic physical properties. Principal among these 1-D properties is the ability for the anisotropic conduction of electricity through the Pt-Pt bonds. The  $\alpha$ -pyridone blue is also a partially oxidized (PO) compound like the POTCP. The partial oxidation (PO) is reflected in the oxidation state of these complexes being a non-integral number. The platinum atom in **(1)** is in an average oxidation state of +2.25. In the case of the **(2)** the average oxidation state of the platinum atom is +2.3. The Pt-Pt bond lengths of **(1)** are 2.774 and 2.877Å. In **(2)** the Pt-Pt bond lengths are on the order of 2.88 Å.

The second type of metal-metal bonded atoms are those of the bridged complexes. In this case the two metal atoms are spanned by an appropriate ligand. Figure 3 shows two examples of platinum bridged dimers. Figure 3a was one of the first Pt(III) complexes synthesized. Until recently when monomeric Pt(III) species were found the only known Pt(III) complexes were of the bridged type. The other example shown in figure 3B is the Pt(II) complex  $[\text{Pt}(\text{CH}_3)_2(\text{SR}_2)]_2$  (5). The bridged Pt(III) dimers have very short Pt-Pt bond lengths. The  $\text{H}_2[\text{Pt}_2(\mu\text{-SO}_4)_4(\text{H}_2\text{O})_2]$  shown in figure 4 has a Pt-Pt bond length of 2.466Å (6,7). In the case of the bridged Pt(II)  $[\text{Pt}(\text{CH}_3)_2(\text{SR}_2)]_2$  the metal-metal distance is not close enough to be called a bond.

Non-bridged dimeric Pt(III) complexes have recently been observed. They have Pt-Pt bond lengths on the order of 2.7-2.8Å. It is likely from Pt-Pt bond lengths in the Pt(III) dimers that bridging contributes to the stability of the

a)



b)

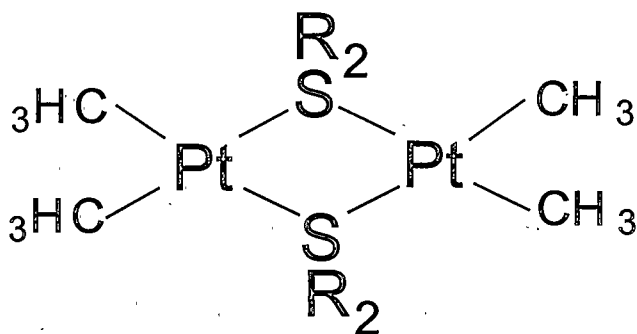


**Figure 3.** a) Structure of the Pt(III)-carboxylato dimer b) Structure of the Pt(II) methyl complex

complex. These types of complexes are significant for the work described here because of the evidence that they are present in the solutions.

Also of interest to the work described here are platinum complexes that are stacked like the example in figure 2 but the platinum distances are not close enough to be considered a metal-metal bond. In these cases the platinum atoms are close enough to interact but the distances are too long for there to be any significant orbital overlap that would result in a strong covalent bond. It is generally accepted that when platinum-platinum atoms are separated by 3Å or less there is a true chemical bond between the two metal atoms.

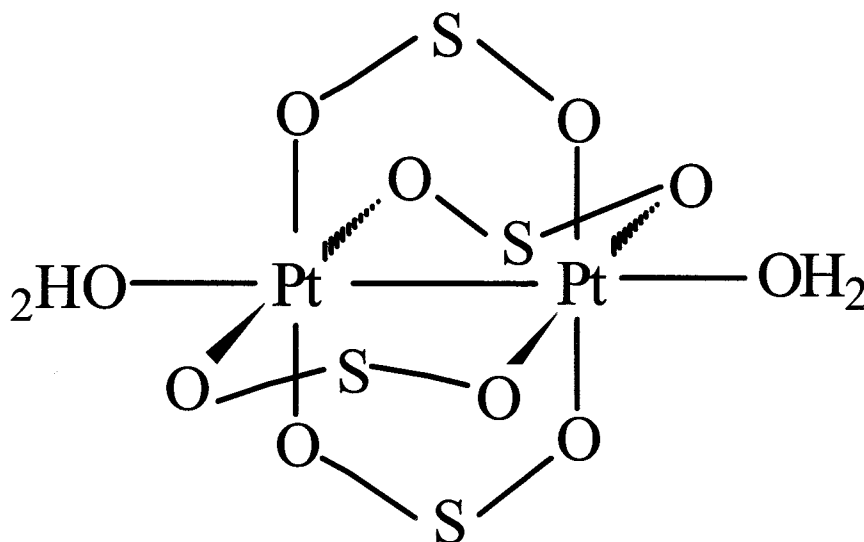


**Figure 4** Depiction of the Pt(III) Complex  $[Pt_2(\mu-SO_4)_4(H_2O)_2]$

## The Tetracyanoplatinate(II) salts (TCP's)

### Tetracyanoplatinate(II) (TCP) in the Solid State

The solid state characteristics of both the  $MPt(CN)_4$  (where  $M=K_2, Na_2, Rb_2, Cs_2, [(CH_3)_3N]_2, Mg, Ca$ ) as well as the POTCP's have been extensively studied (8-12). The TCP's were discovered nearly 150 years ago and were of interest to the early scientists because of the wide range of colors observed for the various salts of the TCP's. In the solid phase the TCP's stack with the platinum atoms on top of each other much like that of a roll of coins (Figure 2). Figure 2 can be used as the structure representation to describe both the TCP and the POTCP because the Pt-Pt stacking is identical in the two different complexes. For our purposes the only difference of significance is the Pt-Pt separations. The colors observed for the TCP's depends upon the counteraction and the content of water hydration (13). A few examples are shown in table 1.

Table 1. Pt-Pt distances and colors of TCP complexes with different cations and contents of water hydration and a few Double Complex Salts

| Complex  | Pt-Pt distance(Å) | Color         |
|--|-------------------|---------------|
| $\text{SrPt}(\text{CN})_4 \cdot 5 \text{H}_2\text{O}$                | 3.6               | Colorless     |
| $\text{SrPt}(\text{CN})_4 \cdot 3 \text{H}_2\text{O}$                | 3.09              | Violet        |
| $\text{MgPt}(\text{CN})_4 \cdot 7 \text{H}_2\text{O}$                | 3.16              | Dark Red      |
| $\text{MgPt}(\text{CN})_4 \cdot 4.5 \text{H}_2\text{O}$              | 3.36              | Yellow        |
| $\text{BaPt}(\text{CN})_4 \cdot 4 \text{H}_2\text{O}$                | 3.32              | Yellow-Green  |
| $\text{BePt}(\text{CN})_4 \cdot 2 \text{H}_2\text{O}$                | 3.16              | Dark Red      |
| $\text{K}_2\text{Pt}(\text{CN})_4 \cdot 3\text{H}_2\text{O}$         | 3.42              | Yellow        |
| $[\text{Pt}(\text{NH}_3)_4][\text{Pt}(\text{Cl})_4]$                 | 3.25              | Green         |
| $[\text{Pt}(\text{CN-iso-C}_3\text{H}_7)_4][\text{Pt}(\text{CN})_4]$ | 3.15              | Red-Violet    |
| $[\text{Pt}(\text{CNC}_2\text{H}_5)_4][\text{Pt}(\text{CN})_4]$      | ?                 | Bright Yellow |
| $[\text{Pt}(\text{CNR})_4][\text{Pt}(\text{CN})_4]^*$                | Varies            | Varies        |

R= any alkylisocyanide or arylisocyanide

Referring to table 1 it can be seen that the color of the solid complexes does not change in the same direction of the absorption spectrum as the water content varies. Some salts have a red shift in their visible spectrum upon losing water in the lattice and others will have a blue shift. An example of this is the comparison of the strontium and magnesium salts of the TCP's. In the case of the strontium salt as the  $\text{H}_2\text{O}$  hydration decreases the Pt-Pt separation also decreases. The opposite is the case with the magnesium salt where a decrease in  $\text{H}_2\text{O}$  hydration causes a lengthening of the Pt-Pt separation. Since the cations and the isolated anions do not absorb in the visible region of the spectrum they cannot be the reason for the different colors observed in these complexes.

Yamada was the first to determine that there was a relationship between the color of the TCP compounds and their Pt-Pt separation (13). Yamada observed that the absorption bands of these compounds shifted to longer wavelength on

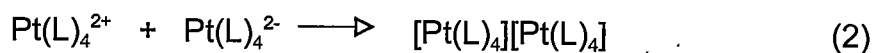
going to a shorter Pt-Pt separation. Yamada showed that the platinum-platinum separation results in the colors observed for the different cations and contents of hydration. The Pt-Pt separations of the TCP salts range from 3.09Å to 3.7Å. For the TCP's the Pt-Pt distance is usually termed as a separation because the metal-metal distance in these complexes are not close enough to constitute a metal-metal bond. In the case of the TCP's the electrostatic interactions of the ligands do not favor the atoms stacking on top of one another. This arrangement puts ligands of the same relative charge in close proximity to one another. Because of unfavorable electrostatics it is assumed the packing energies for the TCP's and their respective alkali and alkaline earth metal counter cations are responsible for the stacked structures.

#### Tetracyanoplatinate(II) in the Solution State

All of the colored solid state TCP's gives clear solutions in all solvents. The only work that studied whether there are metal-metal interactions in solution is the work by Adamson (14,15). Adamson used emission and absorption data to conclude that there is some Pt-Pt aggregation in solution. Adamson concluded that there was some Pt-Pt aggregation in solution because the absorption spectra did not obey Beers Law. There have been a few other papers dealing with the solution studies on the TCP's but these have mostly dealt with the assignment of the electronic transitions (12,16).

Double Salt Complexes

Included in table 1 along with the TCP's are a few representatives of the double complex salts (DS). The term double salt arises from the fact that these complexes consist of a cationic platinum complex and an anionic platinum complex. The DS complexes are formed simply by combining two oppositely charged square planar platinum complexes according to equation 2.



These compounds also stack in a similar fashion to the TCP's where the platinum atoms are on top of one another as in figure 2. In the case of the DS, this type of atom arrangement occurs for two reasons. Like the TCP's the favorable packing energies for the platinum atoms causes this type of atom arrangement, but in the case of the DS the electrostatic interactions contributes to this form of atom arrangement.

All the double complex salts contain square planar platinum(II) complexes with one metal center tetracoordinate to negatively charged ligands and the other metal center tetracoordinate to positively charged ligands. Magnus's Green salt which has the formula  $[\text{Pt}(\text{NH}_3)_4][\text{Pt}(\text{Cl})_4]$  (4) was described over 150 years ago but not until the middle of this

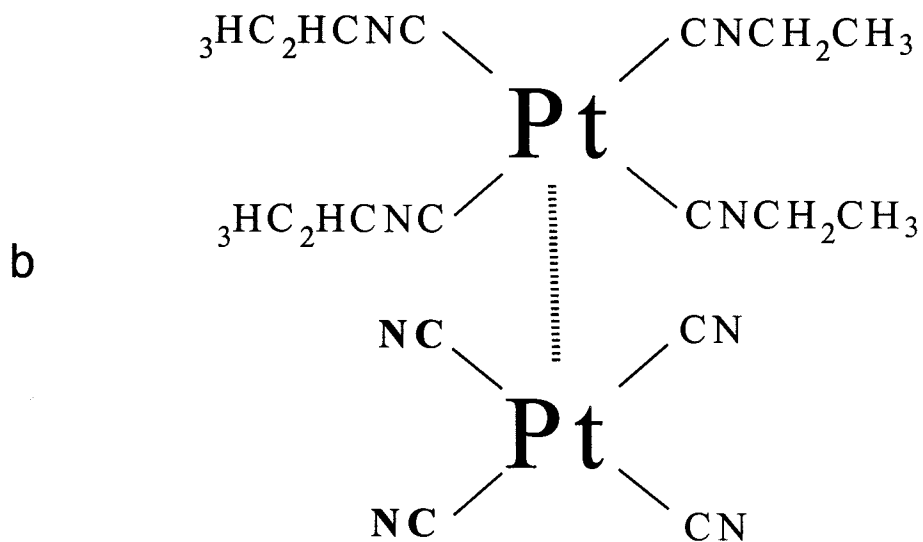
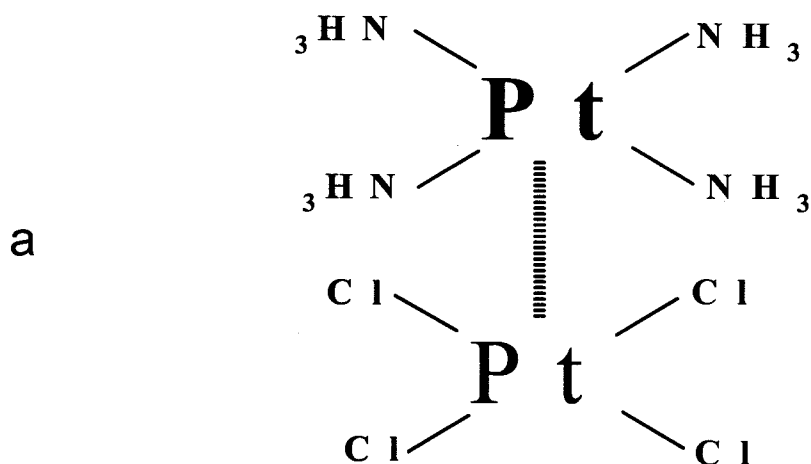


**Figure 5.** a) Depiction of Magnus Green Salt and b) the ethylisocyanidecyano double salt.

century was the structure correctly formulated (17). More recently single crystals have been obtained on more of the double complex salts (18). Because of the low solubility exhibited in most solvents it has been difficult to obtain single crystals of these complexes (19,20). The electrostatic attraction by the ligands leads to the decreased solubility of the DS compared to the TCP's. Low solubility has also prevented solution studies. Figure 5 shows the DS complexes (4) and the tetraethylisocyanideplatinum(II) tetracyanoplatinate(II)  $[\text{Pt}(\text{CNC}_2\text{H}_5)_4][\text{Pt}(\text{CN})_4]$  (5).

### Partially Oxidized Tetracyanoplatinates (POTCP)

#### Solid State Properties of the Partially Oxidized Tetracyanoplatinate(II) Complexes

When the TCP's are exposed to less than 0.5 electron equivalents of oxidant a new class of interesting compounds is formed. Partial oxidation (PO) of the Pt(II) complex results in small needle like crystals that have anywhere from a bronze sheen to a copper color sheen (8). These complexes are termed the partially oxidized tetracyanoplatinates (POTCP) because of the non-integral oxidation state of the platinum atom. The best known example of the POTCP is compound (2). PO results in the Pt-Pt separation decreasing down to 2.8Å to 2.95Å depending on the counter cation used. The decrease in the Pt-Pt

separation gives rise to 1-D physical properties. One of the most interesting properties of these complexes is the 1-D metallic conductivity that arises from delocalization of the electrons in the overlapping Pt  $5d_{z^2}$  orbitals. The shorter Pt-Pt separation in the POTCP complexes is a true metal-metal bond. When metal-metal separations are less than  $3\text{\AA}$  it is believed that there is covalent bonding between the metals. Table 2 shows the Pt-Pt bond distances for some of the POTCP.

Included in table 2 are the physical properties of two PO bisoxalatoplatinates (POBOP). The POBOP complexes are formed in a similar fashion as the POTCP's and also have nearly identical physical properties. The stacking of the platinum atoms in the POBOP's are similar to that in the POTCP complexes. This 1-D stacking and the new Pt-Pt bond give rise to the anisotropic physical properties observed in both complexes. All the known POBOP's have shorter Pt-Pt bonds than the known POTCP's. The POBOP like the POTCP have ligands that result in unfavorable electrostatic interactions. It has been suggested that the shorter Pt-Pt separations in the POBOP are the result of  $\pi$ -type interactions between the oxalate ligands (21,72).

Table 2. Bond distances of partially oxidized complexes

| Complex   | Oxidation # | Type | Pt-Pt $\text{\AA}$ |
|---|-------------|------|--------------------|
| $\text{K}_{1.75}\text{Pt}(\text{CN})_4 \cdot 1.8\text{H}_2\text{O}$           | 2.25        | CD   | 2.96               |
| $\text{K}_{1.62}\text{Pt}(\text{ox})_2 \cdot 2\text{H}_2\text{O}$             | 2.38        | CD   | 2.85               |
| $\text{H}_{1.6}\text{Pt}(\text{ox})_2 \cdot 2\text{H}_2\text{O}$              | 2.40        | CD   | 2.80               |
| $\text{K}_2\text{Pt}(\text{CN})_4\text{Cl}_{.32} \cdot 2.6\text{H}_2\text{O}$ | 2.32        | AD   | 2.88               |
| $\text{K}_2\text{Pt}(\text{CN})_4\text{Br}_{.3} \cdot 7.3\text{H}_2\text{O}$  | 2.30        | AD   | 2.887              |
| $\text{MgPt}(\text{CN})_4\text{Cl}_{.28} \cdot 7\text{H}_2\text{O}$           | 2.28        | AD   | 2.985              |

The anisotropic properties arise because the distance between the Pt-Pt chains is upwards of 9Å. This is compared to the in-chain Pt-Pt separation which is less than 3Å for all the PO compounds. The conduction of electricity along the Pt-Pt chain is some  $10^5$  greater than perpendicular to the chain. These complexes also polarize light parallel to the chain axis.

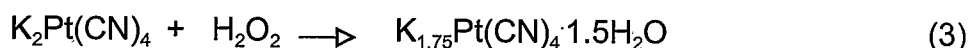
When the PO compound (2) was initially found early in this century it was formulated as a mixed complex containing five Pt(II) and one Pt(IV) molecules (22). This gives very nearly the exact stoichiometry of the PO complexes when the oxidation state is averaged over all the atoms. Five Pt(II) atoms and one Pt(IV) atom add up to a total charge of +14. If this is delocalized over all six platinum atoms the average oxidation state of each platinum would be +2.3. This is indeed the oxidation state in (2) which is the complex that was studied early in this century and described by Levy (18).

### Two Different Types of PO Compounds

For the POTCP's there are two different types of compounds that can be formed (8). These consist of the anion-deficient (AD) and the cation deficient (CD). The AD POTCP are deficient in halide ion and are found according to equation 1. They have the general formula  $K_2Pt(CN)_4X_{3.3} \cdot 2H_2O$  (where X = Br or Cl). These compounds can be made simply by mixing the Pt(II) and the corresponding trans di-halo Pt(IV) species together in a 5Pt(II):1Pt(IV) ratio in

many solvents. Upon evaporation, copper colored needles are deposited in the reaction vessel. The first evidence that the AD PO compounds were not mixed valence species was their IR spectrum. IR studies showed that the chlorine atoms were no longer bound to the platinum atom in the PO compounds (8).

The CD-POTCP is deficient in counter cation and is formed according to equation 3. The general formula for this compound is  $K_{1.75}Pt(CN)_4 \cdot 1.5H_2O$  (6).



This type of compound is formed by heating Pt(II) in the presence of hydrogen peroxide under acidic conditions. Upon slow cooling the copper colored CD-POTCP crystallizes. Table 2 indicates whether each of the PO compound are AD or CD. The CD-POTCP has also been made using electrochemical procedures (23).

Non-stoichiometry arises from the non-integral oxidation state of the platinum atom. The average oxidation number for (2) is +2.3 and for (6) +2.25. A good method for remembering the difference between the AD and the CD is that in the AD case the halide is in non-stoichiometric proportions and in the CD case the cation is in non-stoichiometric proportions. In the case of the POBOP only the CD type have been found. The most common representative of the POBOP is the  $K_{1.62}Pt(ox)_2 \cdot 2H_2O$  (7).

A term that is commonly used when referring to the PO complexes is the degree of partial oxidation (DPO). It is the measure of the amount of oxidation

that takes place. It is used as a relative correlation between the Pt-Pt bond distance and the oxidation state in the PO complexes. The above DPO's for the two POTCP are 0.3 for **(2)** and 0.24 for **(6)**. Referring to table 2 it is seen that the complex with a DPO of 0.3 compared to 0.24 has a shorter Pt-Pt bond. The DPO varies for both the AD and the CD depending upon the counter-anions and counter-cations used but the correlation always holds true that the larger the DPO the shorter is the Pt-Pt separation.

The correlation of the DPO and the Pt-Pt bond distances is also seen in the few known Pt(III) complexes. All the known Pt(III) complexes are dimeric with a Pt-Pt bond whether they are bridging or non-bridging. Whether the complex is bridging or non-bridging is irrelevant when comparing the DPO to the Pt-Pt bond distance. Because Pt(III) complexes have undergone a one electron oxidation they have a DPO of 1 and the Pt-Pt bond distances are between 2.7 and 2.8 Å for the non-bridged Pt(III) complexes (24,25). This is reduced even further for the bridged Pt(III) dimers. This is shorter than any known Pt-Pt bond distance in the POTCP and POBOP.

The oxidation state and the resulting DPO's of the PO compounds were determined using x-ray crystallographic methods. From the crystal structure all the platinum atoms are crystallographically identical. If the platinum atoms are crystallographically identical they must be in the same oxidation state. The determination of the molecular formula can be described using **(2)** as an example. In the case of **(2)** it was found that every unit cell contains two

platinum atoms. For every unit cell there is a hole for one halide atom, which gives .5 halides for every platinum atom. Only 60% of the holes that will accommodate a halide in the unit cell are occupied resulting in a total of .3 halides for every platinum atom. This gives the formula for **(2)** with a platinum oxidation state of +2.3 and a DPO of 0.3. The early hypothesis of the AD complexes like **(2)** and **(3)** being mixed valence Pt(II) and Pt(IV) species was disproved by IR methods and this was reaffirmed using crystallographic methods (11). However, the X-ray structure was needed of **(6)** to determine whether it was a mixed valence compound or not. Unlike **(2)** where there is a fairly intense IR band for the M-X there is no similar intense band for the M-OH.

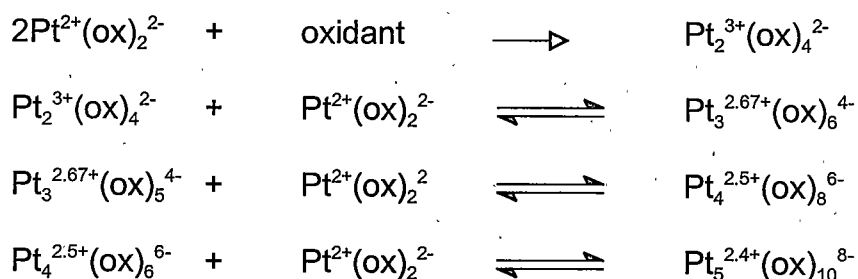
#### Solution Studies on the Partially Oxidized Compounds

The solution chemistry leading to the POTCP's is a major part of the research that is described here. The study of the solution properties of the PO compounds has not been the objective of many researchers because the 1-D solids lose their unusual anisotropic physical properties when dissolved. Additionally many of the PO compounds that form 1-D columns are not very soluble in water, although the lack of water solubility is not the case with **(6)**. The POTCP compounds do have a diminished solubility compared to the unoxidized TCP but most of the POTCP salts are still slightly soluble in water.

Partially Oxidized Bis-Oxalato Platinates Solution Chemistry

The POBOP does not give both the AD and CD form. It is only found in the CD form. The POBOP that has received the most attention to its solution behavior is (7). The solutions of the POBOP formation and their subsequent dissolution have been studied and have been shown to hold a rich solution chemistry (9,26-28). Keller proposed that the POBOP forms in a stepwise manner beginning with oxidation of the Pt(II) oxalate to give the Pt(III) dimer. This is then followed by further oligomerization until the solids precipitate out of solution as the copper colored needle like crystals. Scheme I below shows the oligomerization process proposed by Keller for the formation of the POBOP.

Scheme 1

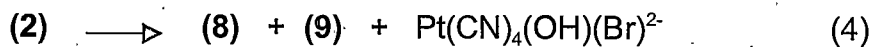


The initial step is oxidation of the Pt(II) to a dimeric Pt(III) complex. Various oxidants have been used for this first step including  $\text{Ce}^{4+}$ ,  $\text{H}_2\text{O}_2$  and  $\text{Pt}(\text{Cl})_6^{2-}$ . Three more non-integral platinum oxidation steps then follow the initial step. Each subsequent oligomer in scheme I gives a new electronic absorption

band in the visible region of the spectrum. With the addition of each platinum oxalate the absorption band is shifted to lower and lower energy. The pentamer has an overall oxidation state of +2.4. This is near the oxidation state of +2.38 that is observed in the solid crystal of (7). The crystal structure reveals that (7) is made up of repeating pentamers (8). This evidence suggests there are no multinuclear species in these solutions larger than the penta-nuclear species. Once the pentamer is formed the solubility is reduced enough to allow precipitation of (7).

#### Anion Deficient Partially Oxidized Tetracyanoplatinate Solution Chemistry

The solution chemistry of the anion-deficient (AD) POTCP is fairly limited (29). Complex (2) is made by simply combining the  $\text{Pt}(\text{CN})_4^{2-}$  (8) and the  $\text{Pt}(\text{CN})_4(\text{Br})_2^{2-}$  (9) in a 5:1 stoichiometric ratio. Saillant used UV-Visible spectroscopy to compare the solutions of the dissolved copper colored needles to the solutions of the starting materials. When the solids are dissolved in water the initial (8) and (9) are present in addition there is some of



the mixed hydrated Pt(IV) species  $\text{Pt}(\text{CN})_4(\text{Br})(\text{OH})^{2-}$  (10). When the solids are dissolved in a .1M solution of KBr it is possible to suppress the hydration which forms (10). In this case only (8) and (9) are observed.

Other studies of these solutions using  $^{195}\text{Pt}$  nmr showed similar results as Saillant (30). The  $^{195}\text{Pt}$  nmr gave singlets at -4724ppm for (8), -3573ppm for (9) and -2434ppm for (10) when (2) is dissolved in pure water. Like the UV-Visible study in solutions of .1M KBr the  $^{195}\text{Pt}$  nmr only shows two resonance's for (8) and (9).

### Cation-Deficient Partially Oxidized Tetracyanoplatinate(II) Solution Chemistry

Of all the different PO compounds the solution properties of the CD-POTCP have received the least attention. Some of this is because no colors are observed in the formation nor the dissolved solutions like the POBOP and the AD-POTCP solutions. It was of interest if the CD-POTCP forms from a Pt(IV) and a Pt(II) like that of the AD-POTCP as seen in equation 1 or if there is a more complicated process like that seen in solutions of the POBOP in scheme 1. If there are oligomers or any association of metal ions present in the formation of the CD-POTCP they do not have visible absorption bands like the POBOP because these solutions are clear like the unoxidized TCP's.

During the initial determination on the feasibility of studying these solutions it was determined that there was a Pt(IV) complex in the reaction solutions when forming the CD-POTCP using hydrogen peroxide. The Pt(IV) that exists in these solutions is of the form  $\text{Pt}(\text{CN})_4(\text{OH}_2)_2^{2-}$  (11).

(11) was described by Russian scientists and they have reported the

formation of this Pt(IV) as the potassium salt  $K_2Pt(CN)_4(OH)_2 \cdot 2H_2O$  (**11A**). The formation and isolation of pure (**11A**) was never achieved by their procedure (31). However,  $^{195}Pt$  nmr reveals that (**11**) is the dominant species present when the TCP's are oxidized with sufficient amounts of hydrogen peroxide under acidic conditions. This Pt(IV) is also the dominant species any time the conditions and oxidant used result in a larger than one electron oxidation of the TCP's.

Of considerable interest to the work described here are the reports by Levy of a purple Pt(III) crystal formed by oxidation of (**8**) with nitric acid and perhydrol (22). Purple colors are not observed in the reaction solutions when POTCP compounds are formed but when a one-electron oxidation of TCP is done, a purple color is observed after two weeks. To date there has been no characterization of any purple complexes concerning the platinumcyanides. The purple color observed in the oxidized TCP solutions is comparable to that seen in the formation of the POBOP. In the case of the POBOP it is believed this color is the result of the trimeric platinumoxalate shown in scheme I. This color is also similar to that of the platinum blues (Figure 1) which are all tetrameric and result in blue or purple colors. It may be reasonable to expect that the purple color seen in the oxidized solution of the TCP's is also a trimeric or tetrameric species. It is reasonable to compare the solution colors of the oxalates and the cyanides because the colors exhibited by these complexes are the result of Pt-Pt interaction. On the other hand one must be cautious comparing Levy's purple solid with the purple solutions because of the large difference in the Pt-Pt

interactions between the solid phase and the solutions. It would not be surprising if a purple tetramer that existed in solution gave some other color upon crystallization. For example the dimeric oxalate gives yellow solutions but it would be possible for the crystalline dimer to be purple. This is the direct result of the packing energies for these complexes. The solid phase can give drastically different Pt-Pt separation distances than the same compound in solution. Hartley concluded that the complex reported by Levy was most likely not a Pt(III) species but was a mixed valence species with stacking of Pt(II) and Pt(IV) centers (32). However, the assumptions by Hartley were made before many Pt(III) complexes had been synthesized.

Piccinin and Toussaint also reported a Pt(III) species in 1967 but their crystal structure is incomplete (33). They reported making the Pt(III) species using  $\text{HNO}_3$  to oxidize  $\text{K}_2\text{Pt}(\text{CN})_4 \cdot 3\text{H}_2\text{O}$  (**8A**) to  $\text{K}_2\text{Pt}(\text{CN})_5 \cdot 3\text{H}_2\text{O}$  (**12**). The solid species reported on by Piccinin and Toussaint was reported to also be purple like that described by Levy. They also referenced Levy's 1912 paper for the synthesis of this compound.

### Platinum(II) Isocyanide Complexes

#### Chemistry Effects on the Platinum Atom From the Isocyanide Ligand

Because of the highly anisotropic physical properties of the PO platinum

cyanides and oxalates, other ligands have been studied to determine if they also form complexes having similar anisotropic physical properties. Some of the interest lies with ligands that can be derivatized so the ensuing PO compound could be attached to surfaces and in essence one could make a molecular wire that can be bound to a surface. This would continue with the further miniaturization of electrical circuitry. Isocyanides are one type of ligand that can be derivatized because of the ability to alter the terminal alkyl group. To date none of the isocyanides studied have been susceptible to partial oxidation.

The isocyanides stabilize metals to a greater extent than the cyanides do in low oxidation states. This is probably due to the fact that isocyanides are fairly good reducing agents. Their stabilization of low oxidation states is apparent in the Pt(I) species  $[\text{Pt}(\text{CNC}_2\text{H}_5)_6][\text{BF}_4]_2$  (**13**). (**13**) has a Pt-Pt separation of 2.583Å. The crystal structure has been solved for the Pt(I) methyl isocyanide  $[\text{Pt}(\text{CNCH}_3)_6][\text{BF}_4]_2$  (**14**) and the crystal structure of the ethyl isocyanide is described in this thesis (34,35). This species has some unique characteristics. It is one of the few stable Pt(I) species that has been characterized by  $^{195}\text{Pt}$  nmr,  $^1\text{H}$  nmr and x-ray crystallography. Its stability is also unique because of the unsaturation at the metal centers. The structure of these complexes is seen in figure 5. A good overview of isocyanides can be found in the references listed and all those therein (75,76).

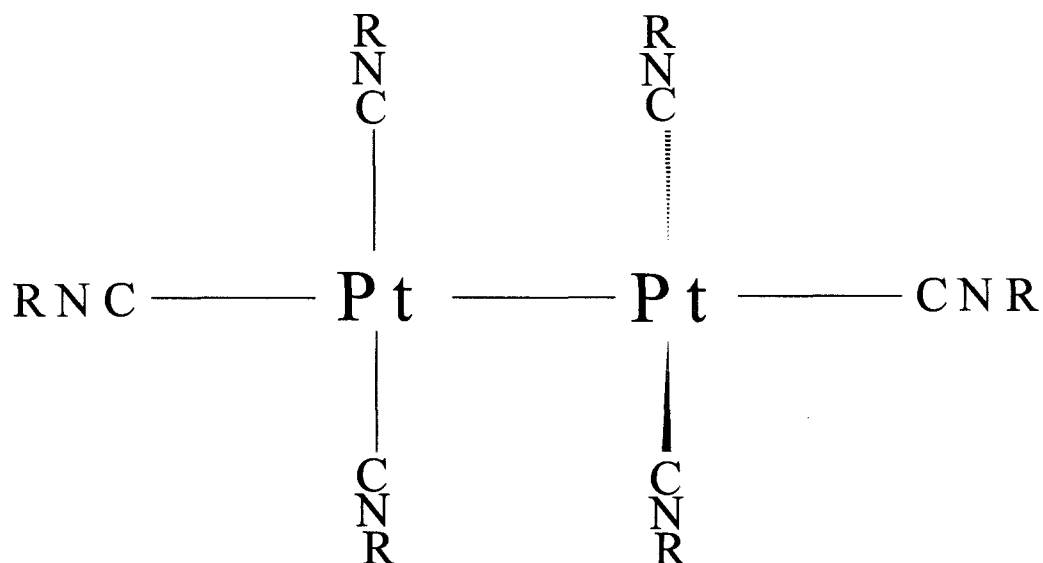


**Figure 6.** Depiction of the Pt(I) unsaturated isocyanide complexes.

The result of the unsaturation is that there is a ligand along what would be the metal-metal bonding axis. This Pt(I) species contains a Pt-Pt bond that is shorter than any of the dimeric Pt(III) that have been found. It is also shorter than all the known bridged Pt(III) complexes except for the one used in figure 4. Cyanides on the other hand form stable complexes in high (+4) oxidation states.

Molecular orbital (MO) considerations that are described later indicate that removal of electrons from the  $d_{z^2}$  orbitals in Pt(II) complexes is necessary to form strong metal-metal bonds. The Pt(I) isocyanide mentioned above is a special

case where there is unsaturation at the metal that makes the metal-metal bond possible. The higher the oxidation state of a metal-metal bonded complex the shorter this bond will be. Removal of electrons the antibonding orbital would give a higher bond order. Finding isocyanides that will allow the metal to undergo partial oxidation has not been done. To date there are no known platinum isocyanides that exist in oxidation states higher than +2. Because the isocyanides prefer to be in lower oxidation states it is unlikely without altering the substituents on the isocyanide to get the platinum to oxidize.

Isocyanide ligands are also susceptible to nucleophilic attack when coordinated to a metal-although most organic solvents are poor enough nucleophiles they result in the rate of nucleophilic attack being very slow. The rate of attack is sufficiently slow enough in acetonitrile that it does not impede the solution studies of these complexes. In acetonitrile at 25°C one usually has up to one hour before any significant changes are seen in the UV-Visible absorbance of the isocyanides. When the isocyanides are dissolved in water at 25°C there are changes seen in the UV-Visible spectrum after 30 minutes. If the solution studies are done as low as 7°C there are no changes in the spectrum after 2 hours. The mechanism for the nucleophilic attack on the isocyanide by water has been studied and described by Balch (36,37). The UV-Visible studies done here were done within 15 minutes of dissolution and this showed no degradation of the ethyl isocyanides.

## Vapochromic Double Salts

### Solid State Properties of the Vapochromic Double Salts

One interesting property associated with the isocyanide complexes when they are combined with the TCP's is the resulting vapochromic properties of the resulting DS. Vapochromism is the ability of these complexes to change color when exposed to solvent vapors. The vapochromic properties in these solid complexes give changes in the color of the complex when exposed to volatile organic compounds (VOC's) (38,39). The color change observed is reversed when the solvent is removed from the presence of the isocyanide complex. The most useful vapochromic complex for the detection of VOC's are of the type  $[\text{Pt}(\text{CNR})_4][\text{Pt}(\text{CN})_4]$  (where  $\text{R} = \text{C}_6\text{H}_4\text{-C}_n\text{H}_{n+1}$   $n > 5$ ) (Figure 7). The first vapochromic complexes contained tetracyanopalladate as the anion (37). These complexes are potentially useful for both environmental and industrial detection of VOC's. In most cases the eye can see the change in color of the vapochromic solid. The magnitude of the shift is different for the various solvents when exposed to a vapochromic complex as is shown in table 3.



**Figure 7.** Arylisocyanideplatinum(II) tetracyanoplatinate(II) vapochromic complex.

Table 3. Absorption for solid state films of I when exposed to VOC's

| Solvent                         | Absorption max(nm) | Shift(nm) |
|---------------------------------|--------------------|-----------|
| None                            | 548                |           |
| MeOH                            | 544                | -4        |
| EtOH                            | 554                | 6         |
| 2-PrOH                          | 554                | 6         |
| Et <sub>2</sub> O               | 558                | 10        |
| CH <sub>3</sub> CN              | 559                | 11        |
| Hexanes                         | 561                | 13        |
| Acetone                         | 562                | 14        |
| Benzene                         | 567                | 19        |
| CH <sub>2</sub> Cl <sub>2</sub> | 569                | 21        |
| CHCl <sub>3</sub>               | 578                | 30        |

For the vapochromic complexes to be effective as environmental sensors for VOC's they must be insoluble in the solvents that they will be exposed to yet still change color when exposed to the solvents being investigated.

Solution State Properties of the Double Complex Salts

Our interest lies with double complex salts like those that exhibit vapochromic properties but are soluble in either aqueous or organic media. As with most of our research we are interested in investigating which species exhibit metal-metal bonding in solution. It is believed that the metal-metal interaction in the solid phase is the cause of the extensive colors exhibited in these double complex salts much like the colors of the TCP salts. In the case of the TCP salts when they are exposed or depleted of water a color change occurs. The change in the content of water hydration disrupts the lattice resulting in a different Pt-Pt separation and hence a different color. To have the ability to alter the vapochromic complexes for environmental uses or the electrical properties of the POTCP it is of significant importance to understand the solutions leading up to the solid state products.

Our solution studies were carried out on the tetraethylisocyanide tetracyanoplatinum  $[\text{Pt}(\text{CNC}_2\text{H}_5)_4][\text{Pt}(\text{CN})_4]$  (5) double complex salt because of its slight solubility in acetonitrile and high solubility in water. This solubility allows us to study the metal-metal interaction in solution. The ethylisocyanide double complex salt does possess vapochromic properties like the aryl isocyanides. It gives a change in color from yellow to red when exposed to water vapor but because of its solubility in water it begins to dissolve. This ethylisocyanide complex is not favorable for practical use as a vapochromic compound for two

reasons. The ethylisocyanide complex only shows vapochromism towards water and it is soluble in this solvent. Secondly there is no demand for the detection of water vapor. However this complex does have vapochromic properties and it is easily made. These reasons make it a useful example of these complexes to study the metal-metal interactions in the solution state.

### Mixed Cyanide/Isocyanide Platinum(II) Complexes

In addition to the tetrakisocyanideplatinum(II) complexes Isci and Mason assigned the electronic spectra for bismethyldicyanoplatinum(II) and bisethylidicyanoplatinum(II) (57). These complexes have received no attention beyond the work of Isci and Mason. The crystal structures have been solved for the two mixed complexes and described here. The bond lengths of the mixed complexes have been analyzed and attempts have been made to position the two strong field ligands in respect to their position in the spectrochemical series. Isci and Mason made suggestions that the CNR was in fact a slightly stronger  $\pi$ -acids than the  $\text{CN}^-$  ligand. The crystal structures of the bisisocyanidedicyano complexes are studied and conclusions are made on the  $\pi$ -acid strengths of the two ligands.

A similar complex to the mixed isocyano/cyano is the cis- $\text{Pt}(\text{CH}_3)_2(\text{CNCH}_3)_2$  that was studied by Pudaphat (41). The few known

(bisisocyanide)(biscyano/bismethyl) platinum(II) complexes containing the three strong field ligands CNR, CN<sup>-</sup> and CH<sub>3</sub> all give the cis arrangement. The complexes structured here may give some information on the small differences that exist between the ligands in regard to the thermodynamic cis/trans-influence.

### Bonding Descriptions for the Pt-Pt Complexes

An appreciation of the molecular orbital bonding descriptions for metal-metal complexes is helpful in the understanding of the chemistry involved with these complexes. All the Pt(II) TCP's are d<sup>8</sup> square planar complexes. Figure 8 shows a simplified MO sketch for the interaction of two platinum atoms. Figure 9 expands the view of figure 8 to only include the HOMO and LUMO of two interacting platinum complexes. The MO diagram would suggest there is no metal-metal interaction for the complex since the a<sub>1g</sub> and a\*<sub>2u</sub> are both full and thus there would be no net bonding interaction (figure 9A). However the a<sub>1g</sub> and a<sub>2u</sub> derived from dz<sup>2</sup> orbitals are lowered in energy compared to the a<sub>1g</sub> and a<sub>2u</sub> that are derived from p<sub>z</sub> orbitals (9,42). This repelling arises because the a<sub>1g</sub> and a<sub>2u</sub> are non-degenerate molecular orbitals that are of similar symmetry. This results in a net bonding energy for the TCP's as shown in figure 9B. Krogmann and Gray have termed this as a configuration interaction. The configuration interaction gives a small net bonding interaction in the TCP's and this is evident

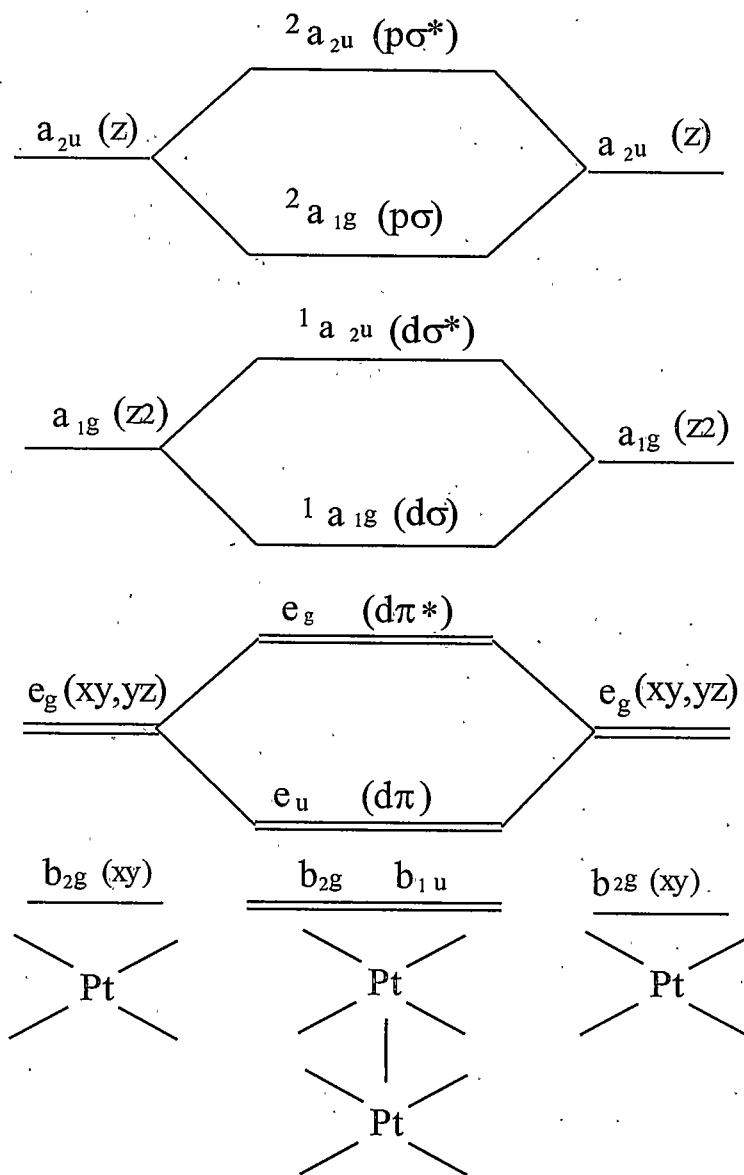


**Figure 8.** Simplified MO sketch of two interacting square planar platinum complexes.

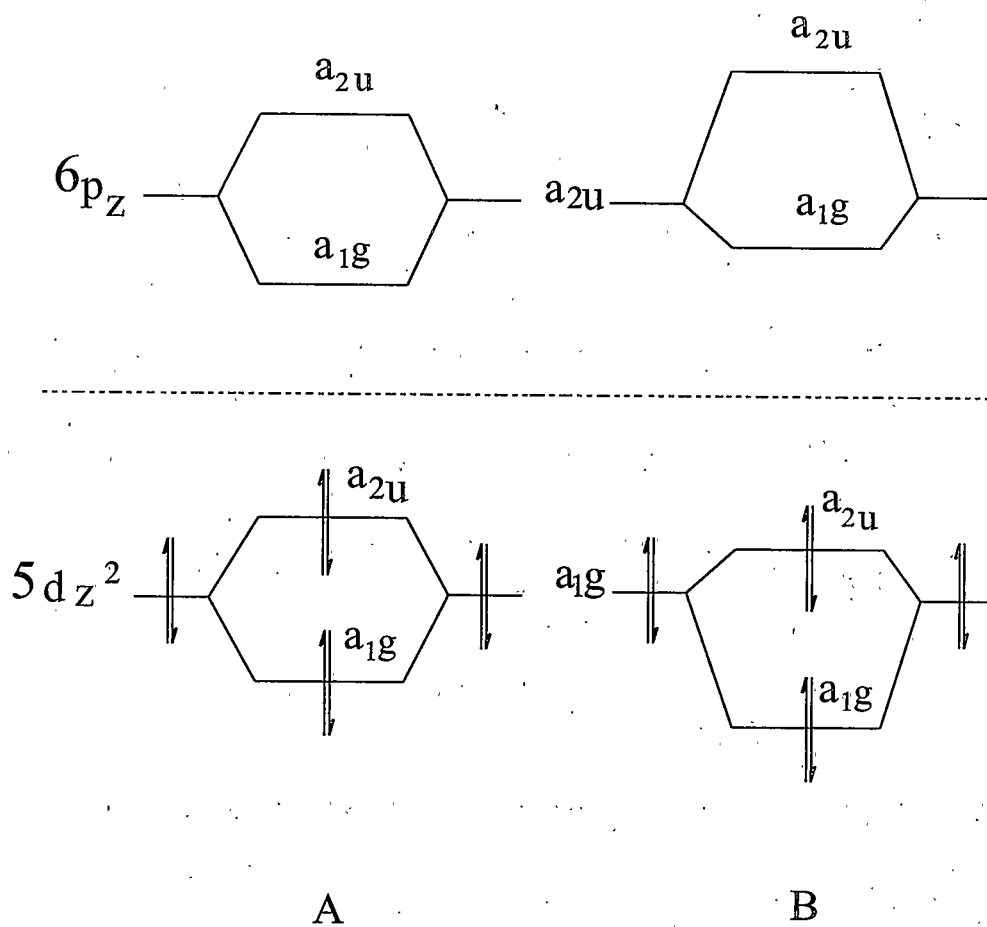


**Figure 9.** a) Two platinum atoms interacting giving no net bonding interaction b) two platinum atoms interacting with a "configuration interaction" resulting in a net bonding interaction for the two platinum atoms.

in the Pt-Pt distances which are all greater than 3Å. As the configuration interaction becomes larger the resulting Pt-Pt separation is shorter. The electronic transition energy moves to lower energy the larger that the configuration interaction is (13).

A similar treatment for metal-metal interactions was done by Mann et. al. (73,74). The favorable metal-metal interactions of the dinuclear tetraphenylisocyaniderhodium(I) was rationalized with a molecular orbital depiction that is identical to the treatment shown in figure 9. The symmetry between the platinum and the rhodium species is the same so the molecular orbital treatment would be identical. The rhodium isocyanides give similar solid state complexes as the platinum cyanides where there is metal-metal interactions in both the platinum and rhodium cases with the metal-metal distances greater than 3Å. The major difference between the two systems is in the solution properties. The rhodium complexes give metal-metal association into the solution state where the platinum cyanides only give association in oxidized solutions and when mixed with a planar counter-cation.

One would expect a resulting stabilization of a Pt-Pt complex if electrons were effectively removed from the  $\sigma^*$  orbital. This is the case in the POTCP's. It is more appropriate to view these complexes in a MO band model. Figure 10 shows the band model of a POTCP platinum chain complex. Figure 11 is the band model for a chain of Pt(II). In figure 10 it is seen that upon PO the removal of electrons from bands that are mostly antibonding in character causes a net

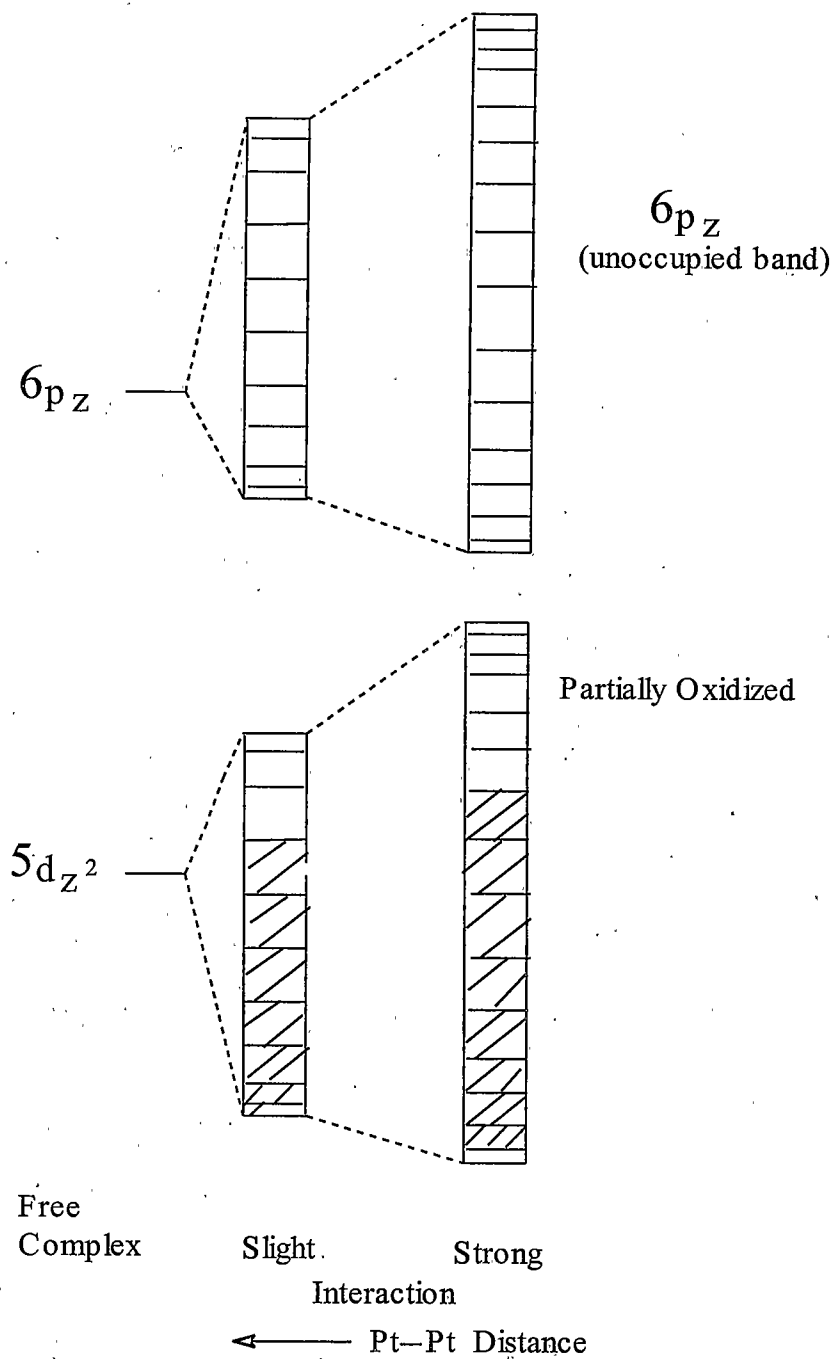


Figure 10. Band model for the POTCP chain compounds.

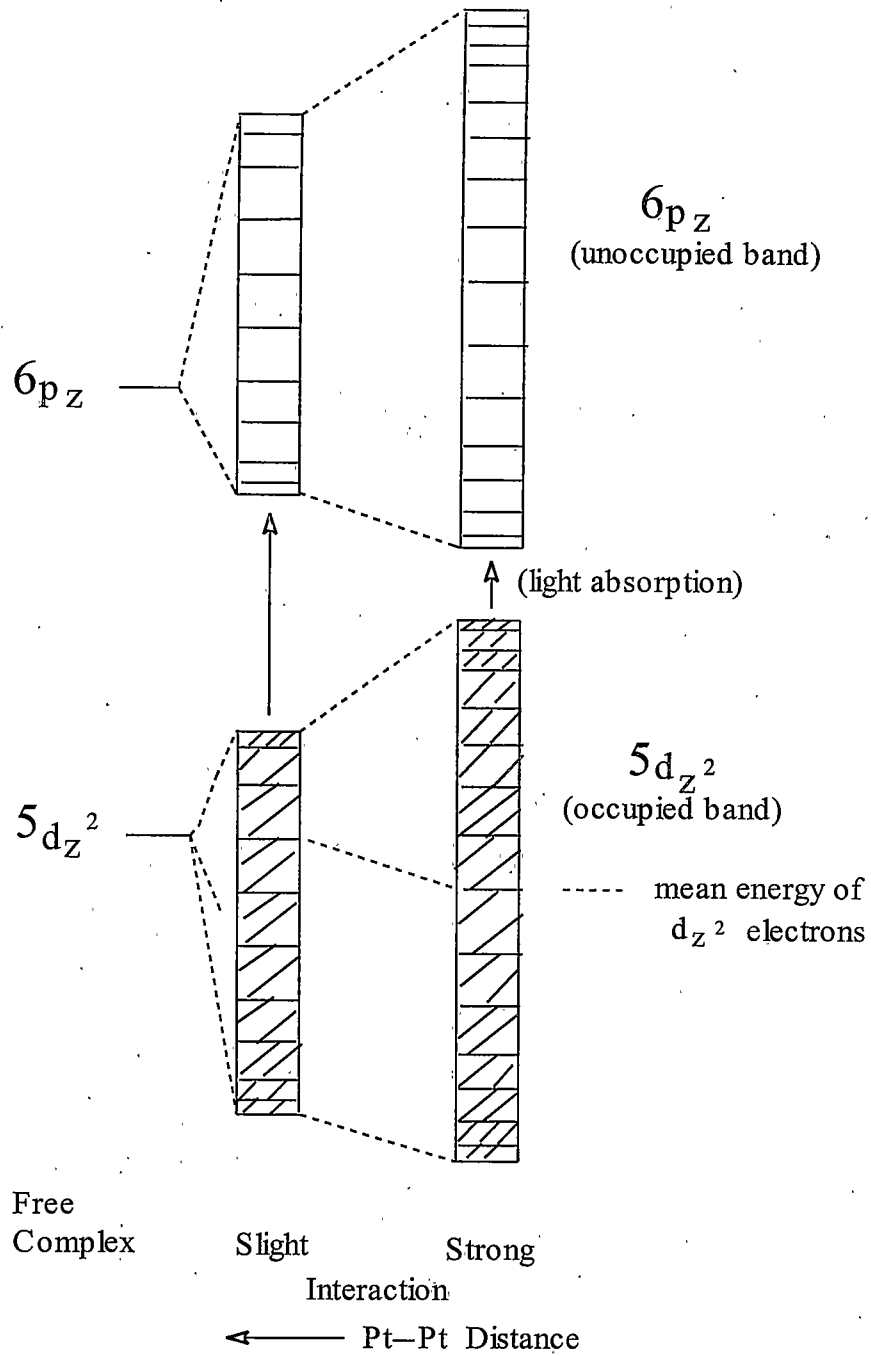


Figure 11. Band model of a chain of platinum(II) compounds.

stabilization and thus a shorter Pt-Pt bond. This is correlated with the DPO described earlier where the more electrons that are removed the lower in energy the molecule becomes and the shorter the Pt-Pt bond.

It would seem logical from the MO depiction in figure 9 that one would be able to suggest the inherent stability of the dimeric Pt(III) complexes. The dimeric Pt(III) complexes have  $d^7$  electron configurations giving a total of 14 electrons to accommodate on the correlation diagram. When describing this on the MO diagram it would appear the Pt(III) dimers should be more stable than the POTCP complexes. Only needing to fill 14 electrons on the MO diagram would result in a much more energetically favorable bonding situation than the POTCP. There must be larger electronic effects that take precedence causing the Pt(III) dimers to not be all that common. However, the few that exist do have shorter Pt-Pt separations, which is what the MO diagrams suggest.

### $^{195}\text{Pt}$ Nuclear Magnetic Resonance

$^{195}\text{Pt}$  nmr spectroscopy gives us a powerful tool to probe the solution chemistry of the TCP's and their partially oxidized compounds. The  $^{195}\text{Pt}$  chemical shift affords us useful information on the species present in solution. The chemical shift is dependent on both the ligands surrounding the platinum atom and the oxidation state of the metal. Although there is overlap of where the

different oxidation states of Pt occur in the spectrum, the oxidation state of the Pt species can be nearly assigned by where the chemical shift occurs in the spectrum assuming there is some knowledge of the ligands attached to platinum.

The one bond coupling constants are also indicative of the oxidation state of the platinum complex. This can be useful when the oxidation state of different species in solution are unknown. On going to a higher oxidation state the couplings decrease due to less s character involved in the bonding. In the case of square planar platinum(II) complexes the hybridization is  $dsp^2$  which has a 25% s character. Octahedral platinum(IV) complexes on the other hand are  $d^2sp^3$  which correlates with only about a 17% s character. The  $^1J_{Pt-C}$  in the platinum cyanides are on the order of 250Hz smaller for the Pt(IV) species than their Pt(II) counterparts (43,44).

Unfortunately any species present in solution that are monomeric Pt(III) can not be detected because they are paramagnetic. However, if the Pt(III) species exist as a dimeric Pt(III) species or any even numbered multinuclear species they are then diamagnetic and nmr detectable. Broad peaks of greater than 200Hz in width generally give a good indication that metal-metal associated species are present in the solution. The broadening of dimers occurs for two reasons. The first is that these complexes have higher molecular weights compared to their monomer counterparts. This results in a slower tumbling rate and a broader signal. Secondly the Pt(III) dimers have faster relaxation times which also causes broadening of the resonance.

The chemical shift range for  $^{195}\text{Pt}$  spans about 15,000ppm. The slightest change of the electronic influences surrounding the platinum atom result in a change in its chemical shift. In some cases exchange of only a single ligand on a platinum complex can result in a chemical shift change of up to 1000ppm. The  $^{195}\text{Pt}$  chemical shifts of hundreds of various complexes can be found in the reviews done by Pregosin (43,44).

The substituents surrounding the Pt nucleus can be determined with near certainty by the  $^{195}\text{Pt}$  chemical shift using comparative methods (43,44). For example in the case of oxidation where two oxygen atoms are added to the platinum center the chemical shift observed for the new complex can be compared to other well known oxidation's where two coordinated oxygen atoms are added to the Pt nucleus. The comparative method is described in great detail later in this thesis.

## EXPERIMENTAL METHODS

Preparation of Compounds

Starting Materials  $\text{K}_2\text{Pt}(\text{Cl})_4$  (**15**) was obtained from Alfa Aesar and used without further purification. KCN was obtained from J.T. Baker and used without further purification. The monopersulfate compound Oxone<sup>TM</sup> was also obtained from Aldrich and used without further purification. The 99+%  $\text{K}^{13}\text{CN}$  and the 30% solution of hydrogen peroxide were obtained from Aldrich chemical and used without further purification. Tetra-butylhydrogen peroxide was obtained from Fisher scientific and used without further purification. All alkylating agents including methyl iodide, ethyl iodide,  $[(\text{C}_2\text{H}_5)_3\text{O}][\text{BF}_4]$  and  $[(\text{CH}_3)_3\text{O}][\text{BF}_4]$  were obtained from Aldrich and used without further purification. The  $\text{Cs}_2\text{SO}_4$  and the tetra-n-butylammonium chloride were obtained from Aldrich Chemical and the  $\text{BaSO}_4$  was obtained from J.T. Baker Co. and were used without further purification. Anhydrous  $\text{CH}_2\text{Cl}_2$  was obtained by distillation over  $\text{P}_2\text{O}_5$ .

Preparation of  $\text{MPt}(\text{CN})_4 \cdot \text{XH}_2\text{O}$  (M=Ba,  $\text{K}_2$ ,  $\text{Na}_2$ ,  $\text{Cs}_2$ , [t-n-butylN]<sub>2</sub>) (**8A-8D**) The  $\text{K}_2\text{Pt}(\text{CN})_4 \cdot 3\text{H}_2\text{O}$  (**8A**) was made by adding a slightly greater than 4 mole equivalents of KCN to a concentrated solution of (**15**) and allowed to stir for one

hour. The reaction was dried and brought back up in a minimal amount of warm water (50°C) and placed over a NaCl ice bath. The crystals were then washed, filtered with a little cold water and collected from a fine porosity fritted filter. It is necessary to repeat the crystallization process at least four times to obtain about 96% of the TCP.

$\text{BaPt}(\text{CN})_4 \cdot 4\text{H}_2\text{O}$  (**8B**) was prepared by addition of a small excess of barium chloride to a fairly concentrated solution of compound (**8A**), resulting in a green solid precipitating out of the solution immediately (22). The green solid was collected over a fine fritted filter. Re-dissolving the collected green solid in warm water (60°C) and then cooling over an ice bath results in bright yellow needle like crystals of the form (**8B**). The yield obtained for the Ba salt by way of the K salt was 91.4%.

$\text{Na}_2\text{Pt}(\text{CN})_4$  (**8C**) was prepared by ion exchange. A concentrated solution of (**8A**) was prepared in water and ran through a Dowex 50W-8X  $\text{Na}^+$  charged cation exchange resin. Compound (**8C**) was collected from the ion-exchange column and dried. No further purification was carried out.

$\text{Cs}_2\text{Pt}(\text{CN})_4 \cdot 2\text{H}_2\text{O}$  (**8D**) was prepared by the method of Mafly et al. (19) 4.0g of (**8C**) was dissolved in 14.5ml of hot  $\text{H}_2\text{O}$  (75°C), to this was added 1 eq of  $\text{Cs}_2(\text{SO}_4)$  (2.86g). An immediate white precipitate of  $\text{BaSO}_4$  results. The reaction was stirred for 30 minutes then the  $\text{BaSO}_4$  was filtered off over a fine fritted filter. The  $\text{BaSO}_4$  was washed 3 times with warm water, the filtrate was then dried and brought back up in a minimal amount of hot water and cooled

over a NaCl ice bath. The resulting white crystals were filtered off and washed with cold water. The recrystallization was repeated 3 more time on the filtrate obtaining a 89% yield.

(t-n-butylN)<sub>2</sub>Pt(CN)<sub>4</sub> (**8E**) This was prepared similar to the literature method with small modifications (45). 4.0g of (**8A**) were dissolved up in 10ml of water in a separation funnel. A stoichiometric amount of the tetra-n-butylammonium chloride was added to the solution of (**8A**). The resulting mixture was then extracted 3 times with CH<sub>2</sub>Cl<sub>2</sub>. The collected organic phase was dried over MgSO<sub>4</sub> and then the solution was dried on vacuo. Recovery of platinum salt = 95%.

Preparation of K<sub>2</sub>Pt(ox)<sub>2</sub> (**16**) The complex was prepared by the method of Krogmann and Dodel using K<sub>2</sub>Pt(Cl)<sub>4</sub> and K<sub>2</sub>C<sub>2</sub>O<sub>4</sub> (17,19).

Preparation of K<sub>2</sub>Pt(ox)(CN)<sub>2</sub> (**17**) .2g of K<sub>2</sub>Pt(ox)<sub>2</sub> (**16**) was dissolved in 5ml of distilled water and heated to 55°C. To this was added .054g (2mole eq.) of K<sup>13</sup>CN. The mixture was stirred for one hour holding the temperature at 55°C and then dried. The solid after drying contained a mixture of yellow and red. The <sup>195</sup>Pt nmr indicated three different species present in different concentrations. Pt(ox)<sub>2</sub><sup>2-</sup> (-525ppm) << Pt(CN)<sub>4</sub><sup>2-</sup> (Pentet with <sup>1</sup>J<sub>Pt-C</sub>=1029Hz) < Pt(ox)(CN)<sub>2</sub><sup>2-</sup> (triplet with <sup>1</sup>J<sub>Pt-C</sub>=1195Hz). The <sup>13</sup>C spectrum shows a 1:4:1 triplet at 125ppm for the Pt(CN)<sub>4</sub><sup>2-</sup> and a 1:6:1 triplet at 131.5ppm for the mixed ligand species. Attempts

at purification were not successful. Slow evaporation initially yields yellow crystals of the starting material (**16**). Further evaporation only results in a yellow and red powder.

Using  $^{195}\text{Pt}$ nmr the distribution of the product species was found to favor the mixed ligand species over the tetracyano species when only 1 eq. of KCN was used. In this case most of the starting material does not react but because of its low solubility its distribution in the final product is small. Nearly all of the remaining starting material will crash out when placed in the refrigerator.

Preparation of  $\text{K}_2\text{Pt}(\text{CN})_4(\text{OH})_2$  (**11A**) 0.5g of (**8A**) was dissolved in 20ml of water at  $25^\circ\text{C}$ . The solution was acidified to  $\text{pH}=1$  with 1M  $\text{H}_2\text{SO}_4$ . .7123g of oxone (1mole eq.) was added to the solution of (**8A**) and allowed to stir for 15minutes. The reaction mixture is then taken to dryness and redissolved in a 50/50 methanol/water mixture. The resulting mixture is then filtered over a fritted filter, washed with the 50/50 solvent mixture and then the filtrate is collected and the  $^{195}\text{Pt}$  nmr or  $^{13}\text{C}$  spectrum is recorded for verification. The  $^{195}\text{Pt}$  spectrum shows a peak at -1305ppm and the  $^{13}\text{C}$  nmr at 97ppm with  $^1J_{\text{Pt-C}}$  of 890Hz. Pure solutions of (**11A**) were never obtained. Drying out of the solution always yielded powdery white solids mixed with clear crystals, which were attributed to the  $\text{K}_2\text{SO}_4$ .

Preparation of the  $\text{BaPt}(\text{CN})_4(\text{OH})_2 \cdot 7\text{H}_2\text{O}$  (11B)

The synthesis used to obtain the crystal structure of  $\text{BaPt}(\text{CN})_4(\text{OH})_2 \cdot 7\text{H}_2\text{O}$  was done using hydrogen peroxide. .02g of (8A) was dissolved in 1ml of 30%  $\text{H}_2\text{O}_2$ . The reaction mixture was then allowed to sit at room temperature. Over the course of one year this reaction was redissolved 4 times in water and allowed to recrystallize. Large square yellow crystal deposited on the fourth attempt at recrystallization.

Partial Oxidation of  $\text{K}_2\text{Pt}(\text{CN})_4 \cdot 3\text{H}_2\text{O}$ 

Partial oxidation of (8A) was done with 30%  $\text{H}_2\text{O}_2$ . The quantities generally required for oxidation with a 30% solution of hydrogen peroxide are on the order of .1ml peroxide for a couple of grams of the TCP's. The procedure for partial oxidation is similar to that of Williams (19). .2g of (8A) was dissolved in 4ml of distilled water at 70°C. To this was added .1ml of 30%  $\text{H}_2\text{O}_2$ . The reaction was stirred for one hour at 70°C. When finished the reaction is allowed to cool slowly to room temperature. The reaction vessel was left open to the atmosphere for 24 hours while the reaction cooled slowly. After cooling the reaction is placed under desiccation and allowed to evaporate down to about 2.5ml. The fine copper colored needles of the form  $\text{K}_{1.75}\text{Pt}(\text{CN})_4 \cdot 1.5\text{H}_2\text{O}$  (6) were then collected on a fine porosity fritted filter and washed with cold water. The needles were stored over a saturated solution of  $\text{NH}_4\text{Cl}/\text{KNO}_3$  so the crystals would not dehydrate. 10% was the maximum yield I ever obtained using this synthesis. Williams reported a yield of 57%.

Partial Oxidation of  $\text{Cs}_2\text{Pt}(\text{CN})_4\cdot\text{H}_2\text{O}$  with  $\text{H}_2\text{O}_2$  The partial oxidation of compound **(8D)** was done using the synthesis described by Maffly et al. (22). 4.0g of compound **(8D)** was dissolved in 14.5ml of hot water (70°C). This was acidified to a pH of 1 using 1M  $\text{H}_2\text{SO}_4$ . To this was added .25ml of 30%  $\text{H}_2\text{O}_2$  and the reaction was allowed to stir while continuing the heating for one hour. The solution was then allowed to stand covered for 24 hours. The partially oxidized compound  $\text{Cs}_{1.75}\text{Pt}(\text{CN})_4\cdot 2\text{H}_2\text{O}$  **(18)** was obtained in about a 90% yield. The final product was not obtained in distinct brown needles but was rather a continuous lump of brown solids. If needles were required they could be obtained by filtering some of the reaction mixture when needles first begin to appear. Needle like crystals were also obtained by taking a 2ml aliquot of the reaction mixture and diluting it to 5ml. Slow evaporation of the solution results in copper needles of the form of **(18)**.

Partial Oxidation of  $\text{Cs}_2\text{Pt}(\text{CN})_4$  with  $\text{HNO}_3$

Partial oxidation of **(8D)**

was also accomplished by dissolving up 100mg of compound **(8D)** in 1.5ml of 2M  $\text{HNO}_3$  and letting the reaction concentrate down at room temperature in an open vessel. After 2 days the copper needles of the form of compound **(18)** begin to appear. This method of synthesis results in larger needles than using hydrogen peroxide but the yield is diminished to 53%.

Oxidation of  $K_2Pt(CN)_4$  using oxone™ Various amounts of oxone were used to oxidize the TCP's but the same procedure was followed for each oxone addition except for the variance in pH. For reactions of pH=1, 1M  $H_2SO_4$  was used and for pH=10, 1M KOH was used to adjust the pH. .1g of **(8A)** was dissolved in 2ml of appropriate aqueous medium. To this solution .08, .25, .5, .75 and 1.0 mole of oxone was added.

Oxidation of  $K_2Pt(CN)_4$  with  $HNO_3$  .05g of **(8A)** was dissolved up in 1ml of various  $HNO_3$  concentrations. The concentration of  $HNO_3$  was varies from 1M to 11M in 1M increments and one reaction was done with 15M  $HNO_3$ . Oxidation was also done by dissolving up **(8A)** in 2ml of 2M  $HNO_3$  heating at 70°C and stirring for one hour.

Oxidation of  $K_2Pt(CN)_4$  with  $Ce^{4+}$  .05g of **(8A)** was dissolved up in 2ml of solution containing various percentages of 1M  $H_2SO_4$  from 2 drops of acid to the entire 2ml of the reaction media being comprised of 1M  $H_2SO_4$ . To this was added 1,2 and 3 electron equivalents of  $Ce^{4+}$ .

Oxidation of  $BaPt(CN)_4 \cdot 4H_2O$  with  $H_2O_2$  Compound **(8B)** was oxidized with hydrogen peroxide using various amounts of oxidant as well as adjusting the pH of the solution between neutral and a pH of 1 with 1M  $HNO_3$ . The quantities of peroxide varied from 2 equivalents to the entire reaction medium consisting of

30% H<sub>2</sub>O<sub>2</sub>.

Preparation of [Pt(CNR)<sub>4</sub>][BF<sub>4</sub>]<sub>2</sub> (R = CH<sub>3</sub> (**19A**) and CH<sub>2</sub>CH<sub>3</sub> (**20A**)) The following preparation was taken from Treichel et al (46). 2.5g of (**8E**) was dissolved in 80ml of anhydrous CH<sub>2</sub>Cl<sub>2</sub>. To this was added an excess 6-fold of the appropriate trialkyloxoniumtetrafluoroborate. The reaction was refluxed for 4 hours. The reaction was then taken to dryness and redissolved in a minimal amount of acetonitrile. Upon addition of ethyl acetate a white solid consisting of the isocyanide crashes out of solution. The above macro-recrystallization is repeated to obtain a second batch of the platinum isocyanide. R=CH<sub>2</sub>CH<sub>3</sub> <sup>1</sup>Hnmr = t, 1.1ppm: q, with Pt satellites at 4.02ppm <sup>4</sup>J<sub>Pt-H</sub>=14Hz; <sup>195</sup>Ptnmr= multiplet of 9 at -4821ppm with <sup>2</sup>J<sub>Pt-N</sub>=80.7Hz. Percent yield = 81%. R=CH<sub>3</sub> <sup>1</sup>Hnmr = 1:4:1 singlet and doublet at 3.68ppm <sup>4</sup>J<sub>Pt-H</sub>=15.7Hz; <sup>195</sup>Ptnmr= multiplet of 9 at -4807ppm with <sup>2</sup>J<sub>Pt-N</sub>=85Hz.

Preparation of Pt(CNCH<sub>2</sub>CH<sub>3</sub>)<sub>2</sub>(CN)<sub>2</sub> (**21**) .45g of (**8E**) was dissolved up in 20ml of anhydrous CH<sub>2</sub>Cl<sub>2</sub>. To this was added 10ml of ethyl iodide and the reaction was allowed to reflux for three days. The reaction was then dried and brought back up into solution with a minimal amount of acetonitrile. The solution was filtered and the filtrate collected and placed in a desiccator containing ethyl acetate for crystallization by diffusion. Beginning after one-week small clear needle like crystal appeared. <sup>195</sup>Ptnmr = p, -4762ppm with <sup>2</sup>J<sub>Pt-N</sub>=82Hz.

$^1\text{Hnmr}$  = triplet of a quartet containing the platinum satellites with  $^4J_{\text{Pt-H}} = 13.8\text{Hz}$ ;

$^2J_{\text{N-H}} = 2.19\text{Hz}$ ;  $J_{\text{H-H}} = 7.18\text{Hz}$ .

Preparation of  $\text{Pt}(\text{CNCH}_3)_2(\text{CN})_2$  (22) .45g of (8E) was dissolved in 20ml of anhydrous  $\text{CH}_2\text{Cl}_2$ . To this was added 10ml of methyl iodide and the reaction was allowed to reflux for three days. The reaction was then dried and brought back up into solution with a minimal amount of acetonitrile. The solution was filtered and the filtrate collected and placed in a desiccator containing ethyl acetate for crystallization by diffusion. Like its ethyl isocyanide counterpart within about one week clear needle like crystals began to crash out of solution.

$^{195}\text{Pt}$ nmr = p, -4765ppm with  $^2J_{\text{Pt-N}} = 85.17\text{Hz}$ .  $^1\text{Hnmr}$  = 1:4:1 pattern each split into a triplet with  $^4J_{\text{Pt-H}} = 14.24\text{Hz}$ ;  $^2J_{\text{N-H}} = 2.63\text{Hz}$ .

Preparation of [t-n-butylN][Pt(CNCH<sub>3</sub>)(CN)<sub>3</sub>] (23) .45g of the (8E) is dissolved in 15ml of anhydrous  $\text{CH}_2\text{Cl}_2$ . To this is added 10ml of the appropriate alkyl iodide and the reaction is allowed to reflux for one day.  $^{195}\text{Pt}$  nmr analysis shows some formation of (22) the bis-isocyanide however the mono isocyanide (23) is about 70% of the crude products. The reaction is dried and brought up in a minimal amount of acetonitrile and placed in the desiccator containing ethyl acetate for recrystallization. Within one week clear plate like crystals will begin to crash out of the solution. For  $\text{R}=\text{CH}_3$ :  $^{195}\text{Pt}$ nmr = t, -4718ppm with  $^2J_{\text{Pt-N}} = 88\text{Hz}$ ,  $^1\text{Hnmr}$  = 1:4:1 pattern at 3.45ppm with  $^4J_{\text{Pt-H}} = 14.08\text{Hz}$ . For  $\text{R}=\text{CH}_2\text{CH}_3$ :

$^{195}\text{Pt}$ nmr = t,-4721ppm with  $^2J_{\text{Pt-N}} = 81\text{Hz}$ . Percent Yields are not accurate because of the t-n-butylammoniumiodide that also crashes out of solution. The solubilities of the monoisocyanide and the salt are very similar in the ethyl acetate.

Double Complex salt Preparation:  $[\text{Pt}(\text{CNR})_4][\text{Pt}(\text{CN})_4]$  (R =  $\text{CH}_3$  (24) and  $\text{CH}_2\text{CH}_3$  (5)) Equal molar amounts of (8A) and (19A) or (20A) are dissolved separately in dichloromethane. Upon mixing of the two solutions results in an immediate precipitate of the bright yellow salt which is then filtered on a fine porosity filter. Nearly 100% of the DS can be recovered.

Preparation of the Pt(I)  $[\text{Pt}(\text{CNC}_2\text{H}_5)_3][\text{BF}_4]_2$  (13) .1g of compound (20A) was dissolved in 4ml of dry acetonitrile. This was then placed in a desiccator containing ethyl acetate for diffusion. After 3 days long (3mm) square needle like crystals appeared. X-ray crystallography showed these to be that of the Pt(I) complex  $[\text{Pt}(\text{CNC}_2\text{H}_5)_3][\text{BF}_4]_2$ .  $^{195}\text{Pt}$ nmr = -4545ppm.

Preparation of the Continuous Variation Method (CV) Solutions Equal molar solutions of the (8A) and (20A) were prepared made in separate volumetric flasks. The  $[\text{Pt}(\text{CNC}_2\text{H}_5)_4]^{2+}$  and  $[\text{Pt}(\text{CN})_4]^{2-}$  solutions are then mixed in different ratios keeping the total platinum concentration the same in all the solutions (47).

### Instrumentation and Techniques

Nuclear Magnetic Resonance (NMR)  $^{195}\text{Pt}$  nmr spectroscopy was done on a Bruker WM250 spectrometer and a upgraded version, the dpx250 spectrometer. The WM250 was operated with a 10mm broadband probe operating at 53.518MHz relative to the 250MHz of  $^1\text{H}$ . Typical spectral width was 50,000Hz with collection of 1000-50,000scans, 4K data points, no delay between 30us pulses and a line broadening factor of 25-40Hz was typically used. The dpx250 was operated with a single frequency 10mm probe and a broadband 5mm probe. Typical spectral width was 125,000Hz with collection of 1000-50,000 scans, 4K data points, 100us delay and a line-broadening factor of 10-20Hz. Spectra obtained on isocyanides were done using proton decoupling. All  $^{195}\text{Pt}$  chemical shifts were measured relative to a external reference of  $.1\text{M Na}_2\text{Pt}(\text{Cl})_6 = 0\text{ppm}$ .

$^1\text{H}$  and  $^{13}\text{C}$  nmr spectra were recorded on a Bruker AC300 spectrometer and a drx300 spectrometer. The AC300 was equipped with a 5mm  $^1\text{H}/^{13}\text{C}$  dual probe using  $\text{D}_2\text{O}$  as the lock solvent. The drx300 contained a  $^1\text{H}/^{13}\text{C}/^{31}\text{P}/^{19}\text{F}$  quad probe.  $^{13}\text{C}$  spectra were referenced to an external spectrum of  $\text{K}^{13}\text{CN} = 165.71\text{ppm}$ .  $^1\text{H}$  nmr referenced to external TMS.

Ultraviolet and Visible Spectroscopy The UV-Visible measurements were obtained on a HP 8453 diode array spectrophotometer. The spectra were taken

in 1, .1 and .01 cm quartz cells with deionized and distilled water as the solvent. Constant temperature was maintained with a Neslab RTE-110 constant temperature bath. The HP spectrophotometer is fitted with a liquid circulation jacket around the cuvette cell holder. The temperature was maintained accurately within  $\pm 1^\circ\text{C}$ .

X-ray Crystallography X-ray crystallography was performed on a Siemens P4 four circle diffractometer. The source was Mo with  $\lambda = 0.71073\text{\AA}$ . Structures were solved by heavy atom methods and refined by full matrix least squares analysis with statistical weighting. Absorption corrections were made on all intensity data.

pH Measurements pH measurements were obtained on a Radiometer Copenhagen PHM 64 Research pH meter. Two point calibration (pH = 4 and 10) using J.T. Baker Buffer solutions. Temperatures were controlled within  $\pm 1^\circ\text{C}$ .

Equilibrium calculations The equilibrium calculations were carried out using the hyperquad suite of programs developed by Peter Gans (48).

Labeling of the Multinuclear Species The DS multinuclear species in equilibrium are labeled in this paper according to their stoichiometry and following IUPAC rules of cation first followed by the anion. For example the

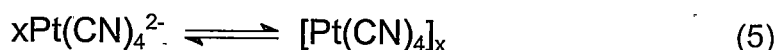
triplatinum species  $[\text{Pt}(\text{CNC}_2\text{H}_5)_4]_2[\text{Pt}(\text{CN})_4]$  is labeled 2,1. The multinuclear species are always labeled with commas but when the solution ratios are referred to the colon is used. Solution ratios also follow IUPAC rules for cationic solution followed by anionic ratio. For example the equal molar ratio of (20) and (8) would be referred to as the 1:1 solution.

Numbering of Compounds      Where numerous salts of a complex exist letters are used after the number for the various solid-state salts. The number without lettering is reserved for the platinum ion of the various salts in solution.

## RESULTS AND DISCUSSION

Solution Studies of the Pt(II) CyanoplatinatesUnoxidized Pt(II) cyanoplatinates

Solution Chemistry of Pt(CN)<sub>4</sub><sup>2-</sup> The solution chemistry of **(8)** is very minimal. Although Adamson has indicated (14,15) evidence of association of the Pt(CN)<sub>4</sub><sup>2-</sup> ions in solution by absorption and emission spectra, the <sup>195</sup>Pt nmr spectra indicate no such action in solution like that seen in equation 5.



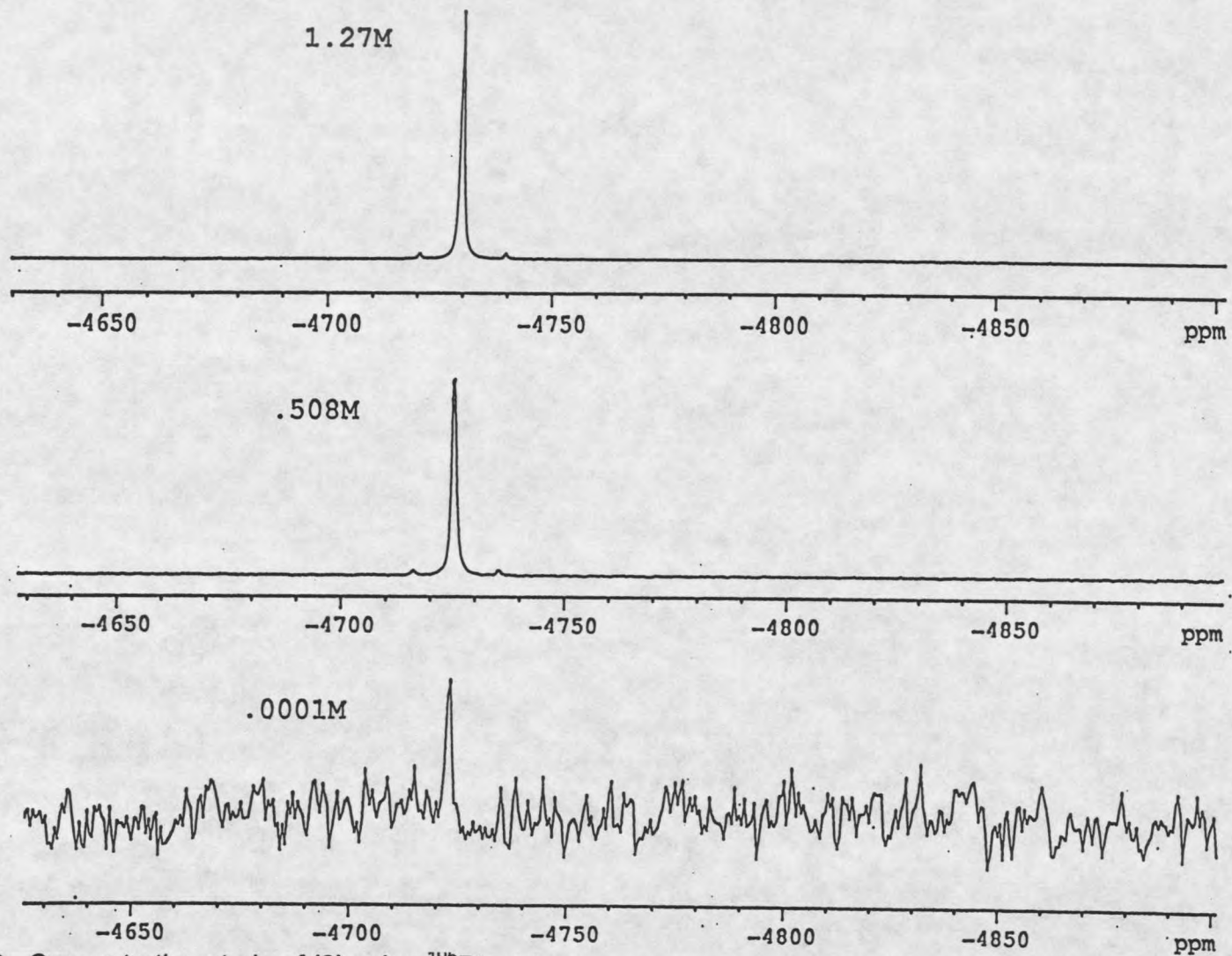
Adamson's absorption and emission data was obtained on the Ba<sup>2+</sup> salt of the TCP. The <sup>195</sup>Pt nmr data shown in figure 12 was obtained for both the potassium and the barium salt.

For both the potassium and the barium salts the <sup>195</sup>Pt nmr spectrum was measured over a large range of concentrations for **(8)**. The potassium salt concentration ranged from 1.0 x 10<sup>-3</sup>M solution of **(8)** to a saturated solution (about 1M). There was no significant change in the <sup>195</sup>Pt nmr chemical shift nor are there any new peaks visible in the spectrum. The chemical shift changed from -4722ppm at 1.0 X 10<sup>-3</sup>M to -4729ppm for the saturated solution. The <sup>195</sup>Pt

nmr on the barium salt was measured over the concentration range from  $9.5 \times 10^{-4} \text{M}$  to a saturated solution (about .1M). The chemical shift stayed constant at -4721ppm with no new peaks arising in the spectrum for the concentration range used. Figure 12 shows the  $^{195}\text{Pt}$  nmr spectra of the concentration study for the potassium salt of **(8)** in water.

The change of 7ppm in the platinum chemical shift seen for the potassium salt of **(8)** is insignificant with respect to Pt-Pt association. Chemical shift changes of 7ppm can be attributed to environmental factors such as temperature. Any dimer or higher oligomer formation will usually result in a change of the chemical shift upwards of 200ppm. Association in solution also results in broadening of the peak due to the higher molecular weight of an associated species compared with its monomeric form. In the event that non-symmetric multinuclear species form it will result in the 1:4:1 singlet/doublet pattern observed for platinum complexes. Association of **(8)** beyond a dinuclear species will form more than one platinum resonance. For example, in the case of a trimeric species of the formula  $[\text{Pt}(\text{CN})_4]_3^{6-}$  the two terminal platinum atoms are magnetically non-equivalent to the central platinum atom, because the central atom sees two bound platinum atoms while the terminal platinum atoms only see one platinum atom.

Adamsons work involving the absorption and emission techniques for the determination of the extent of  $\text{Pt}(\text{CN})_4^{2-}$  association used the barium salt because

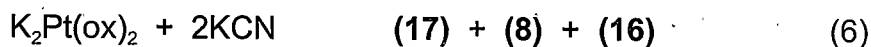


54

Figure 12. Concentration study of (8) using  $^{193}\text{Pt}$  nmr.

their qualitative indications suggested that  $K_x$  for association was bigger with the barium salt compared to the potassium salt. This also allowed them to work at lower concentrations enabling them to stay within the limits of the micrometer cell. Contrary to the concentration concerns when measuring the absorption spectrum,  $^{195}\text{Pt}$  nmr is accomplished easier at high concentrations and is the most straightforward approach for determining if oligomers or any metal associations are forming in solution because of the large chemical shifts that occur in the  $^{195}\text{Pt}$  spectrum. The higher concentrations favor both oligomer formation and their observation by nmr. The higher solubility of the **(8A)** salt versus the **(8B)** salt enables one to obtain solution concentrations about 10X higher by using **(8A)**.

Formation of the mixed complex  $\text{K}_2\text{Pt}(\text{CN})_2(\text{ox})$  (**17A**) The formation of the mixed cyano/oxalate species proceeds to equilibrium giving  $\text{Pt}(\text{ox})_2^{2-}$  (**16**)  $\ll$   $\text{Pt}(\text{CN})_4^{2-}$   $\ll$   $\text{Pt}(\text{CN})_2(\text{ox})^{2-}$  (**17**) when 2 equivalents of KCN are used according to equation 6.



The  $^{195}\text{Pt}$  nmr spectrum in figure 13a shows the 1:2:1 triplet for the mixed species (**17**) with labeled  $^{13}\text{CN}$ . In figure 13b the  $^{13}\text{C}$  nmr spectrum indicates the mixed

species **(17)** is present in solution in nearly twice the amount as **(8)**. The integration for **(8)** at 125ppm and **(17)** at 132ppm in figure 13b are nearly the same but **(8)** has twice as many carbons as **(17)**. When 1 equivalent of KCN is used the percentage of the **(17)** to **(8)** is increased but there is a greater amount of unreacted **(16)** that precipitates out of solution upon cooling the reaction, which has been present in all the solutions so far. Even with its much lower solubility complete removal of **(17)** from the solutions was not achieved. The solubility of **(17A)** and **(8A)** appear to be very similar making it difficult to obtain pure crystals of **(17A)**. A red solid results when the oxalate/cyanide solutions are dried, which is indicative of some stacking of **(8A)** and **(17A)** or the latter with itself. When isolated **(8A)** contains no red hydration phases. The  $\text{CaPt}(\text{ox})_2$  contains a red phase which quickly rearranges to a yellow phase when exposed to the atmosphere. The red color observed here with the mixed ligand reaction is stable to the atmosphere.

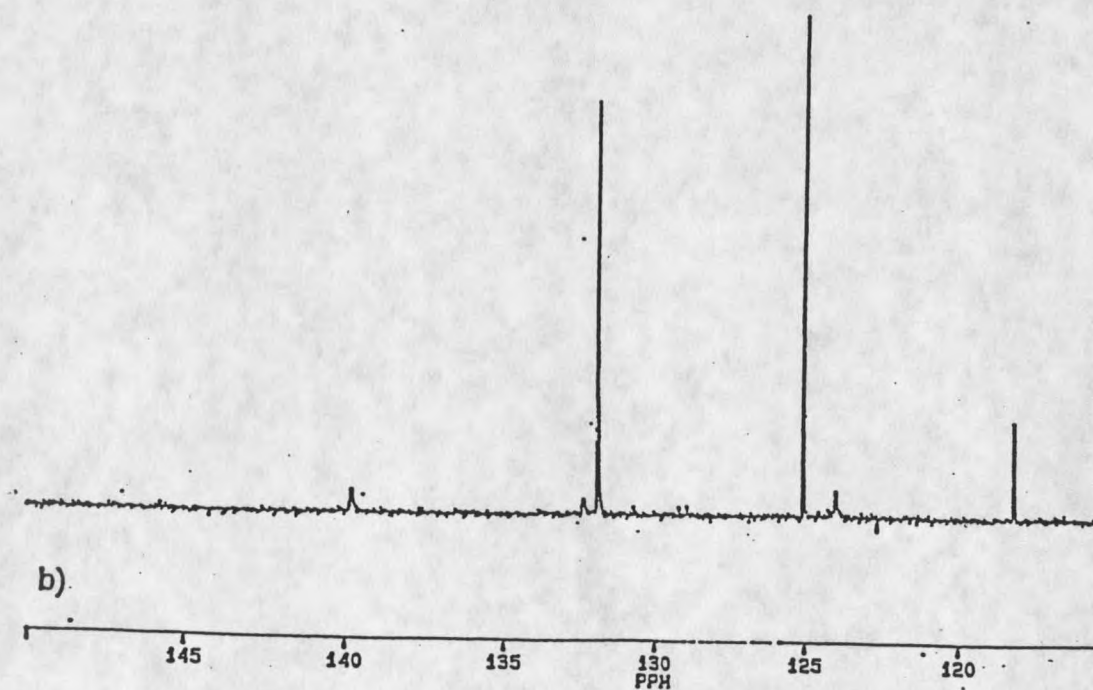
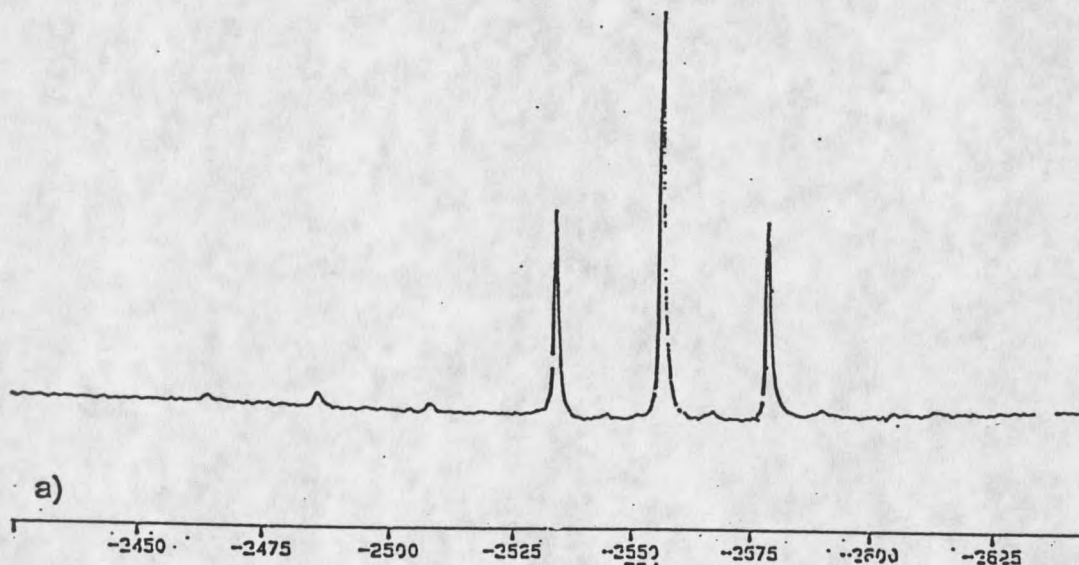
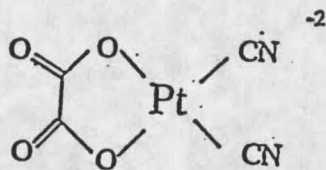
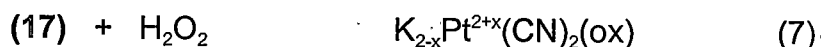


Figure 13 a)  $^{195}\text{Pt}$  nmr of (17) with  $^{13}\text{C}$  labeled CN ligands. b)  $^{13}\text{C}$  nmr of equation 6.

Solution Studies of the Oxidized Pt(II) Cyanoplatinates

Oxidation Reactions using Hydrogen Peroxide

Oxidation of  $K_2Pt(CN)_2(ox)^{2-}$  with  $H_2O_2$  PO of the solution that contains (17) was attempted to see if these solutions would give copper colored PO compounds. It is probable that (17) could form PO compounds according to equation 7



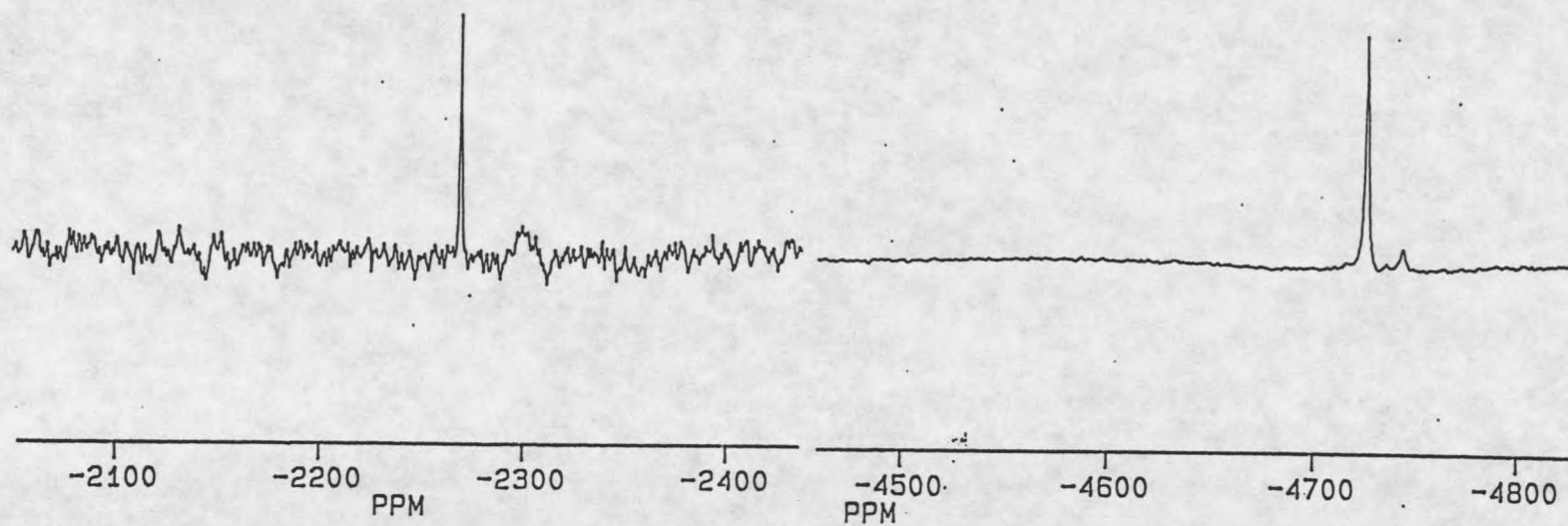
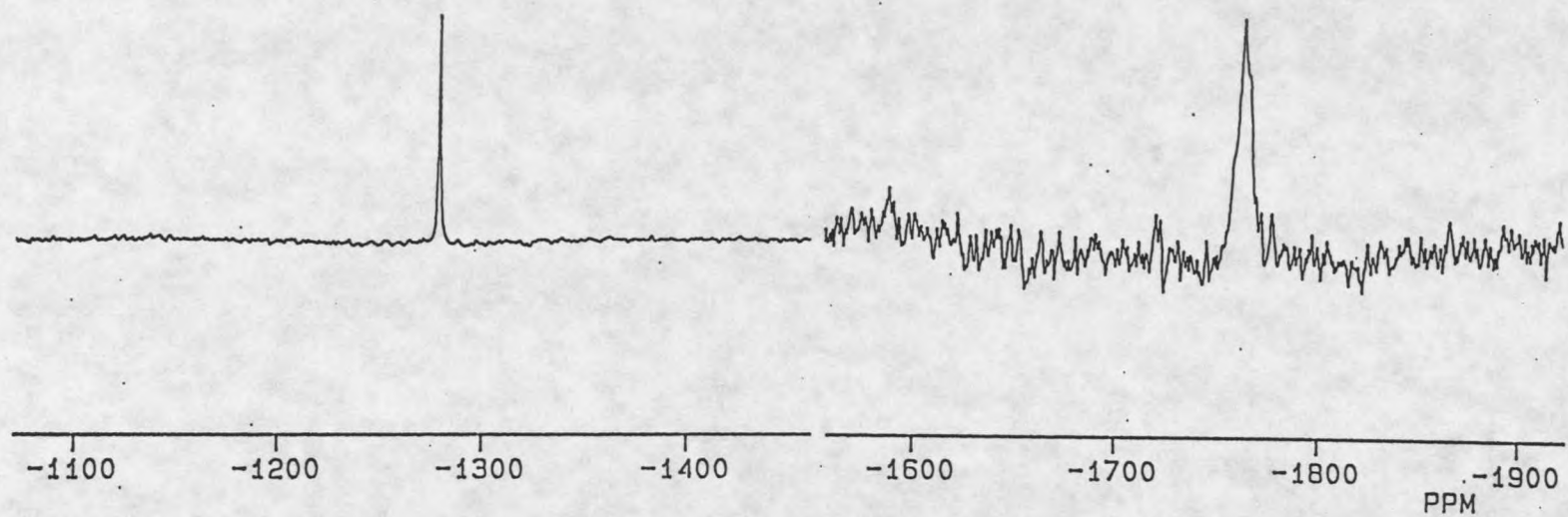
since both the tetra-cyano and the bis-oxalate platinum species do. Oxidation of the solution containing the mixed ligand platinum species (17) with hydrogen peroxide did not result in any formation of PO compounds. One problem is the fact that no pure (17A) has been isolated. The reactants in this reaction consists of all three of the platinum species (16), (17), and (8) all in equilibrium with one another.

The PO was done using the same method as that for the POTCP's and the POBOP's where the appropriate amount of  $H_2O_2$  was added and the reaction was refluxed under heat. The initial (17) was made with labeled  $^{13}CN$ . After heating at  $70^\circ C$  for one hour the  $^{195}Pt$  nmr indicates none of (17) is left after oxidation; however, a new peak that gives a 1:2:1 triplet arises at -4425ppm with  $^1J_{Pt-C}$  of 1028Hz. This new peak is not in a region where the resonances for

complexes with oxygen ligands bound to the platinum center are observed. This indicates that this species is bound to only two cyanides like the starting material  $\text{Pt}(\text{CN})_2(\text{ox})^{2-}$  but contains no oxygen bound ligands. The nmr interpretation indicates a complex containing a platinum-platinum bond each with two terminal cyanides,  $\text{Pt}_2(\text{CN})_4$ . Consequently a complex of this formula would be highly unsaturated and probably very unstable. The characterization of this resonance is left to much speculation.

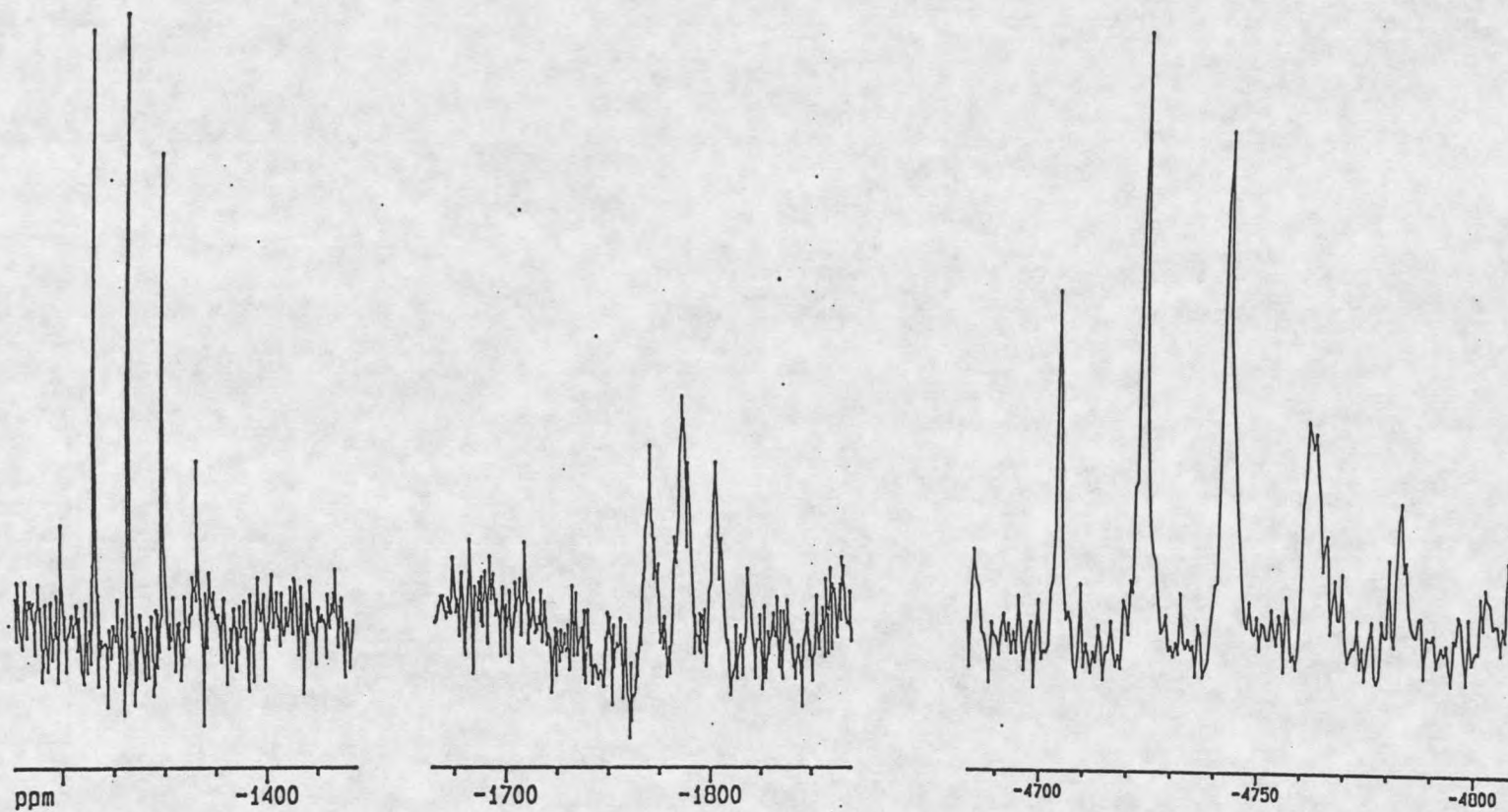
The  $^{195}\text{Pt}$  nmr spectrum also indicates that **(8)** has diminished only slightly in the oxidation reaction. Some of **(8)** has been oxidized to **(11)** and the small amount of **(16)** initially in the reaction solution has all been oxidized to the  $\text{Pt}(\text{ox})_2(\text{OH})_2^{2-}$ . The Pt(IV) oxalate and cyanide species reside at +2875ppm and -1280ppm respectively in the  $^{195}\text{Pt}$  nmr spectrum.

Oxidation of  $\text{K}_2\text{Pt}(\text{CN})_4$  with  $\text{H}_2\text{O}_2$  When the  $^{195}\text{Pt}$  nmr is observed of the solutions for equation 3 before the crystallization of the CD-POTCP there are five different Pt species present in the reaction solution. Figure 14 shows a scaled view of the different peaks present in the  $^{195}\text{Pt}$  nmr spectrum. All the species in this reaction are observed over a 3500ppm chemical shift range. Most peaks in the  $^{195}\text{Pt}$  nmr spectrum can be fully characterized; however, there is some uncertainty with one of the peaks that result in the reaction solutions forming **(6)**. One problem initially encountered when trying to identify all the peaks is that they all result in singlets. For this reason the labeled  $^{13}\text{CN}$  was utilized



69

Figure 14.  $^{195}\text{Pt}$  nmr for equation 3 at solution concentrations near the solubility limit of crystallization of (6).



61

Figure 15.  $^{195}\text{Pt}$  nmr for equation 3 near the solubility limit of crystallization of (6) with labeled  $^{13}\text{C}$ N.

in the oxidation reactions to observe the multiplets. The  $^{13}\text{C}$  labeled cyanide bound to the platinum gave rise to pentets in the  $^{195}\text{Pt}$  nmr spectrum indicating that all species have four cyanides bound to a platinum atom (Figure 15). This did not help with the unidentified species but it did give more certainty to our initial characterization that all species are bound to four cyanide ligands. Figure 15 shows three separate portions of the  $^{195}\text{Pt}$  nmr spectrum. This is done because of the large chemical shift exhibited by the platinum atom. It is not possible to observe the entire chemical shift region within one spectral window. Different windows each comprising a chemical shift range of about 1500ppm are observed by moving the frequency that the nmr pulse is done at.

The four peaks that are characterized occur at -1280ppm, -1776ppm, -4724ppm and -4744ppm while the fifth uncharacterized peak occurs at -2300ppm. The peak at -4724ppm is the starting material (**8**). The peak at -1280ppm is due to the diaquotetracyanoplatinate(IV) (**11**) which was characterized by x-ray crystallography and will be described in a further section. Initially the characterization of the -1280 peak was done by comparison to other platinum oxidations where two oxygen bound ligands are added to a Pt(II) complex. The example used for initial characterization of this peak was the downfield shift on going from (**16**) to  $\text{Pt}(\text{ox})_2(\text{OH})_2^{2-}$ . The platinum resonance shifts 3400ppm downfield (**16**) to  $\text{Pt}(\text{ox})_2(\text{OH})_2^{2-}$  and while going from (**8**) to (**11**) the resonance shifts downfield 3420ppm. The chemical shift of (**11**) is also near the chemical shift of a complex studied by Appleton (49). The complex

$\text{Pt}(\text{Me})_2(\text{CN})_2(\text{OH})_2$  resides at -1383ppm and only differs from **(11)** by the two methyl ligands. Methyl and cyanide ligands have a similar nmr environment around platinum. This method of comparison for predicting where  $^{195}\text{Pt}$  chemical shifts will occur is described in more detail in the  $^{195}\text{Pt}$  nmr section. The nmr characterization was further validated after single crystals of **(11)** were obtained and structured. The pure crystals of **(11)** were dissolved up in  $\text{D}_2\text{O}/\text{H}_2\text{O}$  and its  $^{195}\text{Pt}$  nmr resonance was observed at -1479ppm with a pH=5 and upon acidification to pH=2 the chemical shift went to -1282ppm. The pH was then brought back up to 5, which restored the resonance to -1479ppm region indicating that the change in chemical shift is reversible with protonation/deprotonation of the coordinated water ligands.

The broad resonance at -1776ppm is characterized as the Pt(III) dinuclear species  $\text{Pt}(\text{CN})_8(\text{H}_2\text{O})^{2-}$  **(25)**. This peak is broad and lies in the region that is expected for a dinuclear Pt(III) species with four cyanide ligands on each platinum with water ligands capping the dimer on each end. This chemical shift was also compared to other Pt(III) complexes reported by Appleton (50). Only when water caps the Pt(III) dimer would there be a platinum chemical shift this far downfield due to the oxygen/platinum interaction. Without water on the Pt(III) the chemical shift would be expected around -2300ppm. Therefore, the peak present around -2300ppm is believed to be a Pt(III) dinuclear species not capped with water  $\text{Pt}_2(\text{CN})_8^{2-}$  **(26)**. The broadness of this resonance is also indicative of a dinuclear complex.

The peak arising at -4744ppm was initially very peculiar because of where the chemical shift lies. It is only 20ppm upfield from the Pt(II) starting material. With only a 20ppm difference between these two peaks their structures should be very similar yet the upfield peak is broadened considerably indicating possibly some association with another Pt(II) center. The peak at -4744ppm is the result of the  $\text{Pt}_2(\text{CN})_6^{2-}$  (**27**). Levy's elemental analysis found the yellow solid from these reactions to have the formula  $\text{Pt}(\text{CN})_3$  (22,51,52). This is possible with the loss of CN ligands in acidic media. It was not absolutely evident if the peak at -4744ppm gave a pentet with  $^{13}\text{C}$  because of the overlap with (**8**) at -4724ppm, but is estimated as a pentet. The  $^1J_{\text{Pt-C}}$  in this region is about 1030Hz for these two complexes, which is identical with that of (**8**). Figure 16 shows the  $^{195}\text{Pt}$  nmr chemical shifts of the four characterized species.

Initially this work had peaks occurring at -2600ppm and -1981ppm but were attributed to Cl<sup>-</sup> impurities. Although Pt(IV) species tend to be inert to substitution, the chlorine impurities in solution with the Pt(II) resulted in their addition on the Pt(IV) upon oxidation. The substitution products were that of the dichloro  $\text{Pt}(\text{CN})_4\text{Cl}_2^{2-}$  and  $\text{Pt}(\text{CN})_4(\text{OH})\text{Cl}^{2-}$  species. These were easily avoided by a more thorough purification of the Pt(II) starting material. To be certain that the resonances were due to the dichloro and aquo-monochloro compounds and not coincidental resonance's of anything else, 1 and 2 equivalents of KCl were added to the reaction mixture. This addition was done before adding the oxidant so it would compete with the addition of water on the Pt(IV). This resulted in

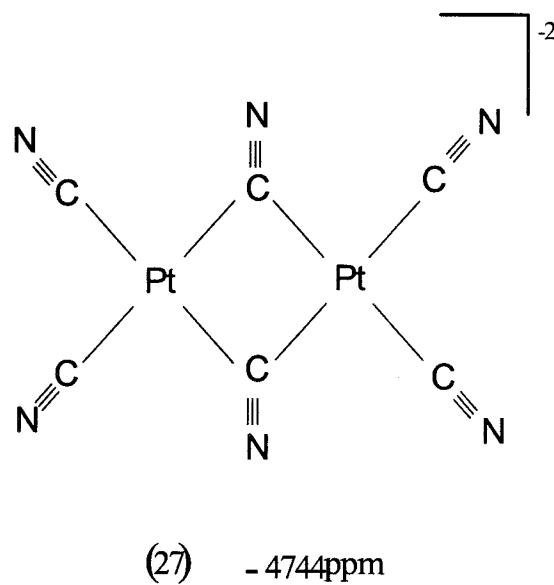
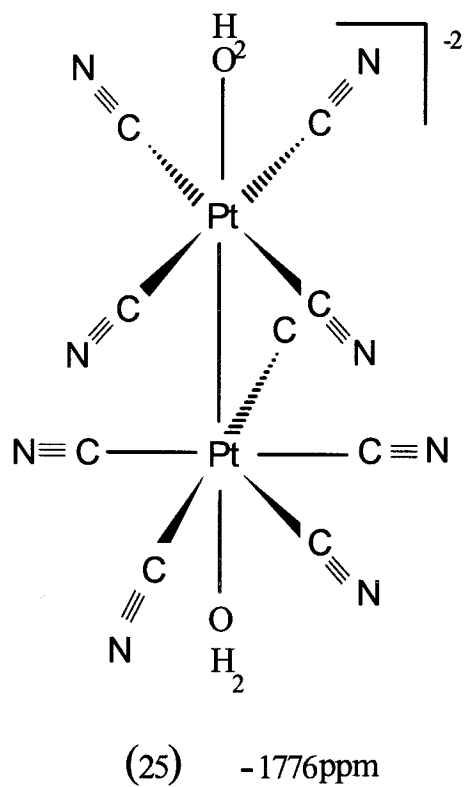
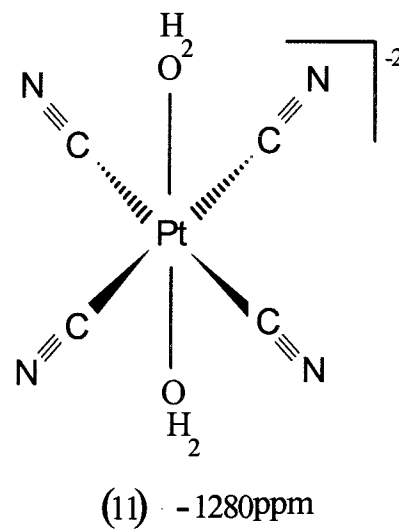
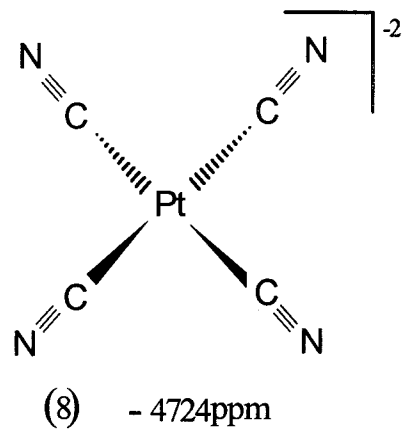


Figure 16. Representations of (8), (11), (25) and (27).

large resonances with good S/N at -1981ppm and -2600ppm respectively for 1 and 2 equivalents of KCl proving these two peaks were due to impurities of Cl in the reactions.

Oxidation of BaPt(CN)<sub>4</sub> with H<sub>2</sub>O<sub>2</sub> .When **(8B)** is oxidized with 30% H<sub>2</sub>O<sub>2</sub> small purple crystals result after the reaction mixture is allowed to concentrate down or ethanol is diffused into the reaction mixture inside of a desiccator. The purple colored solids were only observed when the Pt(II) was dissolved up directly in the 30% H<sub>2</sub>O<sub>2</sub>. If the reaction was done by first dissolving **(8B)** in water then adding a small amount of 30% H<sub>2</sub>O<sub>2</sub> the result was yellow crystals of starting material. The purple crystal would form in reaction mixtures in both a neutral pH (no pH adjustment) and a pH=1 adjusted with 1M HNO<sub>3</sub>. POTCP salts have not been observed for the barium salt in past studies. It was initially hoped that the purple solids were that of a dimeric Pt(III) like that reported by Levy and Piccinin (22,33). When the solid is dissolved and the <sup>195</sup>Pt nmr is observed there is no resonance in the spectrum except the -4724ppm for **(8)**. If solutions were allowed to sit around idle for at least one week the <sup>195</sup>Pt nmr showed the -1776ppm peak from **(25)**. This indicates there are other, probably paramagnetic, species in solution that give **(25)** after the solution became concentrated.

The purple crystals that have been formed so far tend to degrade fairly rapidly after formation; therefore, a complete crystal structure has not been

achieved. A small data set was collected on one crystal giving enough information to discover that two Pt atoms are 3.22Å apart in the crystal. The insufficient x-ray data set indicated the unit cell was very close to that of **(8B)**. With this evidence the purple color in the solid is most likely the result of impurities and not the result of a Pt(III) dimeric complex. When **(8B)** is added to a small amount of 30% H<sub>2</sub>O<sub>2</sub> so as not to let the solid go into solution, the yellow crystals will turn purple after sitting in the oxidant for a few minutes. This appears to be the same action that caused the purple colored solids to crash out of solution. The solutions giving recrystallized purple solids appear to initially give the yellow **(8B)** and then turn purple by surface action of the hydrogen peroxide.

<sup>195</sup>Pt nmr of the solutions made from both the yellow and purple solids gave -4724ppm peak. Observing no peaks in the spectrum except for the Pt(II) indicates that if the purple solids that are seen in the reaction are the result of an oxidized species it must be paramagnetic.

Oxidation of Cs<sub>2</sub>Pt(CN)<sub>4</sub> with H<sub>2</sub>O<sub>2</sub> Various amounts of 30% H<sub>2</sub>O<sub>2</sub> were used to oxidize **(8D)**. Under acidic conditions **(8D)** was subjected to small amounts of hydrogen peroxide and heat, to afford copper needles of **(18)** described in the experimental section.

When **(8D)** was exposed to an excess of 30% H<sub>2</sub>O<sub>2</sub> at room temperature yellow crystals came out of solution after a few days of sitting in a desiccator

containing ethanol. Under these conditions the  $^{195}\text{Pt}$  nmr indicates only **(8)** and **(11)** are present in the reaction solution. The yellow crystals were structured and determined that they contained peroxide in the hydration sphere giving the formula  $\text{CsPt}(\text{CN})_4 \cdot 2\text{H}_2\text{O}_2$ . The complete refinement of the diperoxide-hydrate was not obtained due to poor crystalline quality. The usual crystals for **(8D)** are clear and are singly hydrated.

The  $^{195}\text{Pt}$  nmr spectra of the solutions leading up to **(18)** indicates mostly Pt(II) starting material, a small amount of the Pt(IV) species **(11)** and another small peak at -2398ppm that is unidentified but is in the region of a Pt(III) similar to **(26)**. These solutions do not contain the two peaks at -1776ppm and -2300ppm like the reaction solutions for **(6)**. However, if **(8D)** is heated in an excess of 30%  $\text{H}_2\text{O}_2$  then formation of **(11)** constitutes about 90% of the  $^{195}\text{Pt}$  nmr detectable reaction products. There are other peaks in these spectra that are the result of multi-nuclear species in the solution. Broad peaks arise at -1370ppm, -1750ppm, and at -1780ppm all with widths at half height over 300Hz. There is also a small peak at -4742ppm that is the result of **(27)** like that seen in the formation of **(6)**. The peaks at -1370 and -1750ppm are unknown but are multinuclear because of their large width.

When **(18)** is dissolved it gives only the initial starting material **(8)** in the  $^{195}\text{Pt}$  nmr spectrum. **(18)** was dissolved in basic, neutral and acidic media giving only the -4724ppm peak in the  $^{195}\text{Pt}$  nmr spectrum. The  $^{195}\text{Pt}$  nmr gives the -4724ppm with a good S/N ration in only 4000 scans. The solubility of **(18)** is

sufficient enough to observe other species than the -4724ppm if any are present and nmr detectable.

It is considerably interesting why the different counter-cations for the TCP's result in different  $^{195}\text{Pt}$  nmr spectra when oxidized with 30%  $\text{H}_2\text{O}_2$ . The most likely reason is that the different counter-cations cause the solubilities of the salts to be different. The cations with lower solubility's result in a greater degree of aggregation in solution. For example the potassium salt, the most soluble of all the counter ions, gives the -1776ppm peak and in the case of the cesium salt there is a shifting of this broad resonance as well as new resonance's in the region of the Pt(IV) at -1300ppm. These new peaks are attributed to additional metal-metal association because of their broadness.

#### Oxidation Using the Monopersulfate Compound Oxone

Oxidation of  $\text{K}_2\text{Pt}(\text{CN})_4$  with Oxone<sup>TM</sup> The monopersulfate oxidant oxone was used to study the oxidation solutions because it resulted in reactions that proceeded in a more stoichiometric manner than when  $\text{H}_2\text{O}_2$  is the oxidant but it gives nearly identical reaction solutions with the appropriate amounts of oxidant. Although oxone oxidations proved to occur more stoichiometrically than the other oxidants these were not entirely stoichiometric either.  $^{195}\text{Pt}$  nmr shows the reaction solutions are similar when the POTCP result from solutions using different oxidants. Reactions proceeding in a non-stoichiometric fashion have

been one of the biggest difficulties in fully understanding which complexes in solution are responsible for formation of the POTCP. Also no reactions have given the opportunity to isolate individual species of the partial oxidation reactions. It was of significant interest to find conditions to isolate the Pt(III) complexes and study their role in POTCP formation. There have been reports that are suggestive for the presence of Pt(III) cyanides but none of these reports give absolute characterization of a Pt(III) species whether it is mononuclear or dinuclear (22,33).

The formation of paramagnetic species is chiefly responsible for the non-stoichiometry of the reactions. There is considerable evidence that there are paramagnetic species present in solution which are not observed in the  $^{195}\text{Pt}$  nmr spectrum. One piece of evidence is that the signal to noise ratio decreases considerably in the  $^{195}\text{Pt}$  nmr of oxidized solutions of the TCP's indicating other species are present besides the diamagnetic ones that are observed. Even using a 1000 fold excess of 30%  $\text{H}_2\text{O}_2$  does not give complete oxidation of (8) to (11).

$^{195}\text{Pt}$  nmr and  $^{13}\text{C}$  nmr of oxidized solutions were used to observe the different species present in solution depending on the electron equivalents of oxidant used. Solutions with less than .5 electron equivalent of oxidant result in solutions that resemble those when hydrogen peroxide is used as the oxidant in the formation of the POTCP. Using less than 1 electron equivalent of oxone gives the greatest amount of species present in solution. Less than 1 electron

equivalent of oxidant results in a total of 7 species in acidic media and 6 in neutral media. The seven resonance's that are observed in acidic media is two more resonance's than are seen in the peroxide oxidations done under acidic conditions. All the  $^{195}\text{Pt}$  nmr signals are the same as when peroxide is the oxidant except for the two additional peaks at -4764ppm and +1011ppm. The -4764ppm region would indicate a Pt(II) with four cyanides. The -4764ppm resonance results from further association of **(27)** to give the  $\text{Pt}_3(\text{CN})_8^{2-}$  **(32)**. The other new resonance is a tetraquo species that is present in small concentrations in these reactions. Figure 17 shows the  $^{13}\text{C}$  nmr of the oxone oxidation of **(8)** with .3 electron equivalents of oxone. The further addition of more than one electron equivalent of oxone results in the disappearance of the resonance at -2300ppm.

More than 1.5 equivalents results in the -1280ppm peak being the only peak present in the initial nmr analysis. When these solutions sit around for at least a week the -1776ppm peak begins to appear in the spectrum. These reactions obviously contain other species besides **(11)**. To form the dinuclear Pt(III) without any Pt(II) present would only come about from association of Pt(III) monomers. When Pt(II) is present it can combine with the Pt(IV) to give the Pt(III) dimer. This is the case in the 1 electron equivalent reactions. The one electron equivalent reactions give the greatest amount of dinuclear **(25)** after sitting around for one week. Little of **(25)** results from a Pt(III) monomer because the  $^{195}\text{Pt}$  nmr indicates from the S/N that **(11)** and **(8)** constitute the majority of

the reaction species.

The oxidation reactions done with oxone are pH dependent. All the other oxidants used in these studies only give oxidized products in acidic media. Oxone will give products in neutral and basic media but the solution species vary with the pH. The lower the pH for the reaction solution, the more products that are observed in the  $^{195}\text{Pt}$  nmr spectrum. Oxidation's done in acidic media initially give seven different species in solution. Neutral reaction solutions give five species in solution. Reactions in basic media result only in the formation of (11) at -1300ppm. No matter how large or small the amount of oxidant that is added to the reaction (11) is the only product observed under basic conditions. Using up to four electron equivalents of oxone still only result in about 30% of the species present being that of the Pt(IV) at a pH=10.

The neutral and acidic oxidation solutions both resulted in a new peak at +1013ppm that is not observed in the peroxide oxidations. This peak occurs as a 1:2:1 triplet in the  $^{195}\text{Pt}$  spectrum at +1013ppm when labeled  $^{13}\text{CN}$  is used and is attributed to the Pt(IV) species  $\text{Pt}(\text{OH})_4(\text{CN})_2^{2-}$ . This species is estimated to be less than 1-2% of the reaction products by nmr and is surely not involved in the formation of the POTCP. It is not believed that neutral solutions result in appreciable amounts of HCN being released from the reaction solutions but some loss of CN in the solution is apparent or  $\text{Pt}(\text{OH})_4(\text{CN})_2^{2-}$  could not form. Like the  $\text{H}_2\text{O}_2$  reaction loss of CN in the reaction solutions result in the formation of (27). Only oxone reactions give further association of (27) to (32).

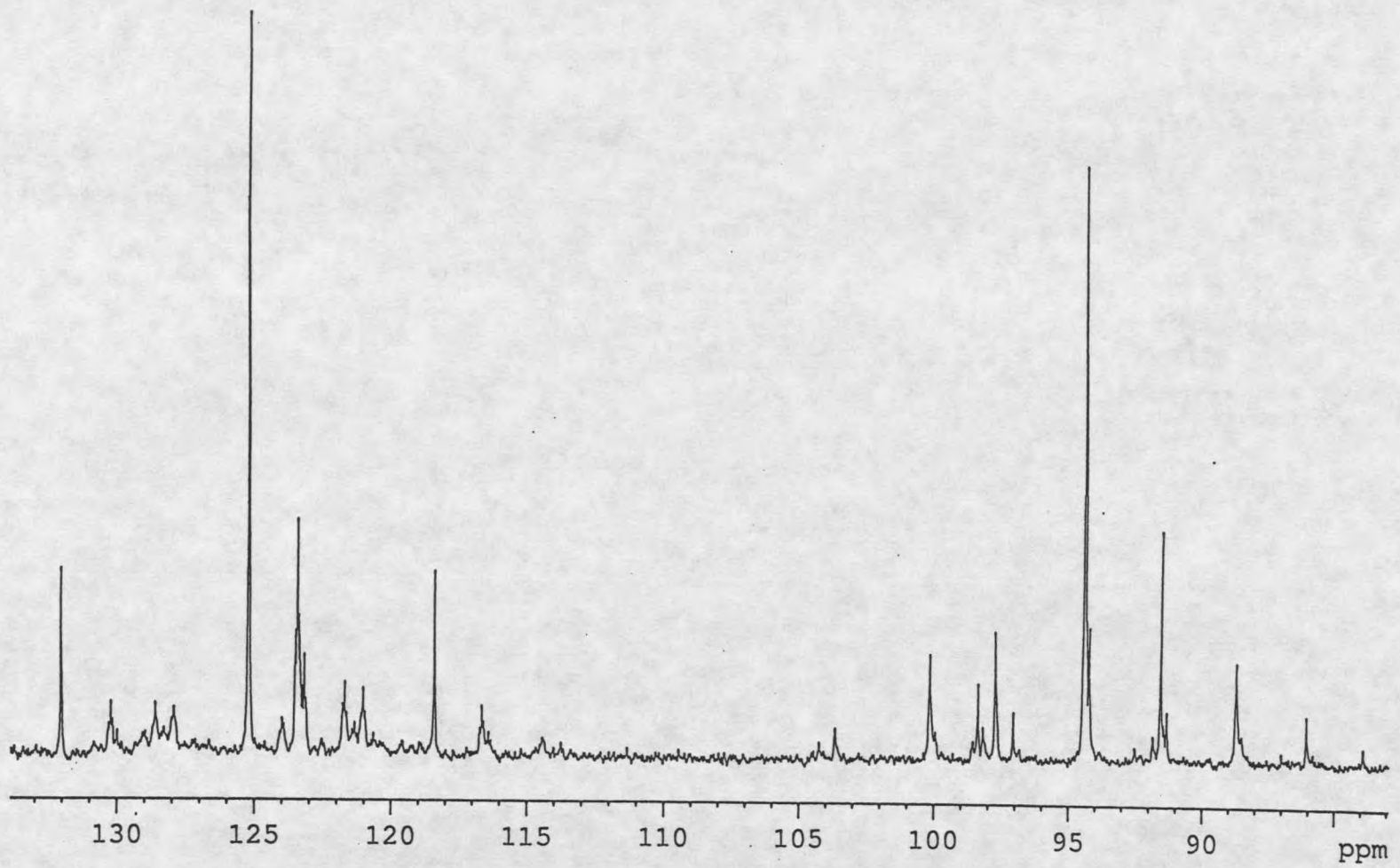


Figure 17.  $^{13}\text{C}$  nmr of the oxone oxidation using labeled  $^{13}\text{C}\text{N}$ .

There is very little difference in the reaction species when the reaction is done under neutral or acidic conditions. The only difference between acidic and neutral reactions are when and how much of each species forms. For example when reactions are acidic and less than .5 electron equivalent of oxidant is used the dimeric Pt(III) resulting in the -1776ppm peak is present in the initial  $^{195}\text{Pt}$  nmr analysis. In basic media the -1776ppm peak appears only after the solutions have sat around idle for at least two days. In both solutions the -1776ppm peak becomes the dominant species in the spectrum after sitting idle for periods longer than two weeks.

The CD-POTCP was obtained using oxone as the oxidant but the crystalline quality and yields are worse than those obtained when using hydrogen peroxide. When a .24 electron equivalent of oxone is used and the reaction is acidified with 1M  $\text{HNO}_3$  to a pH of 1 the copper colored crystalline needles of **(6)** were produced. The copper needles were obtained in about a 10% yield. The poor yield obtained for the POTCP here is most likely due to the large amounts of sulfates present in the solution that are introduced from the oxone. Brown/copper colored solids deposit out of solution immediately if the concentration of the reaction is high enough (about .05M) with respect to the Pt(II). The solids produced under these conditions are not crystalline like those produced at lower concentrations or when  $\text{H}_2\text{O}_2$  is the oxidant. The  $^{195}\text{Pt}$  nmr spectrum obtained on the reactions with less than .3 electron equivalents are identical to those when  $\text{H}_2\text{O}_2$  is used to form the CD-POTCP.

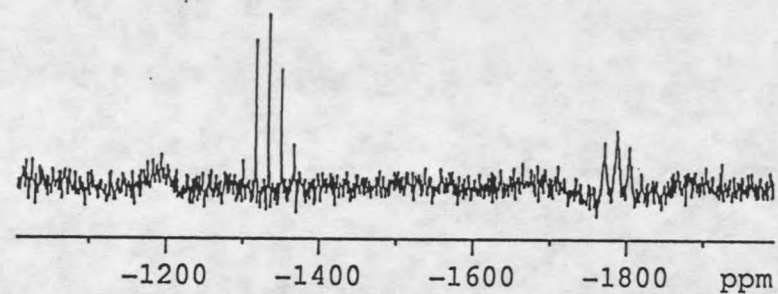
When the electron equivalent of oxone becomes greater than .5 no copper needles were ever produced. The  $^{195}\text{Pt}$  nmr indicates that all the reaction species are present as when copper needles form but they are in different proportions. Most notably is the greater quantities of the Pt(IV).

With greater than .5 electron equivalents of oxone the -1776 ppm peak is not present in the spectrum immediately like when using peroxide but it grows in slowly, starting to appear after a few days of the solution sitting idle at room temperature. This suggests that **(25)** is at least indirectly involved in the formation of **(6)**. The oxone solutions did not afford conditions where any of the solutions species could be isolated. Isolation of the species was desired for further proof of our nmr characterizations of the oxidized species.

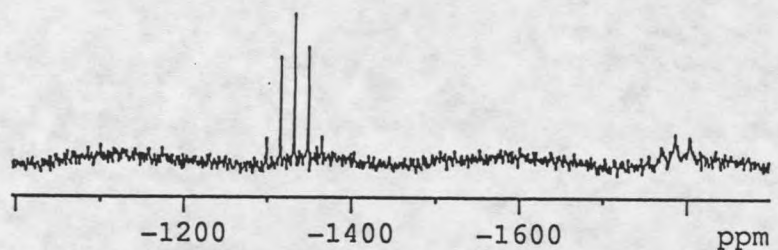
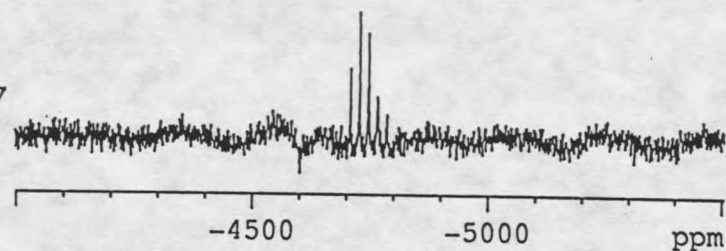
There was little success in the isolation of the solution species that were characterized by nmr, because of this further experiments were done to provide additional evidence of our nmr characterizations. Figure 18 is a  $^{195}\text{Pt}$  nmr study of the solution species over time of the oxone oxidation of **(8)**. It can be seen how **(25)** at -1776ppm becomes more prominent with time and the S/N ratio of **(8)** and **(11)** decrease at -1280ppm and -4724ppm respectively. The spectra seen in figure 18 were done over a period of seven days. It can be seen that after seven days **(25)** becomes a significant portion of the species in the spectrum. With these  $^{13}\text{C}$ N labeled solutions **(27)** is seen when the multiplet for **(8)** becomes unsymmetrical. The  $^{195}\text{Pt}$  nmr peaks for **(27)** also appear to only be present when the -1776ppm peak is present. The symmetry of the pentet at

-1280ppm was also lost in the oxidation solutions but there was no evidence for other species in the region overlapping with **(11)**. Similarly the pentet at -4724ppm due to **(8)** loses its symmetry upon oxidation but this is due to the skewing of the pentet from the overlap with the resonances from **(27)** and **(32)**.

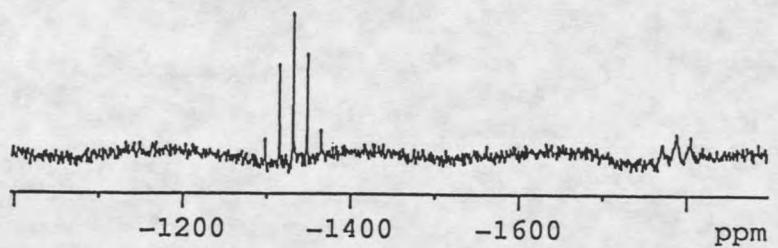
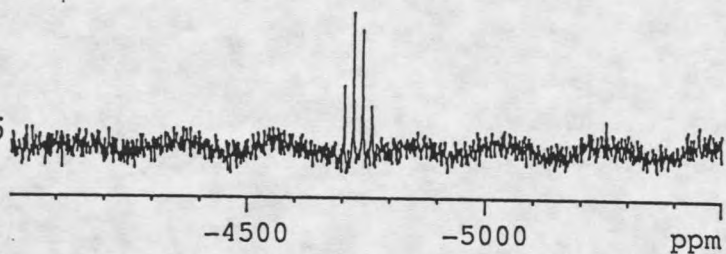
Most of the research with  $^{13}\text{C}$  labeled cyanide was done with the oxone oxidations. The  $^{13}\text{C}$  spectra were done to see if the couplings would also give some insight into the solution species. It is possible to correlate some of the shifts of the  $^{195}\text{Pt}$  nmr spectrum with those in the  $^{13}\text{C}$  spectrum. The  $^{13}\text{C}$  spectra for the oxone oxidation with .25 electron equivalents show the -4744ppm and -4764ppm  $^{195}\text{Pt}$  peak at 123ppm and 121.5ppm respectively. Both of these peaks give complex spectra (Figure 17). The central peak contains 1:4:1 satellites, which are also split into triplets. **(32)** gives a triplet of doublets of a quartet but it does not contain a central peak which should occur with any platinum carbon coupling because there is always some percentage of the species where the CN is bonded to only platinum spin=0 atoms. A structural representation of **(27)** is shown in figure 16 and **(32)** is represented in figure 19 below. The complex spectra of **(27)** and **(32)** can only be assigned using simulated programs, which was not done in these studies.



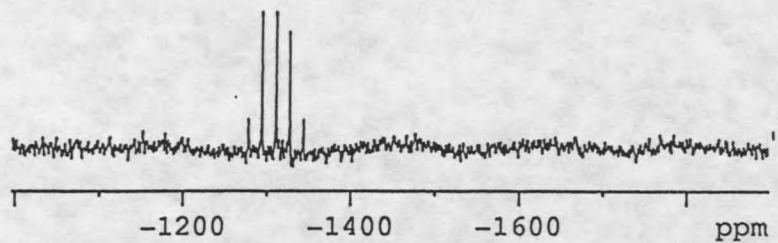
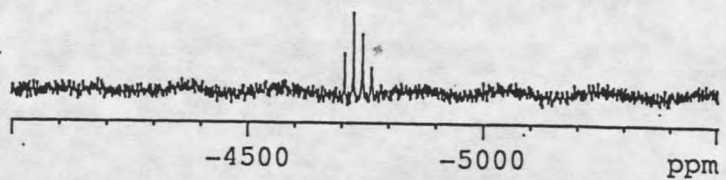
Day 7



Day 5



Day 4



Day 1

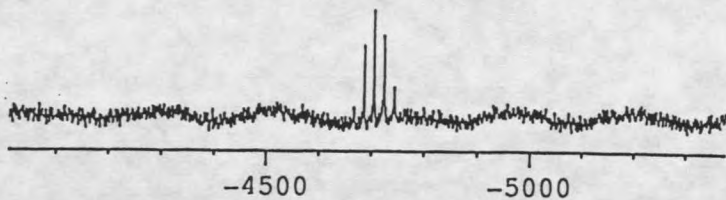
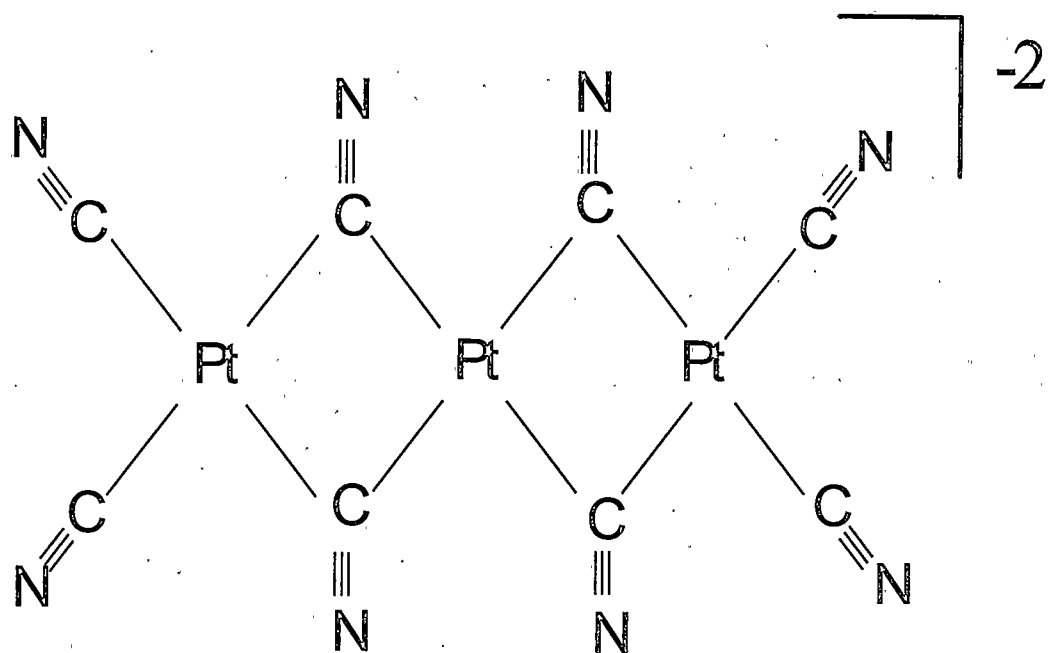


Figure 18.  $^{195}\text{Pt}$  nmr of the .3 electron equivalent oxone oxidation of (8) over a seven day period.

The unlabeled reactions are nearly impossible to obtain a  $^{13}\text{C}$  spectra because the concentration of the reaction can not be increased above .05M with respect to the Pt(II) starting material. If the reaction is done at too high of a concentration the solution turns to a thick white cloudy substance. An unlabeled spectrum was done and with 33,000 scans only a few of the major peaks can be seen and no coupling is observable with the S/N obtained. The peaks for **(27)** and **(32)** are just becoming large enough to be evident in the noise (Figure 20). Also suggestive of the structure for **(27)** and **(32)** is the  $^{195}\text{Pt}$  nmr signal at -4744ppm when  $^{15}\text{CN}$  is used. The peak is broad with an unresolvable multiplet of many. Because peak widths are nearly as broad as the value of the Pt-N coupling the resolution does not allow for the determination of the coupling constants nor the multiplicity. The actual couplings could not be determined from the nmr because of the mess of multiplets.

The difficulty with the nmr spectra of the oxidation reactions involving **(8)** is the number of species that are present in the  $^{195}\text{Pt}$  and  $^{13}\text{C}$  nmr spectra. Unfortunately some of the most interesting platinum compounds are not nmr active. The oxidation state of the platinum in the solid POTCP makes it very likely that there are paramagnetic species present in the reaction solutions leading up to the solid state complexes. Following figure 20 is table 4. Table 4 is a tabulation of the platinum species in the oxidation reactions of **(8)**, which we were successful in correlating the  $^{195}\text{Pt}$  nmr chemical shift with the complexes corresponding  $^{13}\text{C}$  nmr chemical shift.



(32)

Figure 19. Structural representation of the multinuclear complex (32).

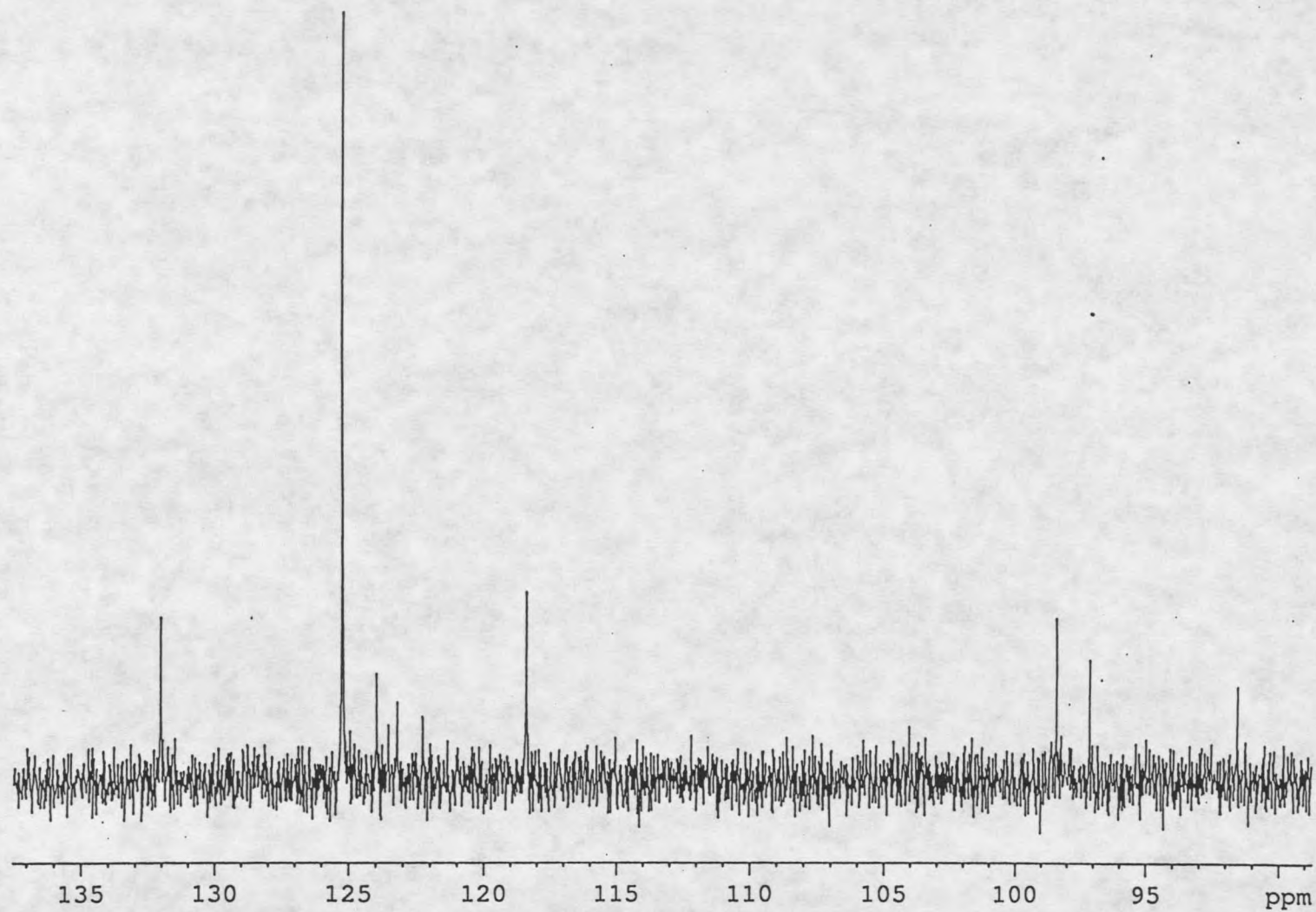


Figure 20.  $^{13}\text{C}$  nmr of the oxone oxidation of (8) with the natural abundance of  $^{13}\text{C}$ N.

Table 4. Corresponding  $^{195}\text{Pt}$  nmr and  $^{13}\text{C}$  nmr chemical shifts for the solution species in the oxidation of **(8)**.

| Species  | $^{195}\text{Pt}$ nmr (ppm) | $^{13}\text{C}$ nmr (ppm) |
|--|-----------------------------|---------------------------|
| $\text{Pt}(\text{CN})_4^{2-}$                  | -4727                       | 125                       |
| $\text{Pt}_2(\text{CN})_6^{2-}$                | -4744                       | 123                       |
| $\text{Pt}_3(\text{CN})_8^{2-}$                | -4764                       | 121.5                     |
| $\text{Pt}_2(\text{CN})_8(\text{OH}_2)_2^{2-}$ | -1776                       | 98                        |
| $\text{Pt}(\text{CN})_4(\text{OH}_2)_2^{2-}$   | -1280                       | 94.5                      |

The number of nmr active species indicates that these oxidations are non-stoichiometric. This can lead to great difficulty in assigning oxidation states to the resulting species. Although the Pt(IV) species **(11)** is nearly 50% of the species in solution with one electron equivalent of oxone and proceeds to be about 95% of the solution species present when two electron equivalent are used this is clearly the most stoichiometric of the oxidation reactions described here. The formation of 50% of the Pt(IV) species with one electron equivalent of oxidant indicates that **(8)** does not afford a Pt(III) species very readily. Even with a one electron oxidant like  $\text{Ce}^{4+}$ , only after addition of an stoichiometric excess of  $\text{Ce}^{4+}$  does any Pt(III) begin to form in solution.

The initial reaction solutions reveal no considerable changes in the UV-Visible spectra like in the case of the oxidation of **(16)**. In the case of **(16)** paramagnetic species result in brilliantly colored solutions. The POBOP reactions give colors within 30 minutes of reaction time. These reactions give four different visible absorption bands depending on the electron equivalents used to oxidize **(16)**. The reaction gives a purple solution, which is attributed to a

tri-nuclear platinumoxalate (27). The visible absorption spectrum was obtained on the TCP reaction solutions after they had turned purple. These solutions give an absorption band at 522nm which correlates with the 510nm absorption band for the trimeric species in the PO of the platinum oxalates (23). This species would be paramagnetic and thus would not be observed in the nmr spectrum.

Absorption bands can indicate whether the species is dinuclear or trinuclear in these systems because the visible absorption bands of these complexes are the result of the metal-metal interaction. Regardless of the ligands present two complexes with similar metal-metal interactions will result in the same or nearly the same color. Without suitable crystals for x-ray crystallography the characterization of this purple species remains speculative; however it is shown below that none of the species characterized by  $^{195}\text{Pt}$  nmr give the purple colors in solution.

#### Characterization of the Dinuclear Species at -1776ppm

When oxone oxidations sat idle for a couple of weeks it was observed that the -1776ppm peak became more pronounced in the  $^{195}\text{Pt}$  spectrum as the solution yielded a purple color. Because of this the -1776ppm peak was initially assigned to the species giving the purple color. However, in some of the oxidation reactions purple solutions were observed without any -1776ppm present in the  $^{195}\text{Pt}$  nmr. For example when the purple color is present in the

HNO<sub>3</sub> oxidation reactions there is no -1776ppm observed in the spectrum. Also the formation of (6) gives a significant resonance at -1776ppm and here the solutions are clear. The -1776ppm peak also results when (8) is oxidized with 1 equivalent of (11) and there is no purple color to the solution. Although with time the solution does give a purple color. Immediately after oxidation using oxone there is -1776ppm present in the nmr spectrum but there is no coloration of the solution. The only coloration is the emergence of a faint yellow color, which is attributed to (11). From these observations it is apparent the purple color is attributed to some other species. The species causing the purple color is most likely paramagnetic since there is no new <sup>195</sup>Pt nmr resonance present. The purple color observed is similar to the reports by Levy (22) and Keller (27).

The peak at -1776ppm also begins to appear at nearly the same time as the peak upfield of (8). This is more than coincidental because (27) should form with the addition of any acid to (8) but this does not occur. Only when acid and oxidant are together will (27) then form. It may be that (27) results from the reduction of one of the oxidized complexes instead of simply losing CN as HCN.

Any time that the -1776ppm peak becomes larger with time there is a corresponding decrease in the signal from (11) indicating it is being reduced to a lower oxidation state (figure 17). Likewise there is also a decrease in the signal of (8). (11) is reduced down to (25) and (8) is oxidized to the dinuclear (25). (11) should be very stable like most other Pt(IV) species. However (11) was very difficult to isolate. It was always present with other species and with time always

appeared to be consumed to form other products in solution.

Some insight into the oxidation state of the -1776ppm peak was attempted by looking at the Pt-C coupling constants. The general rule for Pt-C couplings is that there is a decrease in the  $^1J$  coupling on going to a higher oxidation state. This follows the amount of s-character in the complex. Pt(II) cyanide species are square planar resulting in  $dsp^2$  hybridization. When oxidized to a Pt(IV) oxidation state they then assume the octahedral  $d^2sp^3$  hybridization giving the former more s-character and hence a larger J coupling. The Pt(III) species will not necessarily have J couplings that fall in between the Pt(II) and the Pt(IV) species. Pt(III) species may have various hybridization schemes depending on if they are mononuclear five coordinate species or if they are multinuclear. In this system the -1776ppm peak which is attributable to the Pt(III) dimer has a coupling constant that is actually less than the Pt(IV) species. The error associated with the coupling of this peak is considerable since the peak width at half height is about 600Hz. Because of the width and the value that resulted no conclusions could be made about the oxidation state from the coupling constant. No conditions have yet been found to isolate **(25)** in pure form but the evidence shown here is sufficient to prove **(25)** correlates with the peak at -1776ppm in the  $^{195}\text{Pt}$  nmr spectrum.

### Solution Studies of the Partially Oxidized Tetracyanoplatinates

The  $^{195}\text{Pt}$  nmr spectra of the peroxide reaction solutions leading up to **(6)** and **(18)** show considerable differences. The reaction solution for formation of **(18)** does not contain as many Pt species as the reaction solution leading up to **(6)**. The reactions with **(8D)** contain mostly starting material at -4724ppm and small peaks at -2398ppm and **(11)** at -1285ppm. The PO reactions with **(8A)** contain three more  $^{195}\text{Pt}$  nmr resonances than they do with **(8D)**. The broad dinuclear peaks in peroxide reactions with **(8A)** at -1776ppm and -2300ppm are nearly 50% of the total peak area for all the resonances observed. The Pt(II) starting material and the Pt(IV) di-aquo species make up nearly the rest of the  $^{195}\text{Pt}$  nmr observable species in the solution.

The number of peaks in the  $^{195}\text{Pt}$  nmr spectra reflects the % yield obtained for each of the reactions. Compound **(18)** is obtained in over a 90% yield whereas **(6)** is only obtained in barely over 10% yield. The greater number of species in solution when forming **(6)** compared to **(18)** explains the lower yield for the reaction of compound **(6)**.

### Oxidation Reactions Using $\text{HNO}_3$

Oxidation of  $\text{K}_2\text{Pt}(\text{CN})_4$  with  $\text{HNO}_3$  When low concentrations (1-4M) of  $\text{HNO}_3$  are added to **(8A)** they do not result in readily oxidized solutions. The  $^{195}\text{Pt}$

nmr indicates for these concentrations the Pt(II) starting material remains for up to 2 weeks in the reaction solutions. When higher concentrations of  $\text{HNO}_3$  are used there is not any of **(8)** remaining immediately after the reaction is carried out. This is due to two reasons. 1) **(8)** is consumed and oxidized to a complex in an undetermined oxidation state with no observable  $^{195}\text{Pt}$  nmr resonance and 2) the higher concentrations of acid forms HCN with the ligands and the HCN is evolved from the reaction solution. The latter reason results in the peaks that arise in the  $^{195}\text{Pt}$  spectrum upfield of **(8)** in the oxidation reaction that are carried out under acidic conditions. Loss of CN ligands will result in the platinum atom being unsaturated and while remaining in a Pt(II) oxidation state rearrange to **(27)**. All oxidation reactions done where acid is involved, either as the oxidant or simply to lower the pH the reactions give the peaks upfield of the Pt(II) starting material.

When **(8A)** is combined with 7M  $\text{HNO}_3$  the oxidation of the Pt(II) is readily seen. The light yellow **(8A)** turns to a dark yellow when the acid comes into contact with it followed by a yellow solution when the solid dissolves. The lower concentrations of acid give the yellow solutions after a few hours but with the higher concentrations (>5M) the yellow color is observed immediately after the starting material is dissolved. Similar to the oxone oxidations, if the concentration of **(8A)** is > .05M the solution turns to a white cloudy substance. The reactions will turn white after one day when oxidized with >5M acid and up to four days for the lower acid concentrations.

Reactions that are allowed to sit for 3 weeks give a light purple color. The purple color is similar to that seen when oxone is used for oxidation. However, the  $^{195}\text{Pt}$  nmr spectra of the two reactions are not the same. The purple solutions formed from  $\text{HNO}_3$  oxidation's do not give the broad peak at  $-1776\text{ppm}$  like the oxone oxidations do. The  $\text{HNO}_3$  oxidations give rise to a peak at  $-1460\text{ppm}$  that is even broader than the  $-1776\text{ppm}$  peak.

The visible absorption spectra of these solutions were recorded after the purple color appeared. The purple solutions gave an absorption band at  $536\text{nm}$ , which is very near the  $522\text{nm}$  band present in the purple solutions of the oxone oxidations.

The visible absorption spectra for the purple solutions of both oxone and  $\text{HNO}_3$  oxidation's give nearly the same absorption spectra. This gives further evidence the purple colored compound in solution is not the compound resulting in the  $-1776\text{ppm}$  peak nor the  $-1460\text{ppm}$  peak in the case of the  $\text{HNO}_3$  acid oxidation's in the  $^{195}\text{Pt}$  spectra. The trimeric species  $[\text{Pt}(\text{ox})_2]_3^{-xx}$  resulting from the oxidation of **(16)** gives an absorbance at  $510\text{nm}$ . Because the absorbance in the visible region at  $510\text{nm}$  is due to the Pt-Pt bond of the trimeric oxalate then it is possible a trinuclear platinum cyanide species results in the purple color. The absorbances at  $522\text{nm}$  (for oxone) and  $536\text{nm}$  (for  $\text{HNO}_3$ ) are the only absorbances in these oxidation's that is not due to metal to ligand charge transfer bands (MLCT).

Dilute solutions of **(8)** give MLCT bands at, 216, 255 and  $283\text{nm}$ . On

going to a concentrated solution (about .5M) the absorption obscures the entire region from 190nm to 380nm when using a 1mm-path length cell because of the large molar absorptivities of these bands. Adamson's experiments at concentrations in the 1M range required the use of .0001cm path length cells (14,15). Because of the large absorptivities of **(8)** UV-Vis at high concentrations where multi-nuclear species are favored is not easily achieved. At higher concentrations the bands for **(8)** obscure the spectrum to low energy as far as 400nm without the use of very small path length cells.

When **(8)** is oxidized the solutions are nearly clear but there is a shoulder present off the low energy side of the strongly absorbing MLCT band near 300nm. This shoulder results in the light yellow colors observed in the oxidation reactions. After oxidation the three individual absorption's seen for the  $\text{Pt}(\text{CN})_4^{2-}$  are not resolvable even at concentrations down to about  $1 \times 10^{-5}$  although they are resolvable in unoxidized  $\text{Pt}(\text{CN})_4^{2-}$  solution at  $1 \times 10^{-3}\text{M}$ .

Oxidation of  $\text{BaPt}(\text{CN})_4$  with  $\text{HNO}_3$  Oxidation of **(8B)** with nitric acid gave different reaction products depending on the acid concentration used for the oxidation. When using only 1M  $\text{HNO}_3$  the reaction mixture turned to a white mushy substance after sitting for only 3 days. It is evident that the 1M reaction solutions are not acidic enough to prevent the  $\text{BaNO}_3$  from eventually crashing out of the solution after it has concentrated down by slow evaporation. When 3M  $\text{HNO}_3$  was used the reaction solution resulted in a light orange color over a

period of one week. The orange solution did not give any crystals nor were there any signals in the  $^{195}\text{Pt}$  nmr spectrum. Solution reactions done in 3M and higher acid never resulted in the white  $\text{BaNO}_3$  crashing out of solution.

Oxidation of  $\text{Cs}_2\text{Pt}(\text{CN})_4$  with  $\text{HNO}_3$  When **(8D)** is reacted with  $\text{HNO}_3$  the needle like copper colored crystals of **(18)** result. Varying the concentration of acid results in different yields and quality of crystals for **(18)**. Using 2M  $\text{HNO}_3$  as the reaction medium and oxidant results in the best quality crystals. When 3M  $\text{HNO}_3$  was used the product did not crystallize out as the familiar copper colored needles. Most of the reaction products were lumped together in a brown mass like that described when using hydrogen peroxide as the oxidant. When 4M  $\text{HNO}_3$  is used there is a brown solid resulting within one hour of when the reactants are mixed together. These are also not of good crystalline quality. 1M  $\text{HNO}_3$  also affords good quality copper colored crystals but the yield is not as high as that when 2M  $\text{HNO}_3$  is used. Therefore, the synthesis of **(18)** using  $\text{HNO}_3$  should be carried out using 2M acid.

The cation used has a large effect on the products that form in the oxidation reactions for the platinum cyanides. The  $\text{HNO}_3$  oxidation reactions are also dependent upon the counter cation used. Only a few of the platinum cyanide salts form copper colored needles. This indicates that the solubility of each of the cations plays a role in the resulting species formed in solution as well as in the solid state. The solubility plays a role in the solutions because it effects

the association of the ions. The solid state is effected by the packing energies that result with each of the different cations.

The  $\text{HNO}_3$  oxidation of **(8)** gives oxidized products but the nmr indicates that there are no diamagnetic platinum species present in the solutions. There exists no platinum chemical shift immediately after oxidation but the yellow color gives evidence that there are paramagnetic species present. A good candidate for a paramagnetic species would be the monomeric Pt(III) species.

If these reactions are allowed to stand for over a week a purple solution will result. Only after the purple color develops is there a chemical shift evident at -1460ppm. Since an oxidized diamagnetic species form over time there exists an oxidized platinum species present after oxidation. Immediately after oxidant is added the only  $^{195}\text{Pt}$  signal evident is the starting material when low concentrations of  $\text{HNO}_3$  are used. Similar to the -1776ppm peak the -1460ppm peak is most likely a dimeric Pt(III) species but the difference in chemical shift between the two peaks is too large for them to be the same species. Such a large chemical shift difference would not be the result of any medium effects. Although these effects can be very large in the  $^{195}\text{Pt}$  spectrum they are generally not of this magnitude. Most medium effects such as differing solvents are on the order of 100-300ppm.

Levy described the purple crystal he obtained from the  $\text{HNO}_3$  oxidation of **(8A)** as being a Pt(III) monomeric species. Hartly contended that these solids were most likely the result of Pt(II) and Pt(IV) mixed complexes. Levy's

assumption appears to be correct because the  $^{195}\text{Pt}$  nmr indicate there is no Pt(II) or Pt(IV) species present at the times when the solutions contain a purple color. The purple solids may be other oxidized species besides a form of Pt(III) but with no nmr signal for **(8)** or **(11)** it is shown to not be a mixed Pt(II) and Pt(IV) species.

#### Oxidation of $\text{K}_2\text{Pt}(\text{CN})_4$ with $\text{Ce}^{4+}$

Like the other oxidants used the  $\text{Ce}^{4+}$  does not oxidize **(8)** stoichiometrically. The concentration of acid incorporated into the reaction effects the quantity of **(8)** that undergoes oxidation. Reactions that are acidified with just enough sulfuric acid to make the solution have a pH of one results in a one electron equivalent addition of  $\text{Ce}^{4+}$  only giving a small amount of **(27)**. This is evident by the  $^{195}\text{Pt}$  nmr peak that occurs 20ppm upfield of **(8)**. Addition of two electron equivalents results in both the -4744ppm peak and a broad signal at -2300ppm. Presumably this peak at -2300ppm is due to **(26)** like that described for the peroxide oxidation reaction. Similarly the peak width is 400Hz at half height and it is in the region of the platinum spectrum expected for a Pt(III) species with cyanide ligands bound to the platinum. If the water ligands that cap the Pt(III) dinuclear **(25)** are removed it would result in the new Pt(III) dinuclear resonance shifting to -2300ppm. After addition of three electron equivalents of  $\text{Ce}^{4+}$  **(8)** is completely consumed and more of the -2300ppm peak is present.

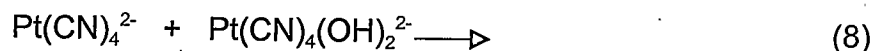
However, the -4744ppm peak for **(27)** is still more prevalent than the oxidized product at -2300ppm. After the reaction solution sat idle for 3 days the  $^{195}\text{Pt}$  nmr spectra was repeated and the resonance for **(27)** at -4744ppm was no longer present. The S/N ratio of the -2300ppm peak did not increase over this time. This indicates the -4744ppm has completely precipitated out of the solution. It is possible that oxidation occurs to **(27)** but this would only account for a small portion of its disappearance because of the large quantity of yellow solid in the bottom of the reaction vessel.

When the reaction solution consists entirely of 1M  $\text{H}_2\text{SO}_4$  the oxidized species present in the  $^{195}\text{Pt}$  spectrum at -2300ppm begins to appear after addition of only one electron equivalent of  $\text{Ce}^{4+}$ , although it is still not stoichiometric. Addition of more  $\text{Ce}^{4+}$  results in more -2300ppm peak but like above the -4744 is still more prevalent. With time this reaction behaved similarly in that the entire -4744ppm peak disappeared giving the yellow precipitate. Unlike oxidation using oxone when the  $\text{Ce}^{4+}$  reactions are acidified to a pH of 1 with a few drops of acid gives rise to the chemical shift upfield of **(8)** without any di-nuclear Pt(III) chemical shifts present.

#### Oxidation of $\text{K}_2\text{Pt}(\text{CN})_4$ with $\text{K}_2\text{Pt}(\text{CN})_4(\text{OH})_2$

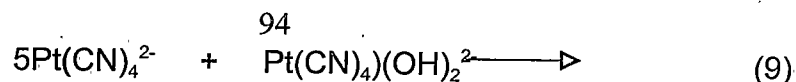
When the potassium salt of **(8)** is oxidized with one equivalent of the Pt(IV) species **(11)** according to equation 8 oxidation takes place but it is a non-

stoichiometric reaction.



Using  $^{195}\text{Pt}$  nmr it was determined the reaction solutions give **(11)**, **(25)**, **(26)**, **(8)**, **(27)** and **(32)**. When the reaction mixture was dried out the solid is purple but quality crystalline solids for x-ray crystallography have not yet been achieved. When the purple solid is dissolved back up into water a slightly yellowish solution results and the  $^{195}\text{Pt}$  nmr gives the same species but in significantly different quantities. The broad peaks due to **(25)** and **(26)** now constitute most of the solution species (Figure 21). The resonances at -4744ppm and -4764ppm for **(27)** and **(32)** have also changed in their respective concentrations in the solution. The total quantities of **(27)** and **(32)** have not increased but the further associated **(32)** is now in the greater amount. Figure 21a shows the six species that are in solution upon mixing **(8)** and **(11)**. For the most part these are the same six species that are present with the other oxidants described here for the oxidation of **(8)**. In 21b it can be seen that there is very little **(11)** and **(8)** remaining when reaction 8 is dried, dissolved back up in  $\text{D}_2\text{O}$  and the  $^{195}\text{Pt}$  nmr is repeated. The change in species distribution results because the drying out of the solution increases the rate of association that forms **(25)** and **(26)** because of the greater solution concentrations.

When the reaction is done with a 5Pt(II):1Pt(IV) ratio like equation 9



the  $^{195}\text{Pt}$  nmr results in nearly the same spectra that is observed for solutions that form the CD-POTCP from hydrogen peroxide. This is the same stoichiometry that is used to synthesize the AD-POTCP. This reaction resulted in copper colored solids but they were not of needle like crystalline quality. Figure 22 shows the  $^{195}\text{Pt}$  nmr of equation 9 reaction solution. The significance of equation 9 compared to equation 8 is the greater proportion of **(8)** in solutions of equation 9 with respect to the other species in solution. The solution species distribution is similar to the peroxide oxidation of **(8)** when **(6)** is synthesized. Since **(11)** oxidizes **(8)** giving the same nmr signals as peroxide oxidations where the POTCP are formed suggests **(11)** is at least indirectly involved in the formation of the POTCP.

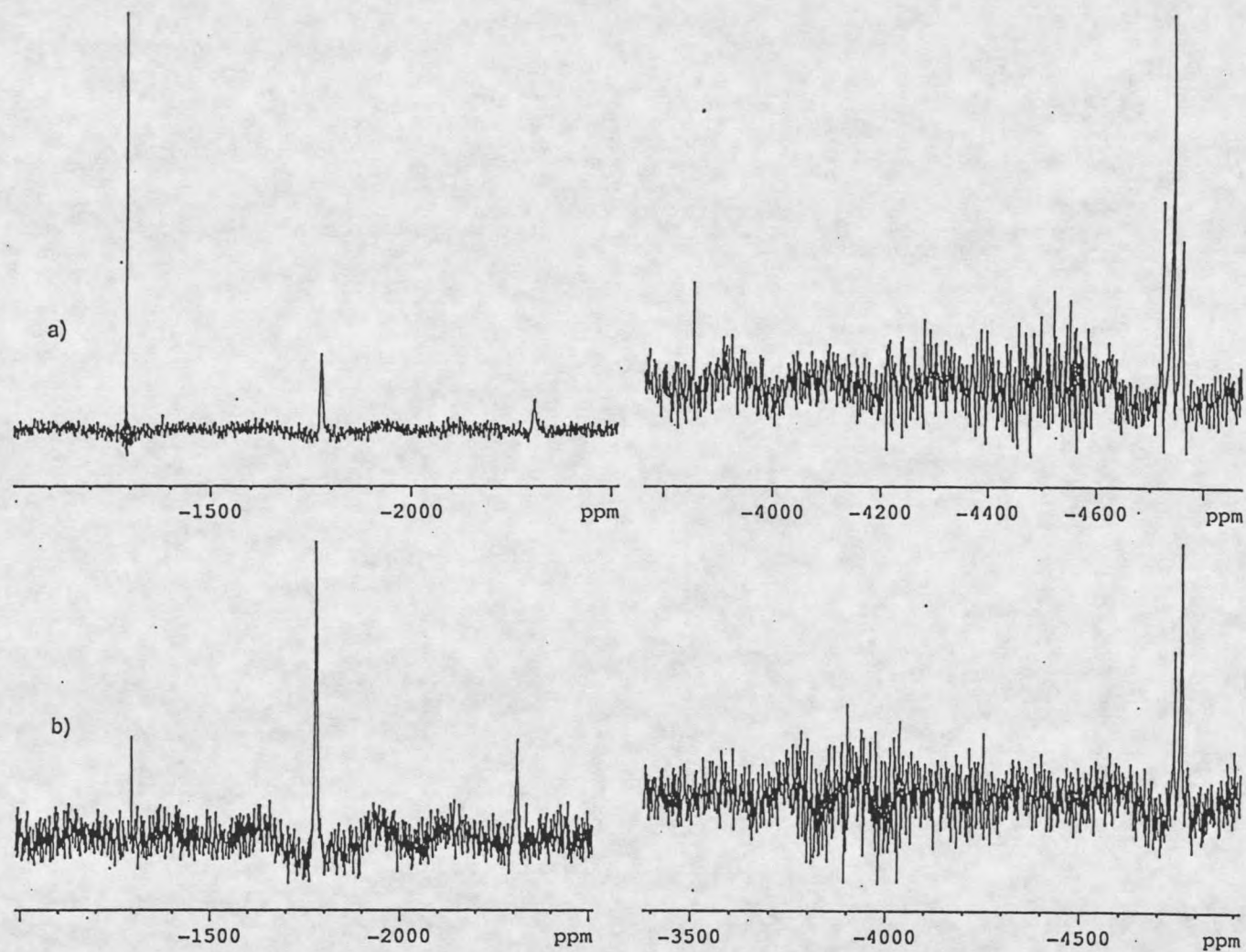


Figure 21. a)  $^{195}\text{Pt}$  nmr of (8) and (11) combined in water. b)  $^{195}\text{Pt}$  nmr of equation 8 after drying and redissolving.

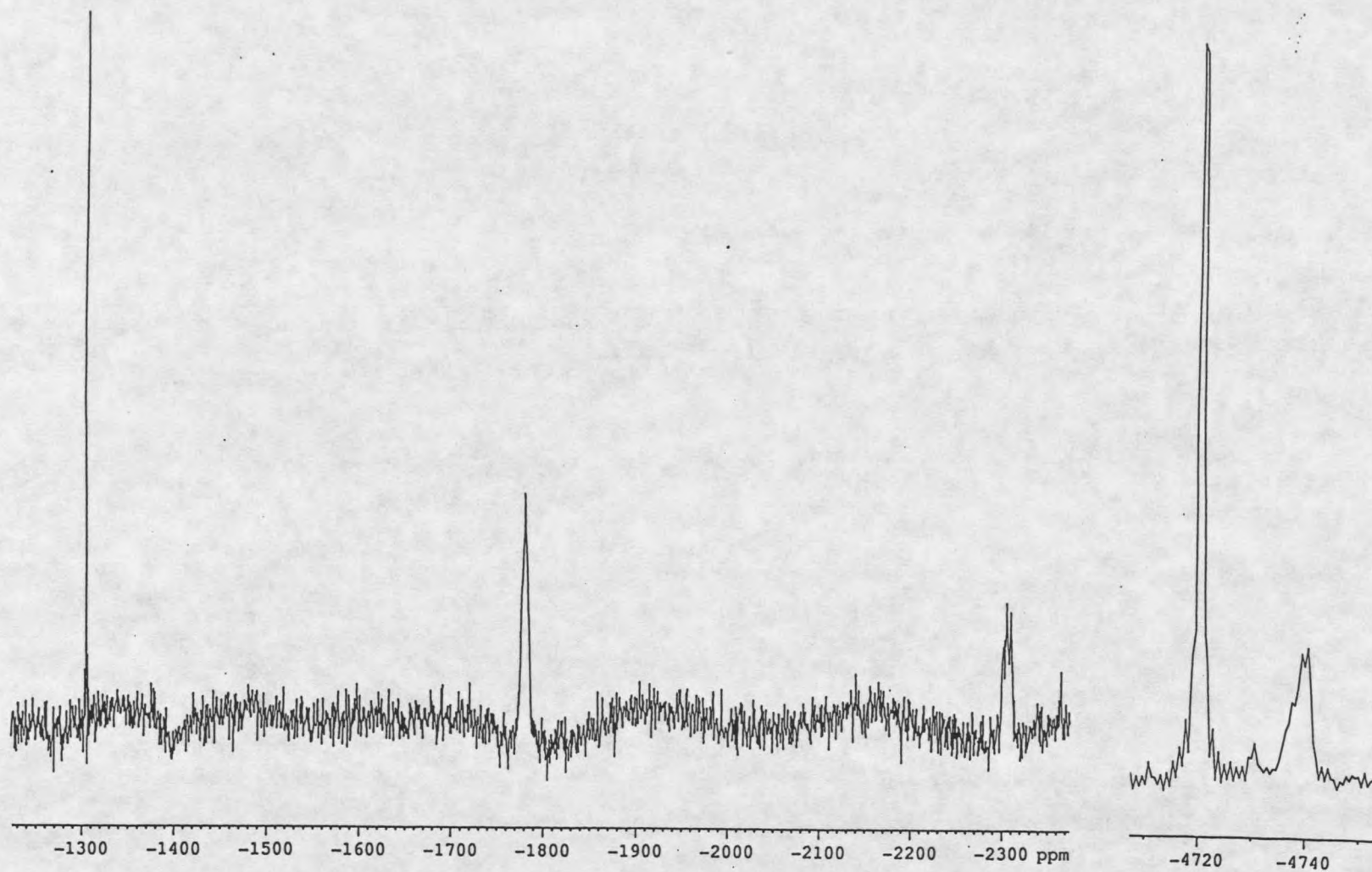


Figure 22.  $^{195}\text{Pt}$  nmr of equation 9.

Species Responsible for POTCP Formation

Complete evidence describing what species in solution are directly responsible for the formation of the CD-POTCP is insufficient. It would be premature to assume they form similarly like the AD-POTCP from a Pt(II) and a Pt(IV). When the copper needles are dissolved in the case of the CD the  $^{195}\text{Pt}$  nmr spectrum is not the same as the  $^{195}\text{Pt}$  nmr spectrum before the copper colored needles are formed. The only peak that is in both solutions is from (8). The -1776ppm and the -1280ppm peaks are not present when the CD-POTCP is dissolved in acidic solutions nor in neutral solutions. These solutions afford other species than (8) when dissolved because the CD-POTCP can be recrystallized from water indicating when the solid dissolves there is some other oxidized species in solution but it is not nmr detectable (23).

These reaction show evidence that the -1280ppm, -1776ppm, -2300ppm, and the -4724ppm peak are not directly responsible for the formation of the copper colored needles even though these three peaks are a significant percentage of the total peak areas before crystallization occurs. However, these three species undoubtedly play a role in the formation of the POTCP but they either react or combine into other paramagnetic species that eventually proceed on to give the copper colored needles. Mass balance would indicate that all or most of these characterized complexes are at least intermediates in the POTCP formation. When forming the POTCP with the cesium salt the % yield is near

90%. By nmr the S/N of the starting material before oxidation and the S/N of the peaks in the reaction solution would indicate most of the platinum complexes are detected in the nmr. The most significant evidence for only indirect involvement of **(11)**, **(25)** and **(26)** is evident in the HNO<sub>3</sub> oxidation's of **(8)**. Copper needles are formed from these solutions but there are no nmr signals at -1280ppm, -1776ppm and -2300ppm like that seen in the oxone and hydrogen peroxide oxidation's of **(8)**.

#### Comparisons of the dianions Pt(CN)<sub>4</sub><sup>2-</sup> and Pt(ox)<sub>2</sub><sup>2-</sup>

The reluctance of **(8)** to oxidize and form multi-nuclear species is due to a number of factors. The cyanide ligands are heavily charged and there is an appreciable amount of repulsion for any association with other ions of like charge. The distances the platinum atoms approach one another in the solid phase of the TCP's is mostly the result of packing energies. Although Krogmann and Gray have demonstrated with their "configuration interaction" that there is a net bonding energy in the TCP's for both oxidized and unoxidized compounds. In the case of the POTCP the stability from the bonding interaction is enough to compensate for the ligand repulsion. The oxidized have a much greater net bonding energy because electrons are essentially removed from anti-bonding orbitals like that demonstrated in figure 10.

**(16)** which forms copper colored needles does not have nearly the

repulsion surrounding the ligands and thus forms a number of oligomeric species in solution when oxidized. However, there are some anomalies with this reasoning. There exists only one of the platinum(II) oxalate salts that stack like the platinum(II) cyanides in the unoxidized solid phase like the depiction in figure 2. The red colored magnesium salt of the bisoxalatoplatinate(II) stacks like the cyanides and it has a Pt-Pt separation of 3.18Å. The color of this complex and its Pt-Pt separation correlate to the platinum cyanides with similar color and Pt-Pt separation. This shows further evidence that the colors of these complexes are only the result of the Pt-Pt interaction and not the counter ion associated with the complex. The greater number of the platinum oxalates though do not stack in the solid phase and the Pt-Pt separations are upwards of 8Å apart. Yet these compounds when they undergo PO give Pt-Pt separations that are shorter than the POTCP's. It has been suggested that the PO of the oxalates may bring added stability to the compound by bonding through the ligands. The distance between the ligands in the PO compounds is less than the van-der Waals radii for pi type oxygen atoms (3.0 Å) as well as pi-oxygen plus a pi-carbon atom (3.3Å) (21).

(16) forms Pt(IV) species much more readily than (8). Even when the oxalate is oxidized with the tert-butylhydrogen peroxide it forms the Pt(IV) species  $\text{Pt}(\text{ox})_2[\text{O}(\text{CH}_3)]_2^{2-}$ , whereas (8) only forms a small amount of the  $\text{Pt}(\text{CN})_4[\text{O}(\text{CH}_3)]_2^{2-}$ . In the case of the cyanide complex it is seen as a broad signal at -1100ppm. For the oxalate there are  $^{195}\text{Pt}$  resonances at -2900ppm and

-2850ppm. The two peaks are the result of the cis and trans-complexes. The high stability constant of **(8)** is also a contributing factor to the difficulty of forming, in isolation the  $\text{Pt}(\text{CN})_4(\text{OH})_2^{2-}$ . There is always some **(11)** that forms readily from **(8)** but the nmr nearly always reveals other species in the oxidation reaction.

#### Investigation of the Pt(IV) $\text{MPt}(\text{CN})_4(\text{OH})_2$

Titration of  $\text{Pt}(\text{CN})_4(\text{OH})_2^{2-}$   $^{195}\text{Pt}$  nmr was utilized to determine the pka values of **(11)**. The error of the pka's is significant due to the inability to obtain pure salts of **(11)** in significant quantities. Removal of all the excess salts, namely potassium and sulfate from the oxone oxidation's was not achieved. Clear plate like crystals were obtained from the oxone oxidations when trying to purify **(11)** by recrystallization. X-ray diffraction showed these crystals to be  $\text{K}_2\text{SO}_4$ . Solvent extraction was used for purification because it resulted in the best isolation of **(11)**. Methanol proved to be the most successful solvent for extraction of **(11)**. However, using methanol to extract **(11)** results in some methanol substitution onto **(11)**.  $^{195}\text{Pt}$  nmr reveals that the methanol substitution product is <5% of the total products in solution. There are also small amounts of the  $\text{Pt}(\text{OH})_4(\text{CN})_2^{2-}$  present in the solution. This species was detected using  $^{195}\text{Pt}$  nmr where a resonance was observed at +1011ppm. Even small amounts of

this product will alter the titration data substantially because of the four coordinated waters.

Upon taking the solution containing nearly 95% of **(11)** from a pH=1 to a pH=4 the chemical shift goes from -1260ppm to -1487ppm. This is a change of about 230ppm for the de-protonation to two protons. The most significant change in the chemical shift occurs between pH=2 and pH=3 giving a estimated pka value of about 2 for **(11)** (Figure 23). There are actually two pka values for this complex but resolving the two is not achieved here. At the pH values where there is a pka inflection the solution color changes from clear to yellow. This occurs near pH=2.5. The intensity of the yellow color increases with increasing pH. The  $\text{Pt}(\text{OH})_4(\text{CN})_2^{2-}$  may have a significant role in the color change observed. The di-aquo species **(11)** does not have an extinction coefficient in the visible region large enough to give this intense yellow color. However, the tetra-aquo species has a considerably higher extinction coefficient in the visible region. This result is because the two water ligands replace two cyanides and the water ligands occur considerably lower in the spectrochemical series than do the cyanides. This will cause lower energy transitions than the tetracyano complexes. For example the hexa-aquo species  $\text{Pt}(\text{OH})_6^{2-}$  gives a yellow solution and the  $\text{Pt}(\text{CN})_6^{2-}$  gives a clear solution. All known complexes that have only cyanide ligands bound to the metal give absorption bands in the UV region only. Conversely the weaker field hydroxide ligand usually gives a band in the visible portion of the spectrum.

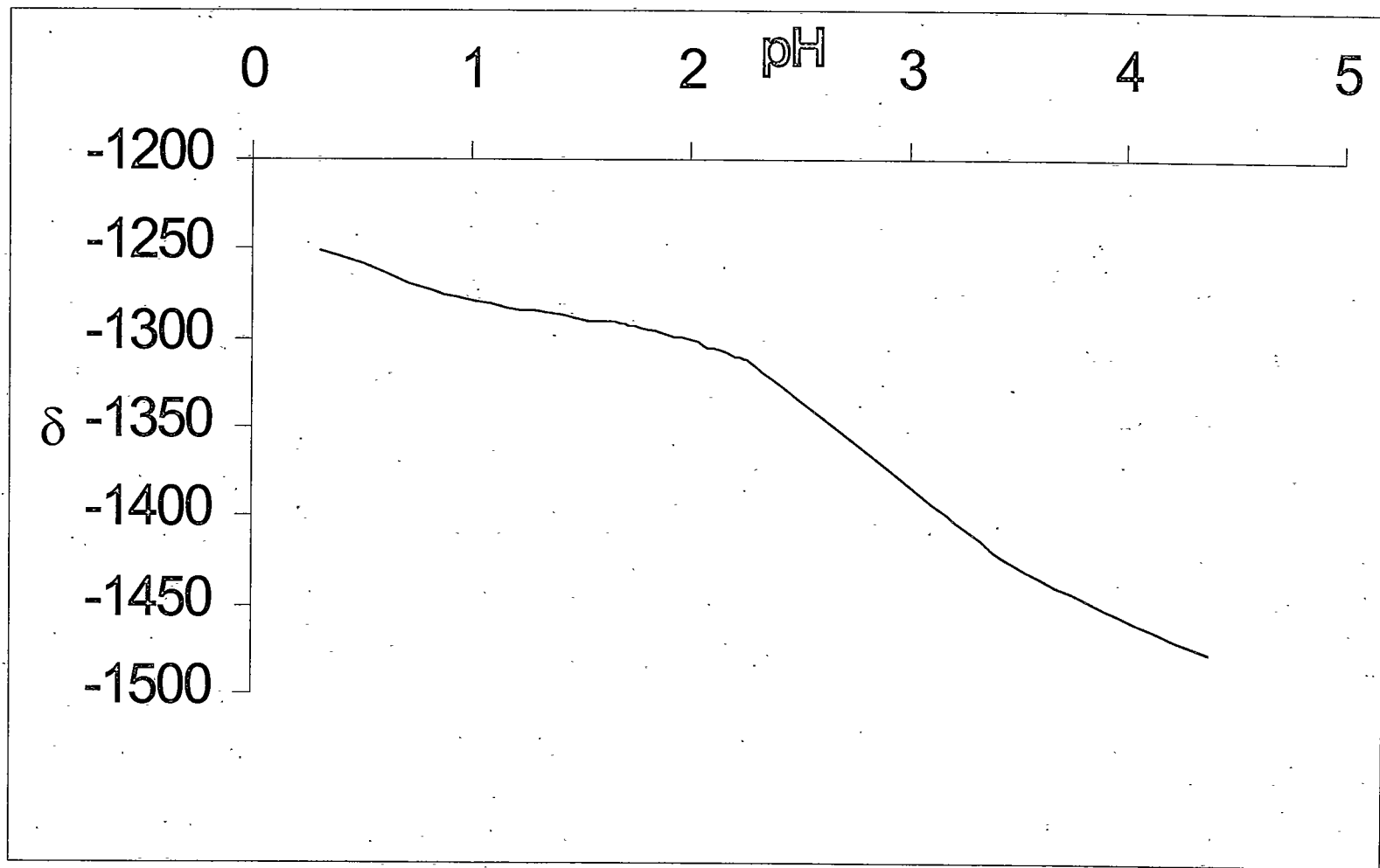


Figure 23.  $^{195}\text{Pt}$  nmr monitored base titration of (11).

After several hours of sitting idle at pH=7 the solution begins to lose its bright yellow color and the pH value drops. This also causes a shift in the nmr signal back downfield. On regenerating the higher pH value the yellow color does not reappear even when the solution is brought up to pH=12 but the  $^{195}\text{Pt}$  nmr signal is returned to -1497ppm. The  $^{195}\text{Pt}$  chemical shifts were regenerated upon the addition of acid followed by the addition of base. The regeneration of the chemical shift shows that the process is an acid/base reaction.

It was not expected that deprotonation results in the bright yellow color observed at a pH of 4. Observing that the bright yellow color disappears and then it is not reproduced suggests that this color is not of the simple deprotonation products but it is that of a degradation product. Whatever this species is it undoubtedly has a very large molar absorptivity constant because its concentration is low yet it gives a bright yellow solution. Also significant is that the pH meter generally took nearly five minutes to stabilize when the color of the solution turned to the bright yellow at pH=4. Acid/Base reactions occur on a much faster timescale than this.

Formation of the Pt(IV)  $\text{K}_2\text{Pt}(\text{CN})_4(\text{OH})_2$  Isolation of **(11)** in large quantities was not achieved. Crystals were finally obtained for the barium salt of the complex by diffusion of ethanol in a desiccator into a peroxide oxidation of **(8)**. The reaction was placed into the desiccator after repeated attempts at obtaining crystals by slow concentration. It is evident that the repeated drying of

the solution is essential for obtaining crystals of the Pt(IV) species because crystallization has not occurred with this compound when peroxide is present. The repeated drying out of the solution effectively rids the reaction mixture of any remaining hydrogen peroxide. All of the oxidations done here except for the formation of the POTCP have not resulted in quality single crystals when hydrogen peroxide is still present.

After the experiments described here and the evidence suggested by the Russian (31) workers it appears what they have reported as the  $K_2Pt(CN)_4(OH_2)_2$  was actually  $K_2Pt(CN)_4 \cdot 2H_2O$ . The two hydrated waters on the Pt(II) complex would give the same elemental analysis as the Pt(IV) complex as they reported it. The Pt(II) species when allowed to dry turns from the yellow tri-hydrated complex to white which corresponds to the di-hydrated complex. They also concluded their product was the Pt(IV) species by conductivity measurements. Conductivity measurements would be inconclusive for analysis because both the Pt(II) and the Pt(IV) complexes are di-anions and both are in solution with potassium as the counter-cation. Although they probably did have some Pt(IV) in their reaction solutions, the Pt(IV) species does not crystallize out before **(8A)**. **(11A)** appears to be very soluble in water. Numerous attempts at isolating **(11A)** have not been successful.

The solutions of **(11)** have only shown the trans form using  $^{195}Pt$  nmr. Upon sitting even for several months no other peaks in the  $^{195}Pt$  nmr spectra arise in the vicinity of the trans species that would indicate conversion to the cis

complex. There may be an appreciable instability to the cis form because of the trans-influence of the cyanide ligand. The  $\text{Pt}(\text{ox})_2(\text{OH})_2^{2-}$  gives both cis and trans forms. The cis-trans isomerization was described by Dunham (30).

Crystal Structure of the  $\text{BaPt}(\text{CN})_4(\text{OH})_2 \cdot 7\text{H}_2\text{O}$  A lot of effort went into obtaining the crystal structure of this Pt(IV) complex. Conventional thinking one would conclude this should be an easy complex to obtain. The oxidation reactions studied here indicate **(11)** is a stable complex but the packing energies in the solid may be the reason it does not give single crystals very easily. **(11)** is mentioned as an intermediate in the chloride anation of **(8)** but what is described does not prove the existence of **(11)** (54). **(11)** is described as the intermediate in the chloride anation of **(8)**. It is suggested that **(11)** results in a band that occurs in the visible spectrum but there has been no absolute identification of **(11)** in the literature. Through  $^{195}\text{Pt}$  nmr we were able to identify this species but it is of unmistakable proof for characterization of a metal complex if the x-ray crystal structure is obtained.

The ORTEP diagram of compound **(11B)** is shown in figure 24. This is followed by the crystallographic data for **(11B)** in tables 5-10.



**Table 5.** Crystallographic data for  $\text{BaPt}(\text{CN})_4(\text{OH})_2 \cdot 7\text{H}_2\text{O}$ 

| Parameter                                 |  |
|---|--|
| Formula                                   | $\text{C}_4\text{H}_{16}\text{BaN}_4\text{O}_9\text{Pt}$ |
| Formula weight                            | 596.6  |
| Space Group                               | Pbca   |
| Unit cell: a (Å)                          | 6.559(1)   |
| b (Å)                                     | 20.594(2)  |
| c (Å)                                     | 22.841(2)  |
| $\beta$ (°)                               | 103.745(8)   |
| volume (Å <sup>3</sup> )                  | 3085.2(4)  |
| Z   | 8  |
| $\rho$ (g cm <sup>-3</sup> ) calculated   | 2.569  |
| absorption coef, Mo K (mm <sup>-1</sup> ) | 11.637   |
| F(000)                                    | 2192   |

**Table 6.** Data collection and structure refinement data for **11**.

| Parameter                       | xx            |
|---------------------------------|---------------|
| 2 $\theta$ range ( $^{\circ}$ ) | 4-75          |
| Unique reflections              | 8110          |
| Observed reflections            | 3703          |
| Number of parameters            | 173           |
| Trans. Factor range             | 0.0984-0.1944 |
| Final R, observed data          | 0.0552        |
| Final wR, observed data         | 0.0277        |
| Final R, all data               | 0.1422        |
| Final wR, all data              | 0.0337        |
| Goodness of fit                 | 1.44          |

**Table 7.** Atomic Coordinates and equivalent isotropic displacement coefficients for 11.

| Atoms | x/a       | y/b       | z/c       | U(eq)    |
|-------|-----------|-----------|-----------|----------|
| Pt    | 0.2463(1) | 0.3984(1) | 0.1373(1) | 0.017(1) |
| N(1)  | 0.4973(1) | 0.273(1)  | 0.1658(3) | 0.044(3) |
| N(2)  | 0.2458(1) | 0.4319(3) | 0.2715(5) | 0.033(2) |
| N(3)  | -0.008(1) | 0.522(1)  | 0.1058(3) | 0.036(2) |
| N(4)  | 0.2329(4) | 0.3657(3) | 0.036(3)  | 0.037(2) |
| C(1)  | 0.4089(3) | 0.3185(3) | 0.1562(3) | 0.022(2) |
| C(2)  | 0.2444(6) | 0.4205(3) | 0.2279(3) | 0.023(2) |
| C(3)  | 0.0804(3) | 0.4788(3) | 0.1179(3) | 0.025(2) |
| C(4)  | 0.2439(7) | 0.3768(3) | 0.052(1)  | 0.026(2) |
| O(1)  | 0.0086(8) | 0.3442(2) | 0.1481(2) | 0.028(1) |
| O(2)  | 0.5058(8) | 0.4492(2) | 0.1221(2) | 0.026(1) |
| O(3)  | 0.9314(9) | 0.2468(2) | 0.0692(2) | 0.032(2) |
| O(4)  | 0.9645(1) | 0.224(1)  | 0.2004(2) | 0.042(2) |
| O(5)  | 0.3338(9) | 0.1912(2) | 0.04(1)   | 0.04(1)  |
| O(6)  | 0.7621(3) | 0.0816(2) | 0.2146(2) | 0.057(2) |
| O(7)  | 1.011(1)  | 0.0761(2) | 0.0965(2) | 0.031(2) |
| O(8)  | 0.2816(9) | 0.1368(2) | 0.1735(2) | 0.036(2) |
| O(9)  | 0.2078(1) | 0.4263(2) | 0.4841(2) | 0.05(2)  |
| Ba    | 0.671(1)  | 0.1548(2) | 0.1188(2) | 0.019(1) |

**Table 8.** Bond lengths (Å) for 11.

| Bond      | Length(Å) | Bond      | Length(Å) |
|-----------|-----------|-----------|-----------|
| Pt-C(1)   | 2.008(8)  | Pt-C(2)   | 2.004(8)  |
| Pt-C(3)   | 2.031(8)  | Pt-C(4)   | 2.000(8)  |
| Pt-O(1)   | 2.026(6)  | Pt-O(2)   | 2.028(5)  |
| N(1)-C(1) | 1.123(1)  | N(2)-C(2) | 1.137(1)  |
| N(3)-C(3) | 1.097(1)  | N(4)-C(4) | 1.131(1)  |

**Table 9.** Bond angles (°) 11.

| Atoms        | Angles(°) | Atoms        | Angles(°) |
|--------------|-----------|--------------|-----------|
| C(1)-Pt-C(2) | 88.9(3)   | C(1)-Pt-C(3) | 179.6(4)  |
| C(2)-Pt-C(3) | 91.4(3)   | C(1)-Pt-C(4) | 91.8(3)   |
| C(2)-Pt-C(4) | 179.1(4)  | C(3)-Pt-C(4) | 87.9(3)   |
| C(1)-Pt-O(1) | 87.7(3)   | C(2)-Pt-O(1) | 90.1(3)   |
| C(3)-Pt-O(1) | 91.9(3)   | C(4)-Pt-O(1) | 89.4(3)   |
| C(1)-Pt-O(2) | 90.8(3)   | C(2)-Pt-O(2) | 93.2(3)   |
| C(3)-Pt-O(2) | 89.5(3)   | C(4)-Pt-O(2) | 87.4(3)   |
| O(1)-Pt-O(2) | 176.4(2)  | Pt-C(1)-N(1) | 178.4(7)  |
| Pt-C(2)-N(2) | 178.6(8)  | Pt-C(3)-N(3) | 177.9(8)  |
| Pt-C(4)-N(4) | 176.6(1)  |              |           |

**Table 10.** Anisotropic displacement coefficients ( $\text{\AA}^2$ ) for (11).

| Atom | $U_{xx}$ | $U_{yy}$ | $U_{zz}$ | $U_{xy}$  | $U_{xz}$  | $U_{yz}$  |
|------|----------|----------|----------|-----------|-----------|-----------|
| Pt   | 0.021(1) | 0.014(1) | 0.016(1) | 0.001(1)  | -0.001(1) | -0.002(1) |
| N(1) | 0.044(6) | 0.023(4) | 0.064(6) | 0.008(4)  | 0.005(5)  | -0.008(4) |
| N(2) | 0.032(4) | 0.042(4) | 0.026(4) | 0.001(5)  | -0.004(2) | -0.01(1)  |
| N(3) | 0.037(5) | 0.021(3) | 0.051(5) | 0.001(1)  | -0.005(4) | -0.003(3) |
| N(4) | 0.036(5) | 0.045(4) | 0.03(1)  | -0.011(4) | -0.002(4) | -0.004(3) |
| C(1) | 0.018(4) | 0.026(4) | 0.023(4) | -0.005(1) | 0.003(4)  | -0.001(3) |
| C(2) | 0.023(4) | 0.023(3) | 0.024(4) | 0.003(5)  | -0.001(5) | 0.001(3)  |
| C(3) | 0.028(5) | 0.018(3) | 0.029(5) | -0.005(3) | -0.011(4) | 0.003(3)  |
| C(4) | 0.028(4) | 0.024(3) | 0.027(4) | 0.01(1)   | 0.002(5)  | -0.001(1) |
| O(1) | 0.033(3) | 0.025(3) | 0.028(3) | -0.007(3) | 0.001(1)  | 0.003(3)  |
| O(2) | 0.022(3) | 0.028(3) | 0.029(3) | -0.008(2) | -0.006(3) | 0.007(2)  |
| O(3) | 0.044(4) | 0.024(3) | 0.029(3) | -0.011(3) | -0.007(3) | 0.001(2)  |
| O(4) | 0.061(5) | 0.029(3) | 0.035(4) | 0.004(3)  | 0.004(4)  | 0.005(3)  |
| O(5) | 0.036(4) | 0.04(1)  | 0.045(4) | 0.005(3)  | 0.001(3)  | -0.006(3) |
| O(6) | 0.108(6) | 0.028(3) | 0.034(3) | -0.003(5) | -0.01(1)  | 0.003(2)  |
| O(7) | 0.041(4) | 0.021(2) | 0.032(3) | 0.007(3)  | 0.003(3)  | 0.004(2)  |
| O(8) | 0.039(4) | 0.04(1)  | 0.03(1)  | -0.001(2) | 0.001(3)  | -0.006(2) |
| O(9) | 0.033(5) | 0.079(5) | 0.039(4) | -0.003(4) | -0.006(3) | 0.021(3)  |
| Ba   | 0.023(3) | 0.016(2) | 0.019(2) | 0.001(1)  | 0.002(2)  | -0.001(1) |

Solution Studies of the Double Complex Salt  $[\text{Pt}(\text{CNC}_2\text{H}_5)_4][\text{Pt}(\text{CN})_4]$

Visible Absorption Evidence of Multi-Nuclear Complexes in Solution

Both the  $\text{Pt}(\text{CNC}_2\text{H}_5)_4^{2+}$  (**20**) and the  $\text{Pt}(\text{CN})_4^{2-}$  (**8**) ions have solution spectra with absorbances resulting from very similar transitions but all transitions occur in the UV region of the spectrum. These transitions all result from metal to ligand charge transfer transitions (MLCT) (16). When acetonitrile solutions of (**20**) and (**8**) are mixed a new band is evident in the visible region of the spectrum. Figure 25 is a plot showing the UV-Visible spectrum of (**8**) and (**20**) overlaid with the spectrum of these two solutions of (**8**) and (**20**) mixed together. In figure 25 the solution concentrations of (**8**) and (**20**) are both at  $5.0 \times 10^{-5}\text{M}$ . The resulting mixed solutions is near  $2.5 \times 10^{-5}\text{M}$ . The new band occurs at 319nm and there is also an additional band becoming apparent at 363nm.

Isci and Mason (55,56,57) described the UV-Visible spectrum of the DS complex in acetonitrile. The acetonitrile solutions only contain one band in the visible region which is attributed to the dimeric  $[\text{Pt}(\text{CNC}_2\text{H}_5)_4][\text{Pt}(\text{CN})_4]$  (**5**). However, in water there is more than one band present in the visible region of the spectrum, which is seen in figure 25 at 363nm. Water is conducive to a greater extent of metal-metal association because the DS complex is 1000X more soluble in water than in acetonitrile. Saturated solutions ( $1.0 \times 10^{-2}\text{M}$ ) of the double complex (DS) salt  $[\text{Pt}(\text{CNC}_2\text{H}_5)_4][\text{Pt}(\text{CN})_4]$  (**5**) in water are a bright

red/orange. The UV-Visible absorption spectrum of a saturated solution shows two absorbance maximum in the visible region. (Figure 26) Their maximum occur at 319nm and 450nm at solution concentrations of  $10^{-2}$ M. The 450nm band obscures most of the visible region from 340nm to 550nm.

Dilution of the  $1.0 \times 10^{-2}$ M solution results in distinctive qualitative evidence of there being a number of multi-nuclear species present in the solutions. Figure 27 is a plot of the DS solution over a 10-fold concentration range. Shown are the spectra ranging from  $1.0 \times 10^{-4}$ M to  $1.0 \times 10^{-3}$ M. Concentrations higher and lower than this range were excluded from figure 27 for simplicity. The  $1.0 \times 10^{-4}$ M spectrum in figure 27 begins to look similar to the DS solution in figure 25 which is at about  $12.5 \times 10^{-5}$ M.

The solution color changes with the dilution from a brilliant bright orange color at  $1.0 \times 10^{-2}$ M to a light nearly transparent yellow at  $1.0 \times 10^{-5}$ M. Dilution from  $1.0 \times 10^{-2}$  M to  $1.0 \times 10^{-4}$  M results in the shifting of the 450nm band to a higher energy maximum at 363nm. The 319nm band does not shift with dilution. The shifting of the broad absorption at 450nm upon dilution is indicative of their being more than one species present under the absorption band. Also the broadness of the absorption band at the saturated concentration level would lead one to suspect the presence of more than one species. Although it is not specifically labeled in figure 27 it can be seen that in the  $10^{-2}$ M solutions this low energy band has a width at half height of nearly 100nm.

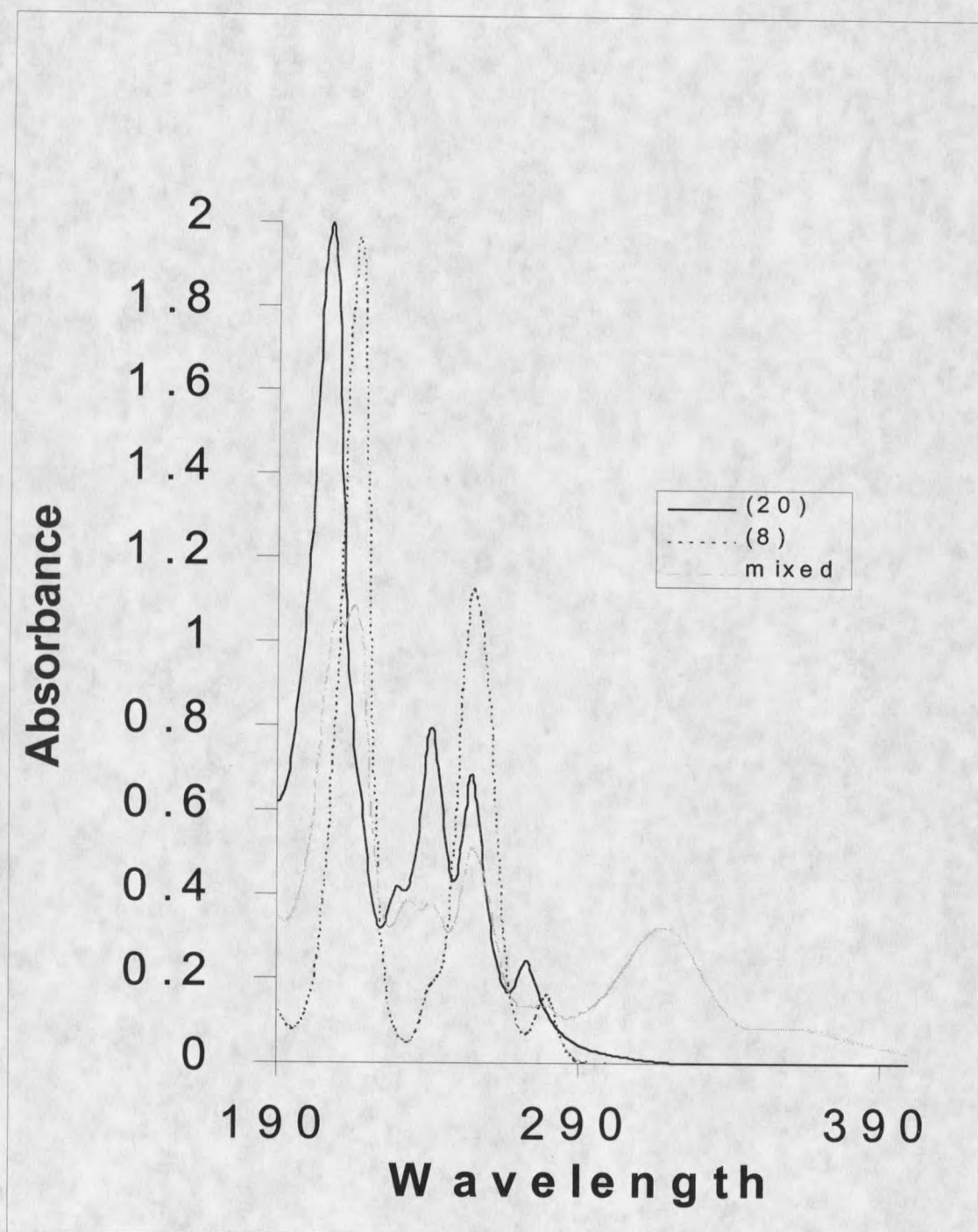


**Figure 25.** UV-Visible absorption spectra of separate equal concentration solutions of (8) and (20) with a spectra of the two solutions mixed together.

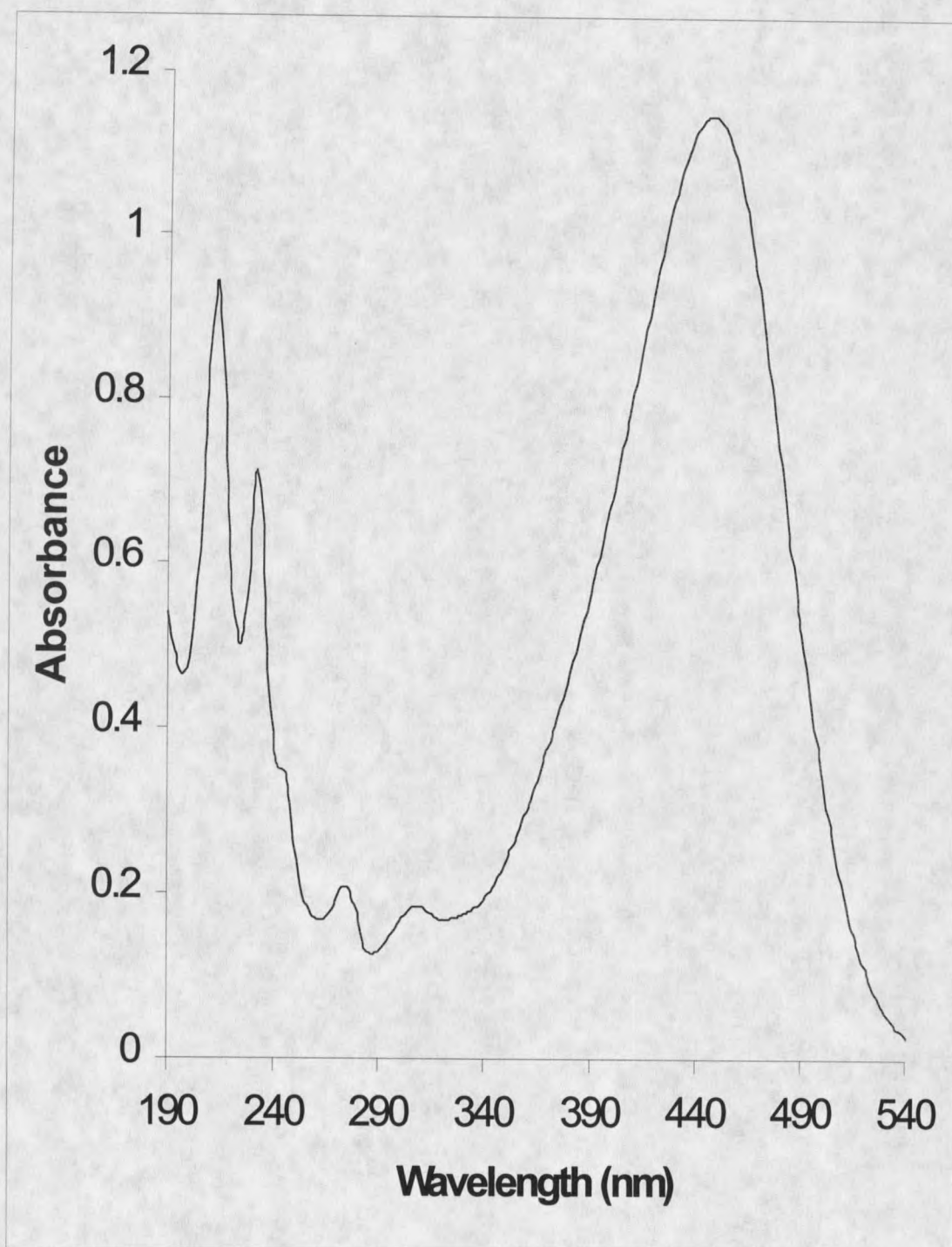


**Figure 26.** UV-Visible absorption spectrum of the  $1.0 \times 10^{-2}$  M DS (5).

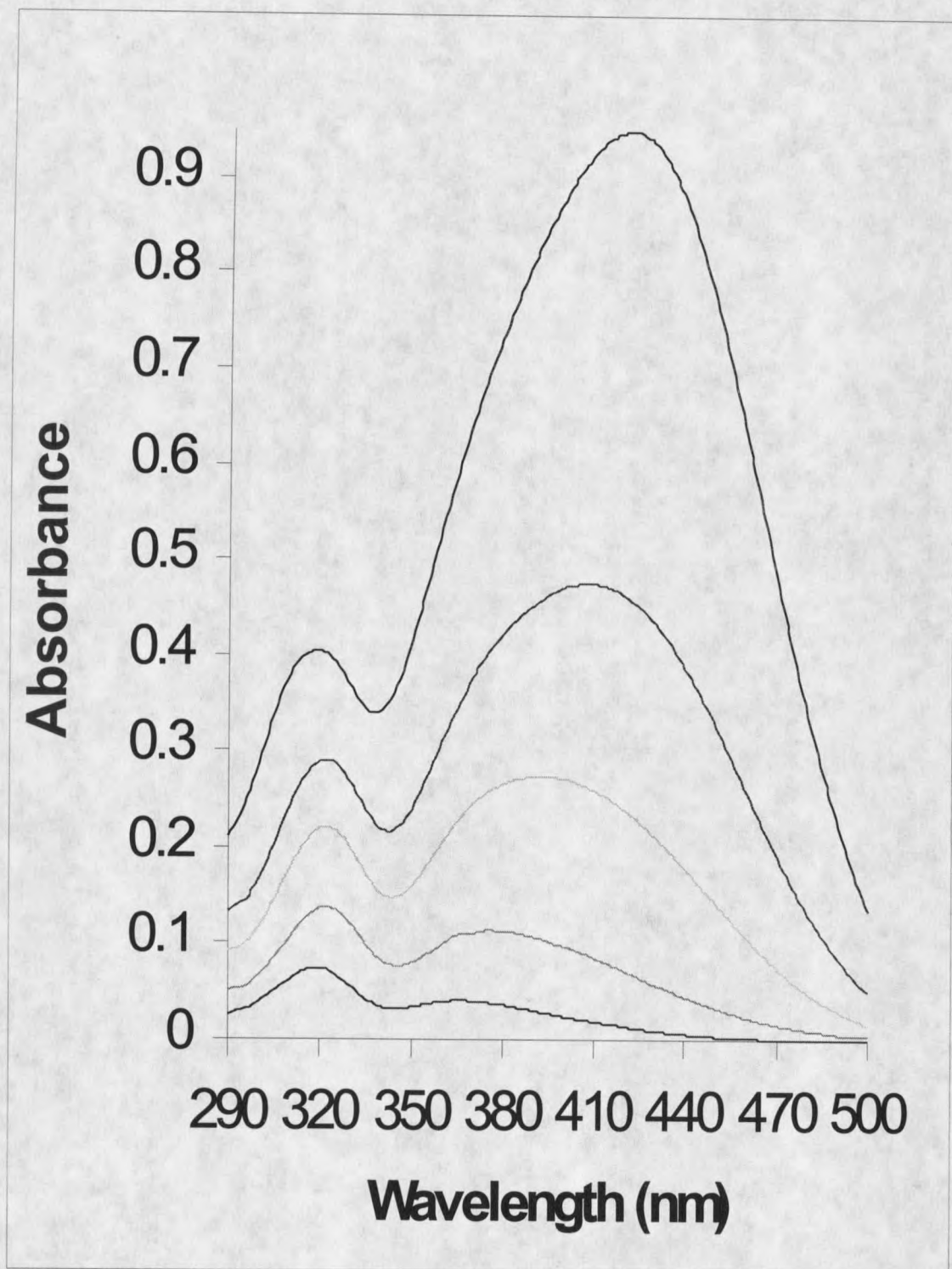


**Figure 27.** The DS (5) diluted over a ten fold concentration range of  $1.0 \times 10^{-3} \text{M}$  to  $1.0 \times 10^{-4} \text{M}$ .

Further dilution of the  $1.0 \times 10^{-4}\text{M}$  solution to concentrations less than  $1.0 \times 10^{-5}\text{M}$  results in the complete loss of the 363nm band with only the 319nm band remaining. This indicates there are at least three species absorbing in the visible region of the spectrum. This includes the dinuclear DS (**5**) at 319nm and at least two species are under the broad band.

Absorption bands in the visible region of platinum DS complexes have been shown to be the result of  $M \rightarrow L$  charge transfer transitions that have been red shifted. Red shifts of this type are known as a Davydov shift (55-59). Most metal-metal complexes give visible bands that result from d-d transitions, which are not intense because of selection rules. Davydov shifts allow MLCT bands, which are totally allowed to shift into the visible region if they result from polarized transitions that is perpendicular to the xy plane. If the polarized transitions occur parallel to the xy-plane the corresponding Davydov shift is a blue shift (59). The greater is the Davydov shift the more intense the band usually is. This helps rationalize the intensity of these bands. The greater is the red shift in the visible spectrum of complexes with platinum-platinum interactions often correlates with a reduction in the Pt-Pt separation distances. In the case of the tetracyanoplatinate(II) salts the Pt-Pt separation distance is predictable by the color of the solid complex (13). For example in the solid TCP's the  $\text{SrPt}(\text{CN})_4 \cdot 3\text{H}_2\text{O}$  has a metal-metal distance of  $3.09\text{\AA}$  with an absorption band near 500nm. The  $\text{MgPt}(\text{CN})_4 \cdot 4.5\text{H}_2\text{O}$  has a metal-metal distance of  $3.36\text{\AA}$  with an absorption band near 350nm.

The bands present in the visible region of the spectrum in the DS solutions are the result of allowed transitions as indicated by their large molar absorptivities. One multinuclear species described in these equilibria has a molar absorptivity of  $57000\text{L}/\text{cm}^{-1}\text{M}^{-1}$ .

Because of the evidence of numerous multinuclear species present in the higher concentration solutions the equilibrium model and equilibrium constants were determined in a stepwise manner. At concentrations of  $1.0 \times 10^{-5}\text{M}$  the solutions contain nearly all dimer. This solution was evaluated first because of the ease of determining the equilibrium constants and the thermodynamic parameters when only one metal-metal associated species is present. Higher concentration solutions were then evaluated. The solutions were then evaluated at  $1.0 \times 10^{-4}\text{M}$  followed by solutions at  $1.0 \times 10^{-3}\text{M}$ . Good overviews of multistep equilibria and the determination of equilibrium constants from spectrophotometric data can be found in the literature (60,61,62).

The equilibria of solutions with concentrations higher than  $1.0 \times 10^{-3}\text{M}$  were not studied because it was apparent at these concentrations there is considerable association of (8) and (20). It can be speculated that more than five associated species are present at concentrations higher than  $1.0 \times 10^{-3}\text{M}$ .

## Modeling the Solution Equilibrium Using Continuous Variation (CV) Method

### Determination of the Stoichiometry of the Solution Species

Stoichiometry of the solution species was determined by the continuous variations (CV) method (47). The CV method is also known as the Job's method. Doing the CV method involves keeping the total platinum concentration constant but varying the ratios of **(8)** and **(20)**. Plotting the absorbance against the ratio of platinum complexes in the solution will result in the maximum absorbance when the mole fractions of each species are equal. An idealized CV experiment for a product that forms in a 1:1 ratio of the two reactants and its absorption band does not overlap with bands from the reactants would give a absorption maximum when the ratio of the two reactants are equivalent.

CV experiments done at a total concentration of  $1.0 \times 10^{-5}$  M show the 319nm absorbance is the result of the di-nuclear **(5)**. The 319nm band is maximized at a .5 ratio of **(20)** to **(8)**, which gives 1:1 stoichiometry. Figure 28 is the Jobs plot of the 319nm band at a concentration of  $1.0 \times 10^{-5}$ M. When CV experiments are done with solutions containing a total platinum concentration of  $1.0 \times 10^{-4}$ M the band at 363nm is maximized when the ratio of **(20)** and **(8)** is 2:1. This is seen in figure 29 where the absorbance is maximized at a .7 ratio of **(20)** to **(8)**, which correlates to a 2:1 stoichiometry respectively. The 2:1 stoichiometry correlates with the tri-nuclear complex  $[\text{Pt}(\text{CNC}_2\text{H}_5)_4]_2[\text{Pt}(\text{CN})_4]^{2+}$  **(28)**.

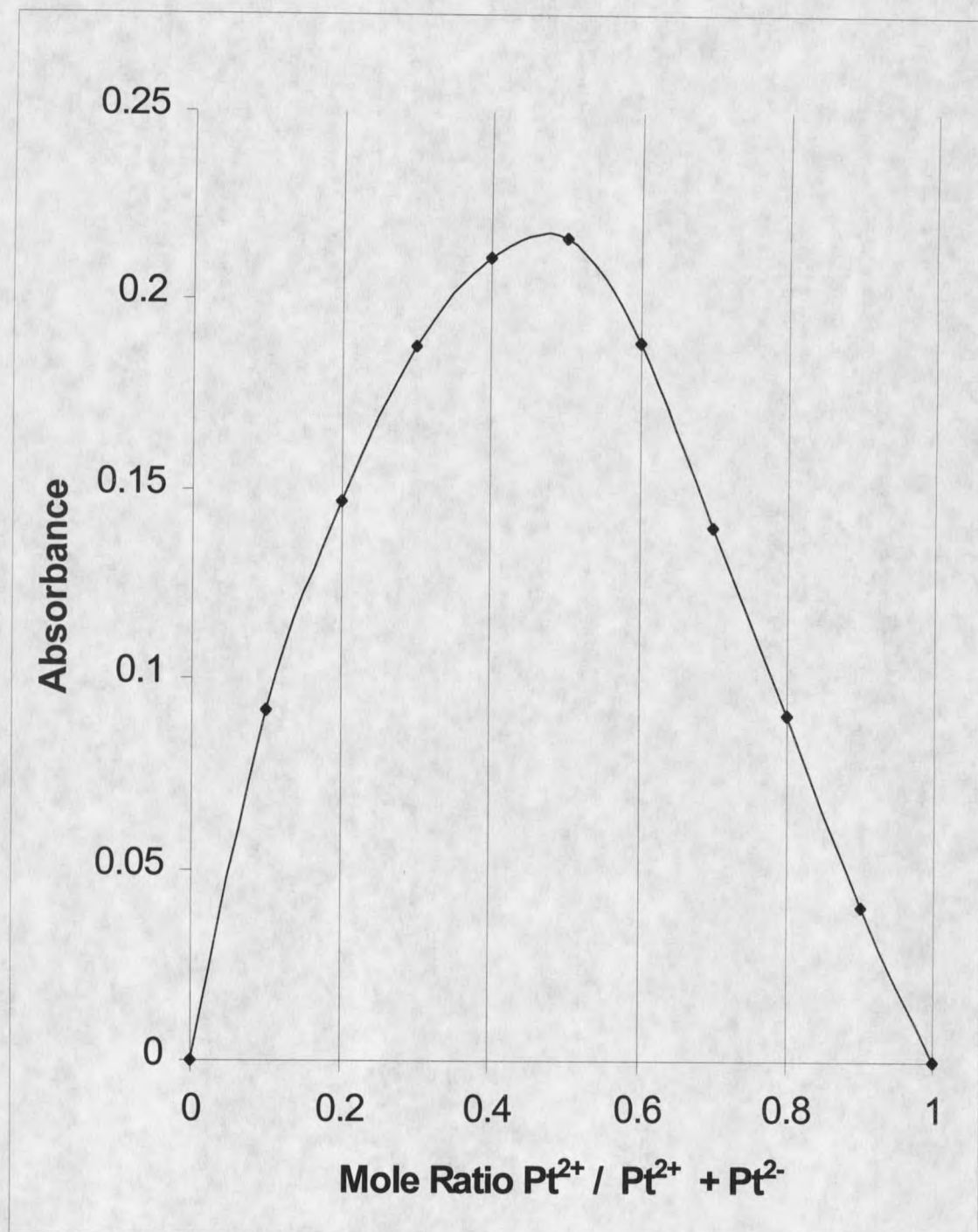


**Figure 28.** CV plot of the 319nm band at  $1.0 \times 10^{-5}M$  in total platinum concentration of **(8)** and **(20)**.

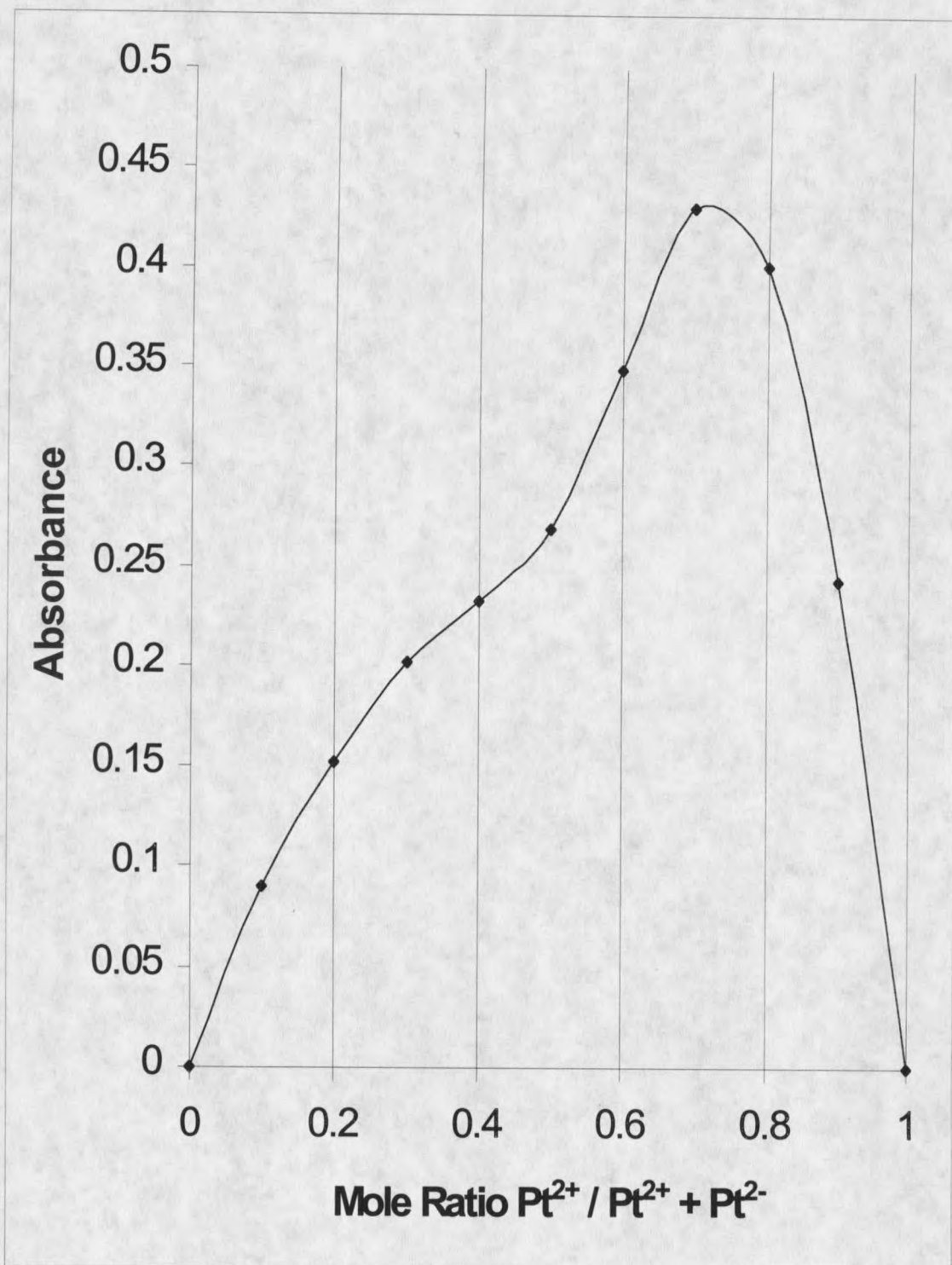


**Figure 29.** CV experiment of the 363nm band at  $1.0 \times 10^{-4}\text{M}$  in total platinum concentrations of (8) and (20).

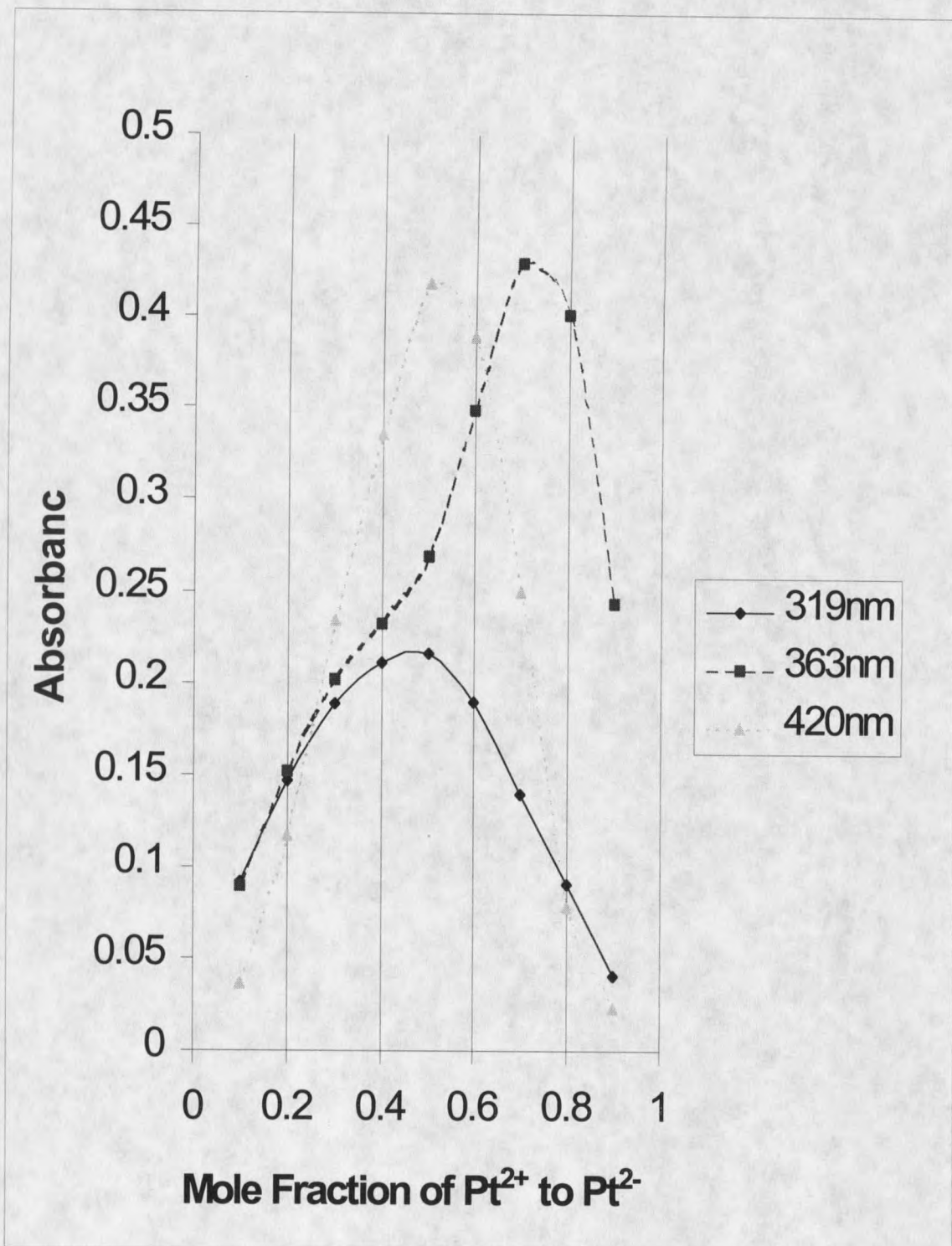


**Figure 30.** CV experiments for the determination of stoichiometry for (5), (28) and (29) at  $1.0 \times 10^{-5}\text{M}$ ,  $1.0 \times 10^{-4}\text{M}$  and  $1.0 \times 10^{-3}\text{M}$  respectively.

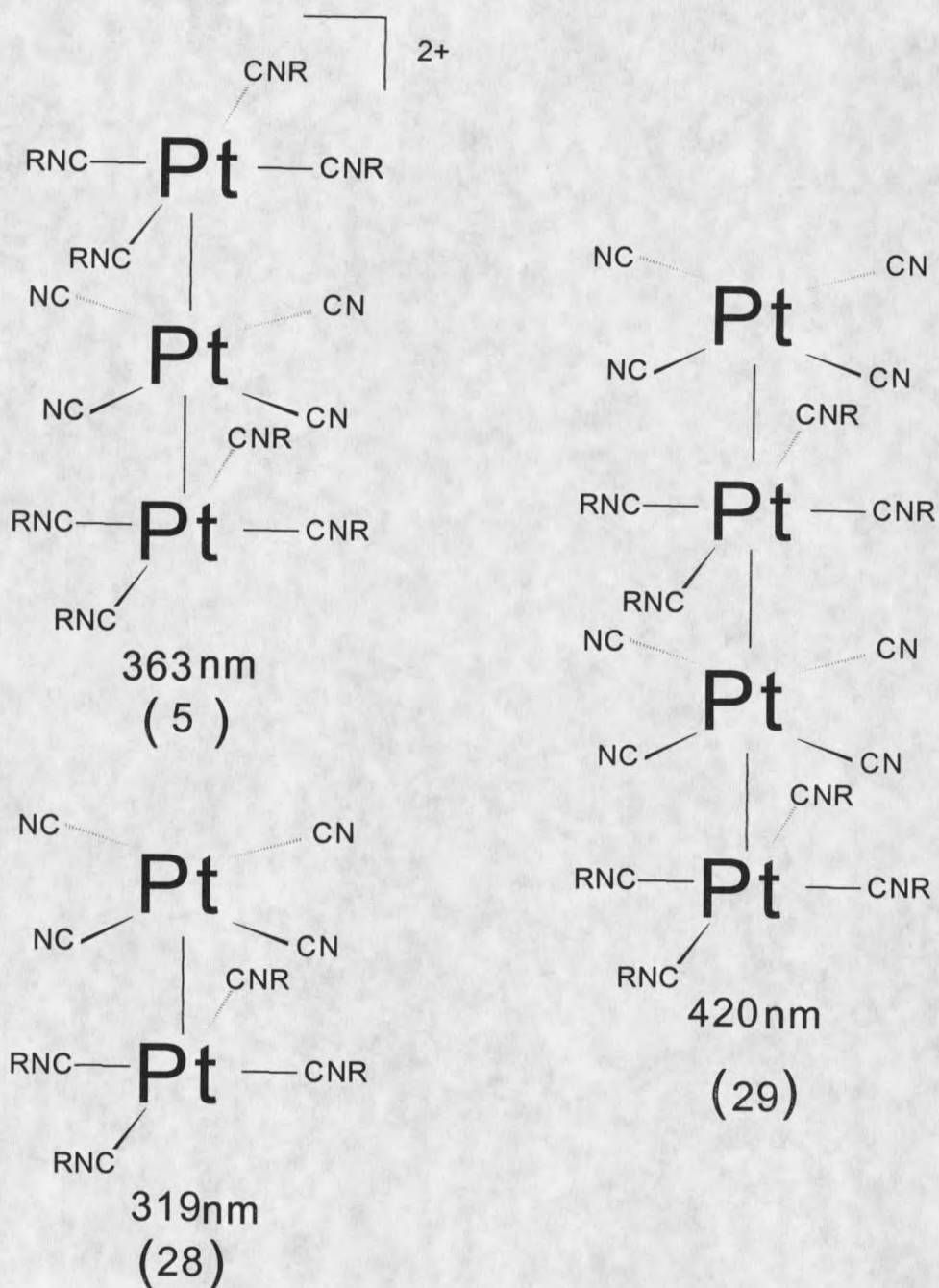


**Figure 31.** Structural representations of the three multinuclear species that result in absorption maximum at 319nm, 363nm and 420nm.

When the CV experiment is done with a total platinum concentration of  $1.0 \times 10^{-3}\text{M}$  and the platinum ion ratios are 1:1, a single band obscures the 370-460nm region of the spectrum. The 420nm absorption maximum is therefore also of 1:1 stoichiometry but the lower energy maximum would indicate it is a higher associated complex than **(5)**. The 420nm band is assigned to the tetra-nuclear species  $[\text{Pt}(\text{CNC}_2\text{H}_5)_4]_2[\text{Pt}(\text{CN})_4]_2$  **(29)**. Figure 30 is an overlay of the CV experiments done at three different concentrations revealing the ratio of **(20):(8)** for the three multi-nuclear species. Figure 31 shows the structural representation of the three multinuclear species characterized in the solutions and each species respective absorption maximum.

Complexes **(5)**, **(28)**, and **(29)** are all evident in the CV experiments at  $1.0 \times 10^{-3}\text{M}$ . Both the 319 and 363nm bands are evident in the solutions when one or the other parent complexes is in excess but as the ratio of the platinum complexes approach's 1:1 the absorbance maximum of the 363nm shifts to 420nm. In  $1.0 \times 10^{-5}\text{M}$  solutions the 319nm band has a positive deviation from Beers's law with increasing concentration. At solution concentrations of  $1.0 \times 10^{-3}\text{M}$  when the tetra-nuclear species begins to appear in the spectrum the 319nm band gives a negative deviation from Beers law. This gives farther evidence that the 420nm band is the result of a tetra-nuclear complex. Although it is not absolutely conclusive for all the species present in solution the CV experiments do give a good qualitative indication of the equilibrium model of the solution. For the CV experiments to be absolutely conclusive the bands for each species must

not overlap. There is some overlap in these solutions but it is not enough to make our qualitative conclusions invalid.

Trimer Formation It initially appeared there was selectivity in the formation of the two possible tri-nuclear complexes. The CV experiments did not initially show evidence for the existence of the tri-nuclear complex  $[\text{Pt}(\text{CNC}_2\text{H}_5)_4][\text{Pt}(\text{CN})_4]_2^{2-}$  (**30**) of 1,2 stoichiometry. Statistically if the 2,1 species forms one would expect the 1,2 species to also be present. It appeared due to the difference in peak intensities that the 2,1 species either formed more favorably than the 1,2 species or the molar absorptivity constant of the 1,2 is much smaller than the 2,1 species.

A closer look at the CV experiments was needed to determine if the 1,2 species formed. Solution ratios of 3:7 in (**20**) and (**8**) should maximize the total concentration of 1,2 like the 7:3 solution ratio maximizes the total formation of (**28**). The CV experiments showed a maximum at 385nm at a solution ratio of 3:7. Figure 32 is an overlay of the two spectra resulting from solutions ratios of 7:3 which maximizes (**28**) at 363nm and the solution ratio of 3:7. As the solution ratio was altered the band at 385nm shifts unlike the 363nm band for (**28**) which does not shift on altering the solution ratios. With changing ratios the 363nm band only increases and decreases in absorbance. This indicates the 1,2 species does not have an absorption maximum at 385nm. Figure 32 also gives some indication that the molar absorptivity constant of the 1,2 species is

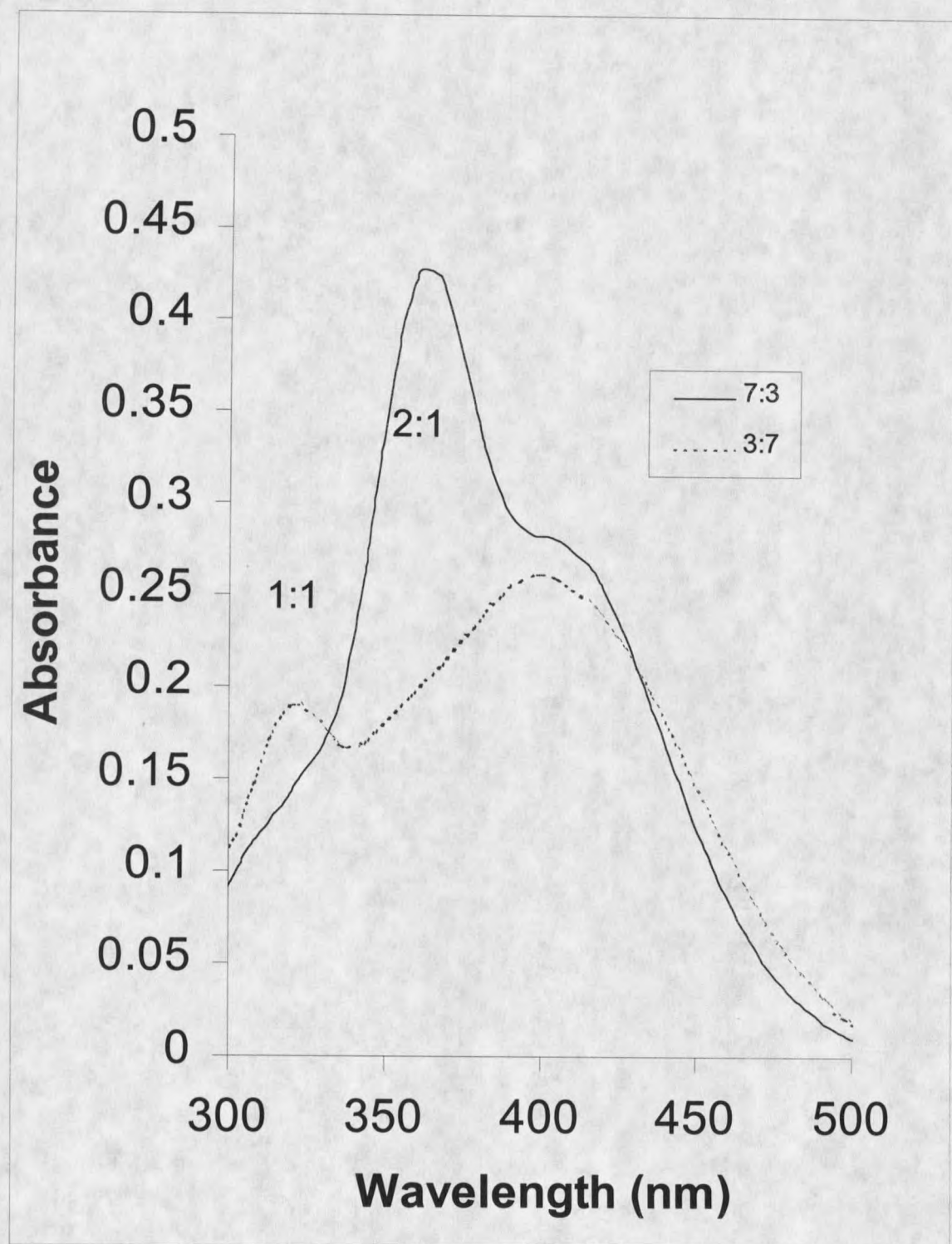


**Figure 32.** Visible spectrum of solution ratios 3:7 and 7:3 of (20):(8) giving the 363nm absorption maxima for (28) and the false maxima for (30) at 385nm.

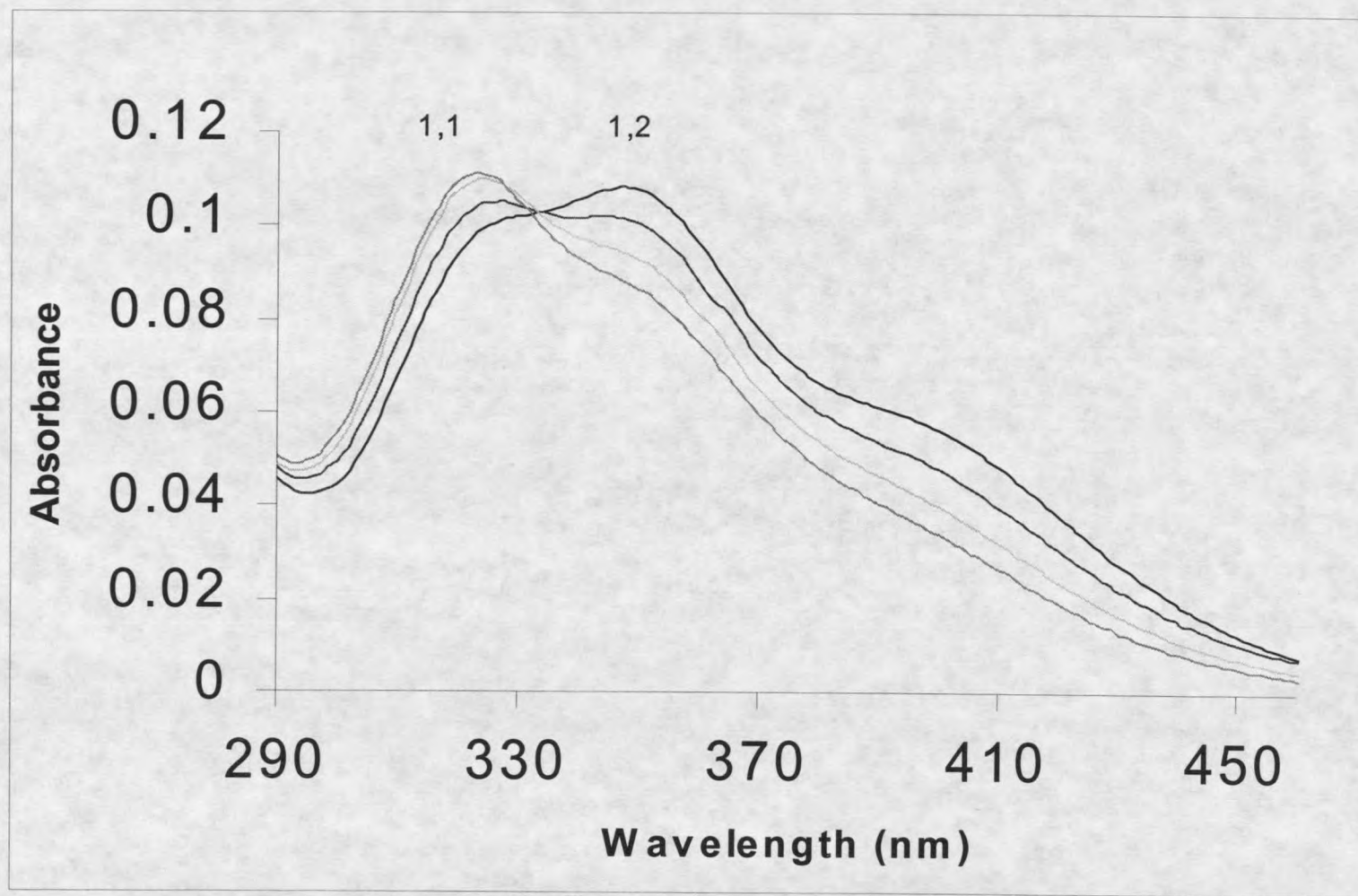


Figure 33. 1:9 solution ratio of (8) and (20) at four temperatures. Absorption maximum of (30) is at 350nm.

smaller than its 2,1 counterpart because the absorbance values are similar at the lower energy region where the 2,2 species absorbs. This reveals the equilibrium of the 2,2 species is the same in the 3:7 and 7:3 solutions ratios, which should be expected.

When the multi-temperature experiments were eventually done the 1,2 species became apparent. Figure 33 shows the visible region of the spectrum for solutions containing a 1:9 ratio of (20) and (8). This ratio will not maximize the total concentration of the trimer but it will maximize its formation with respect to the other multi-nuclear species. A band becomes apparent at 350nm that does not shift with a change in the temperature of the solution. The occurrence of the  $\lambda_{\max}$  for the 1,2 occurring between 363nm and 319nm is likely because of the lack of an isosbestic point between these two wavelengths in the CV experiment. The lack of an isosbestic point indicates that more than two metal-metal associated species are present in this region of the spectrum. If the 1,2 complex had a absorption maximum as far to low energy as 385nm it would result in an isosbestic point between the 1,1 and 2,1 species around 340nm. At the very least the region around 340nm would approximate an isosbestic point.

Additionally if the 1,2 absorbed at 385nm the spectra containing excess cyanide would exceed the absorbance of the excess isocyanide beyond 385nm because the 1,2 would have a shoulder that extended out farther than the 2,1. The opposite is the case when the 3:7 and 7:3 solution ratios are compared in figure 32. The excess isocyanide spectra have a greater absorbance at 400nm

but both solutions have absorption values very near each other at the low energy region of the spectrum. Also the spectra of the 1:9 and 9:1 ratios approach zero absorbance at 400nm revealing that any absorbance in this low energy region is due to the 2,2 species only. The 1:9 and 9:1 solution ratios highly favor an associated species with non-stoichiometric equivalents of one complex or the other. At these ratios it is safe to approximate nearly zero formation of the tetra-nuclear species and thus no absorption at 420nm would be from the tetra-nuclear species. Figure 34 shows the structural representation of the anionic tri-nuclear species (30).

The two main hypotheses were concerning why the 1,2 species is not readily observed in the spectrum like its 2,1 counterpart were not completely explained until the equilibrium constants were determined. The first hypothesis that the 1:2 forms in a lesser quantity than the 2:1 tri-nuclear species was shown to be incorrect via the equilibrium constant calculations which resulted in similar formation constants for the 1,2 and 2,1 models. In all the computer generated refinements of the equilibrium constants the 2,1 constant was a little larger than the 1,2 equilibrium constant. Although the difference is not very much it was the case in every refinement, which makes it statistically significant. There are differences in the tri-nuclear species chemical makeup but it would not seem reasonable for any electronic effects to lead to the difference in formation constants. Most significantly is the fact that statistically it would not be expected for one of the tri-nuclear species to form in a greater quantity over the other one.

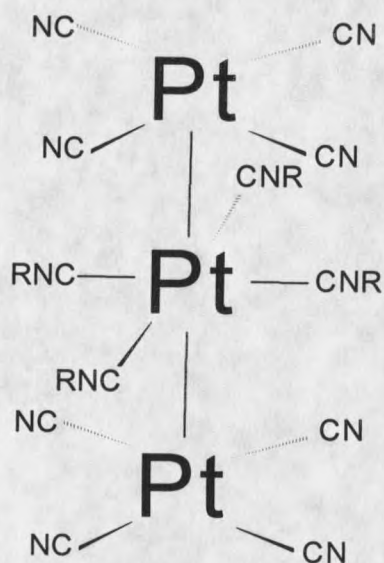


**Figure 34.** Structural representation of the tri-nuclear species (30).

Secondly the possibility that the 1:2 species is formed in similar quantities as the 2:1 but has a much lower absorptivity coefficient than the 2:1 trimer was found to be the case. This was also determined from the equilibrium program. It will be described that both the 2:1 and 1:2 result in solution with similar equilibrium constants and the molar absorptivity constant of the 1,2 species is smaller than that of the 2,1 species. This was expected from the evidence shown in the CV experiments like that shown in figure 32.

Before the computer generated equilibrium constants and absorptivities were obtained attempts were made to determine the reasons for the differences

in the spectrum for **(28)** and **(30)**. The spectra obtained from the CV experiments at 17°C appear to reveal the greater disappearance of the isocyanide complex compared to the cyanide complex. This was done with comparison of the band intensities at 207 and 216nm. Figure 35 shows the UV portion of the spectrum for solutions with 1:7 and 7:1 ratios of **(20)** and **(8)** overlaid with spectra of pure solutions of **(20)** and **(8)**. Typical of all CV experiments, the total platinum concentrations of all solutions in figure 35 are equivalent.

The 207nm and 216nm absorbance bands are the result of transitions in the isocyanide and cyanide complexes respectively. When the spectra of separate, equal concentration solution of **(8)** and **(20)** are ran the highest energy bands show a greater absorbance for the isocyanide than the cyanide. This should be the case since the absorptivity of the isocyanide is slightly larger. However, the 7:1 and 1:7 ratio solutions of **(8)** and **(20)** show a smaller absorbance for the 207nm band. If the associated species did not absorb in this region and there was equal consumption of the monomers it would be expected to see the same absorption band ratio for 7:1 and 1:7 as the 8:0 and 0:8. The larger ratio of the 1:7 solution has two possible explanations. The first is that less of **(8)** is consumed which would give a greater equilibrium concentration of the 2:1 trimer. Secondly is the possibility of the associated species absorbing in this region of the spectrum. The refinement of the molar absorptivity constants proved the latter to be the case.

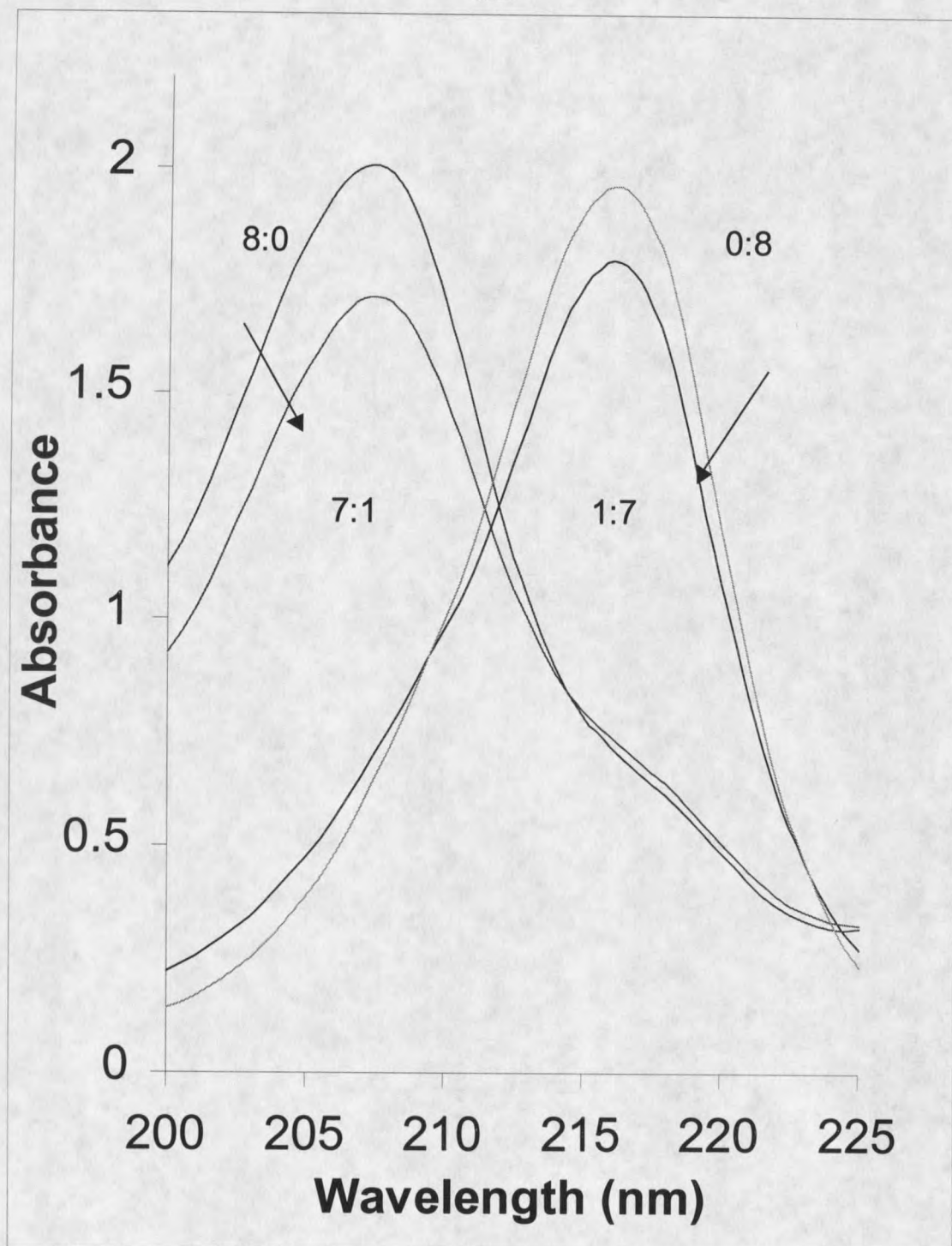


**Figure 35.** 209nm and 216nm UV bands of (8) and (20) and their 1:7 and 7:1 mixtures.

The appearance of dissimilar consumption of monomeric material shown in the 207nm and 216nm bands was fully understood once the molar absorptivity constants were known. The refinement determined the 1,2 complex has a much greater molar absorptivity at 216nm than at 207nm. Thus this would increase the intensity of the 216nm band when the cyanide ion is in excess. This was more noticeable in the spectrum at lower temperatures because this favors even higher associated species than the dinuclear species. Refinement of the equilibrium constants made it possible to conclude that the 1,2 species formed in about the same quantity as the 2,1 but its visible absorbance band is nearly consumed by the more intense band of the 2,1 species.

#### Equilibrium Model Selection

The equilibrium model determined from the CV contains six species all in equilibrium with measurable concentrations at  $1.0 \times 10^{-3}M$  in total platinum complex concentrations. There is evidence for further association than the tetra-nuclear species but it is negligible in the  $1.0 \times 10^{-3}M$  double salt solution concentrations. At  $1.0 \times 10^{-4}M$  in total platinum complex concentration there is not significant enough tetra-nuclear formation for the computer program to refine for it.  $1.0 \times 10^{-3}M$  solutions were studied because they give the greatest concentration of associated species which can still be refined sequentially with

the computer program hyperquad. There are six stepwise equilibrium expressions describing the model as shown in scheme 2.

Scheme 2

| <u>Equilibrium Expression</u>  | <u>Label</u> | <u>Model</u> |
|--|--------------|--------------|
| $\text{Pt}(\text{CNC}_2\text{H}_5)_4^{2+} + \text{Pt}(\text{CN})_4^{2-} \rightleftharpoons [\text{Pt}(\text{CNC}_2\text{H}_5)_4][\text{Pt}(\text{CN})_4]$  | $K_1$        | 1,1          |
| $[\text{Pt}(\text{CNC}_2\text{H}_5)_4][\text{Pt}(\text{CN})_4] + \text{Pt}(\text{CNC}_2\text{H}_5)_4^{2+} \rightleftharpoons [\text{Pt}(\text{CNC}_2\text{H}_5)_4]_2[\text{Pt}(\text{CN})_4]^{2+}$     | $K_2$        | 2,1          |
| $[\text{Pt}(\text{CNC}_2\text{H}_5)_4][\text{Pt}(\text{CN})_4] + \text{Pt}(\text{CN})_4^{2-} \rightleftharpoons [\text{Pt}(\text{CNC}_2\text{H}_5)_4][\text{Pt}(\text{CN})_4]_2^{2-}$                  | $K_3$        | 1,2          |
| $[\text{Pt}(\text{CNC}_2\text{H}_5)_4]_2[\text{Pt}(\text{CN})_4]^{2+} + \text{Pt}(\text{CN})_4^{2-} \rightleftharpoons [\text{Pt}(\text{CNC}_2\text{H}_5)_4]_2[\text{Pt}(\text{CN})_4]_2$              | $K_4$        | 2,2          |
| $[\text{Pt}(\text{CNC}_2\text{H}_5)_4][\text{Pt}(\text{CN})_4]_2^{2-} + \text{Pt}(\text{CNC}_2\text{H}_5)_4^{2+} \rightleftharpoons [\text{Pt}(\text{CNC}_2\text{H}_5)_4]_2[\text{Pt}(\text{CN})_4]_2$ | $K_{4'}$     | 2,2          |
| $2[\text{Pt}(\text{CNC}_2\text{H}_5)_4][\text{Pt}(\text{CN})_4] \rightleftharpoons [\text{Pt}(\text{CNC}_2\text{H}_5)_4]_2[\text{Pt}(\text{CN})_4]_2$  | $K_{4''}$    | 2,2          |

The overall formation constant of the tetra-nuclear species has three possible routes to its formation, which are labeled  $K_4$ ,  $K_{4'}$  and  $K_{4''}$ . It must be remembered that regardless of the mechanism of a reaction the overall thermodynamic parameters will remain unchanged.  $\beta_4$  will contain the thermodynamic data for all of the stepwise constants regardless of which pathway is favored for the formation of the tetra-nuclear species. The overall equilibrium expression for the tetra-nuclear species could also be described as scheme 3.

Scheme 3

$$\beta_4 = K_1 K_x K_y \text{ where } K_x = K_2 \text{ or } K_3 \text{ and } K_y = K_4 \text{ or } K_4' \text{ respectively}$$

$$\text{and if } K_y = K_4' \quad \beta_4 = [K_1]^2 K_4'$$

The most concentrated solution that was used for modeling the solution equilibrium was the  $1.0 \times 10^{-3} \text{M}$  in DS. Although the  $1.0 \times 10^{-2} \text{M}$  solutions undoubtedly have higher concentrations of (5), (28), (29) and (30) the extreme shifting of the visible band indicates significant formation of multi-nuclear species larger than the tetra-nuclear (29). There is also a lack of band resolution at saturated levels. CV experiments done at this high a concentration don't reveal individual bands with changing solution ratios. All the bands overlap into one band at all solution ratios when the total concentration is  $1.0 \times 10^{-2} \text{M}$ . This leaves the determination of the full equilibrium at concentrations where precipitation of the solid DS occurs to be speculative. Sufficient amounts of the tetra-nuclear species are present at solution concentrations of  $1.0 \times 10^{-3} \text{M}$  yet there appears to be only small quantities of higher association.

Double Salt Solution Preparations      No additional salt was used for constant ionic strength for the equilibrium studies. This was initially done because of the low concentrations used in these studies constant ionic strength can be assumed. It was also feared that any added salt would only disrupt ion-ion interactions of interest. All the interactions studied were initially thought to

occur due to significant electrostatic interactions. This ended up to not be entirely the cause of the interactions between **(20)** and **(8)**. After the experiments were run the  $1.0 \times 10^{-3}\text{M}$  DS was observed with a 100X excess of  $\text{Al}_2\text{SO}_4$  and  $\text{KNO}_3$ . The visible absorption bands for the multinuclear complexes showed only small changes in the visible absorption bands. There are shifts in the equilibrium due to the addition of an excess salt but the changes are not drastic to where the interactions are suppressed. Figure 36 shows an overlay of a  $1 \times 10^{-3}\text{M}$  DS solution without the addition of excess salt and one in  $.1\text{M}$   $\text{Al}_2\text{SO}_4$ . The solution pH is 5.5. Thermal expansion was not corrected for because it resulted in  $<1\%$  difference in the equilibrium constants. Refinement of all the equilibrium constants simultaneously, excluding  $K_1$ , was done using the  $1.0 \times 10^{-3}\text{M}$  solutions.  $K_1$  was always held constant during the refinements because it was determined with good accuracy using the low concentration solutions.

Solving of the Equilibrium Constants Visual inspection of the absorption spectrum of the DS solutions clearly reveals that the associated species present in solution also absorb at some of the same wavelengths that their parent complexes do in addition to the new visible bands. Figure 37 is an overlay of the separate **(20)** and **(8)** solutions along with the spectrum of **(20)** and **(8)** mixed together. Conversely it is apparent that there are wavelengths the associated species do not have absorptivities like their parent complexes do.

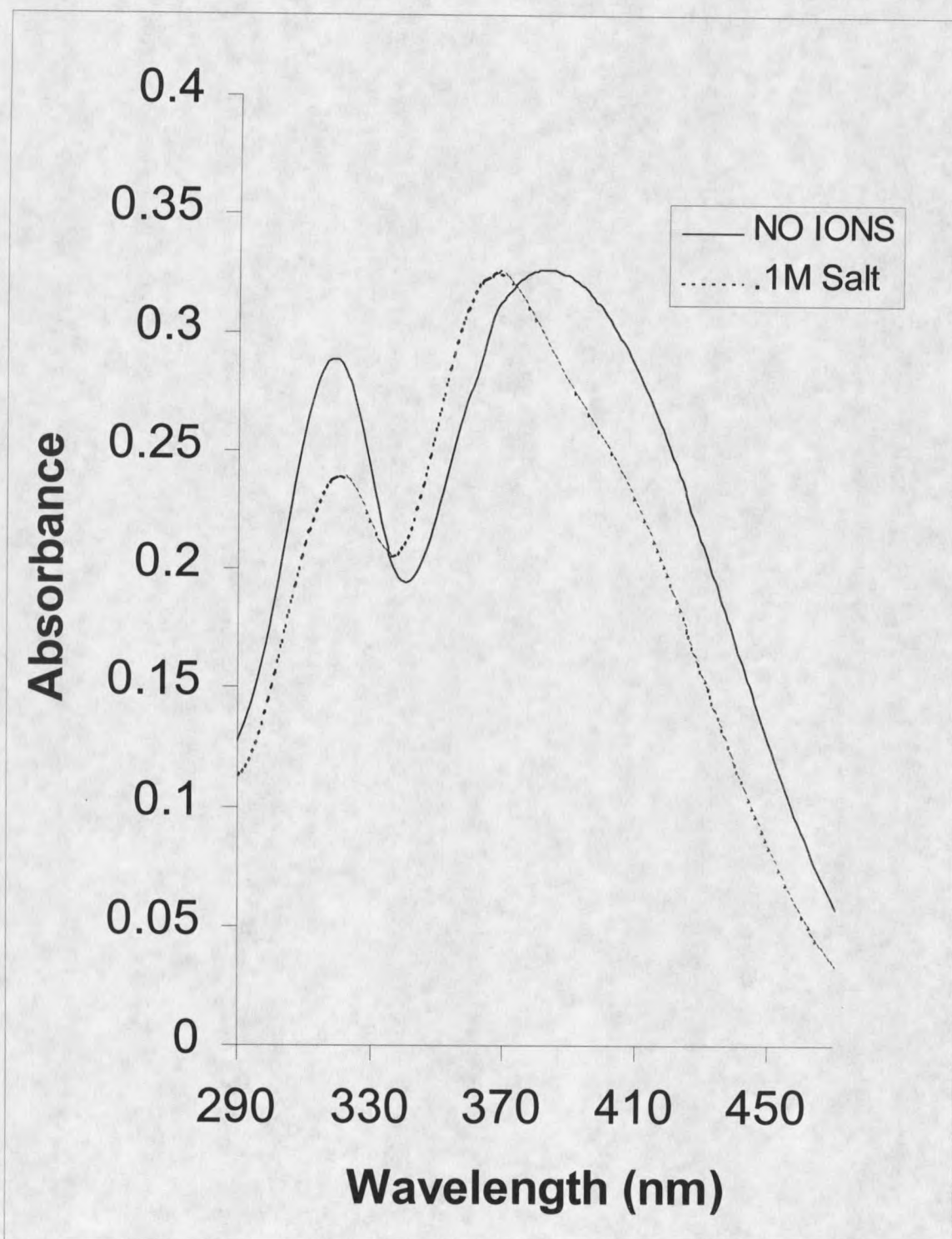


Figure 36. Overlay of two  $1.0 \times 10^{-3} \text{ M}$  solutions in pure water and  $.1 \text{ M Al}_2\text{SO}_4$ .

The disappearance of bands and the addition of new bands in the UV region allow for estimations of the molar absorptivity constants at various wavelengths for the newly formed metal-metal complexes. This is valuable for the computer calculations of the equilibrium constants.

The most recognizable wavelength where no absorption occurs from the associated species is near the band at 255nm. Both of the parent platinum complexes have large absorptivities at this wavelength. When the two parent platinum complexes are mixed in equal molar amounts the absorbance at 255nm drops significantly. This makes it possible to assume an absorptivity of 0 at 255nm for the new species in the solution. However, other higher energy bands do not decrease nearly as much as the 255nm band when the two platinum complexes are mixed. This indicates there is overlapping bands in the UV between the parent complexes and the new associated species. The bands where visual inspection reveals some or all of the associated species have significant absorptivities are at 209, 216, 233 and 242nm.

Further evidence for oligomer absorptivity in the UV region arises from the near existence of isosbestic points or the complete lack of isosbestic points. The parent cyanide **(8)** has a absorption at 216nm and 280nm and the isocyanide absorbs at 209nm and 273nm. These are two examples of where **(20)** and **(8)** have overlapping absorption bands. A continuous variations experiment would result in an isosbestic point in either of these regions of the spectrum if there were only two species absorbing in these regions.

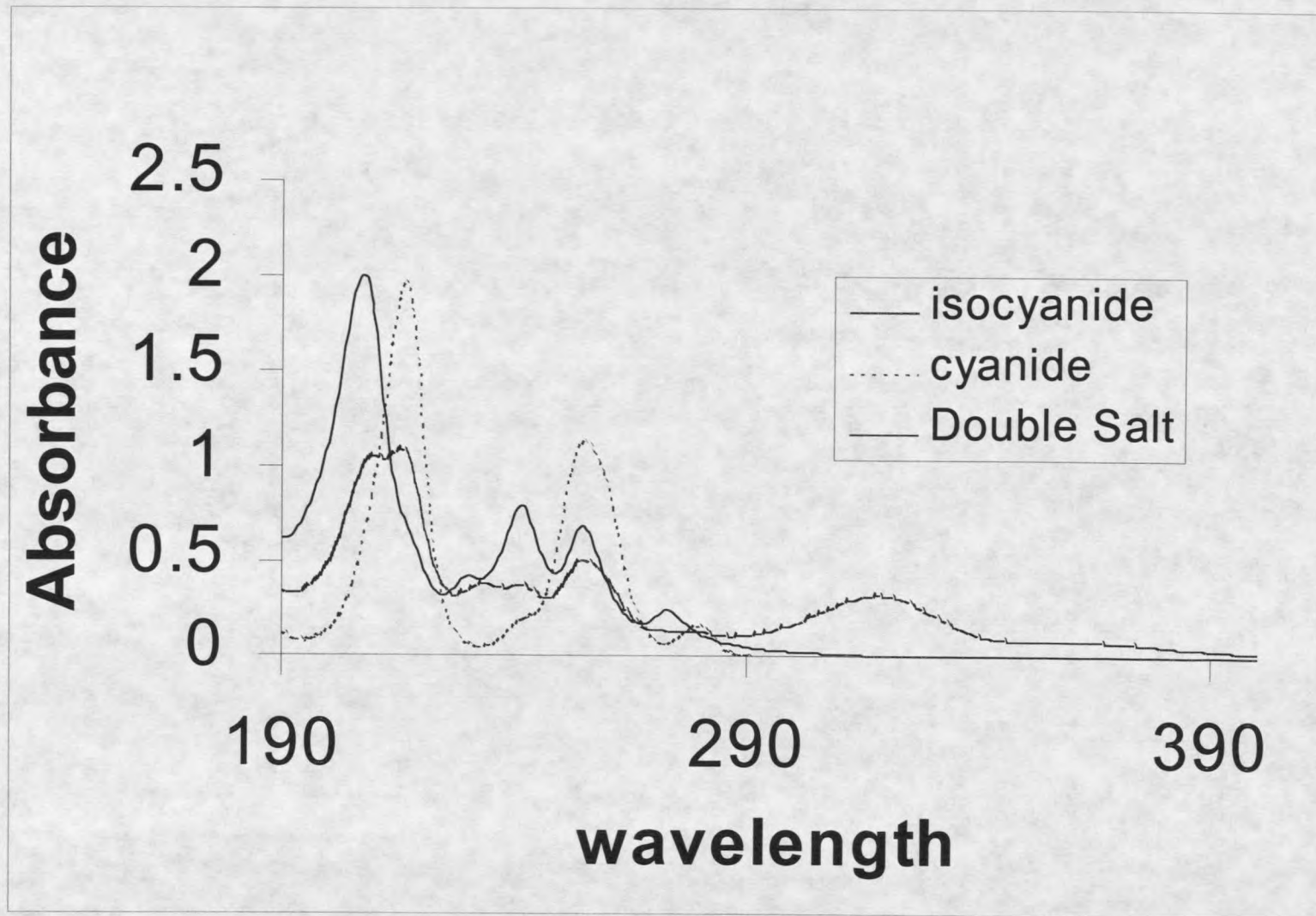


Figure 37. Overlay of the entire UV-Visible spectrum of (8) and (20) and the spectrum of the two ions mixed.

The higher energy region between 209nm and 216nm contains no evidence of an isosbestic point whereas the region between 273 and 280nm does show a partial isosbestic point. It is not a perfect isosbestic point but it is very close. The absorption between 273nm and 280nm due to a third species is very small.

Determination of  $K_1$   $K_1$  for association of the two monomers (20) and (8) was determined first at low concentrations.  $K_1$  was determined from a solution concentration range from  $6.0 \times 10^{-6}$  to  $2.0 \times 10^{-5}$ M. At these concentrations it could be assumed that the only association in solution is that of the dinuclear species. Concentrations greater than  $3.0 \times 10^{-5}$ M in DS begin to give significant concentrations of the higher multi-nuclear species as seen in the visible region of the spectrum at 363nm. A plot of  $C/A^{1/2}$  versus  $A^{1/2}$  gives a slope equal to  $\epsilon^{-1}$ . This relationship is derived from the equilibrium expression in scheme II. Substitution of Beers law into the equilibrium constant expression gives equation 10.

$$K = A/\epsilon / (C-A/\epsilon)^2 \quad (10)$$

Figure 10 is further transformed into equation 11, which is in linear form.

$$C/A^{1/2} = A^{1/2}/\epsilon + 1/K^{1/2} \epsilon^{1/2} \quad (11)$$

Isci and Mason used this method for solving the equilibrium constant for the dinuclear species of the DS in acetonitrile solution (55). This equation is only valid if the dinuclear species does not have overlapping bands with other species. The  $1.0 \times 10^{-5}$  M solution is assumed to contain >95% proportion of the dinuclear species compared with any other multi-nuclear species. The solution concentrations of  $6.0 \times 10^{-6}$  to  $2.0 \times 10^{-5}$  M used in the determination of  $K_1$  contained nearly no 363nm band similar to that seen in figure 35. Calculations of  $K_1$  at all concentrations gave equilibrium constants within 5%.

The acetonitrile solutions of the DS near the solubility limit are similar in spectra to the dilute solutions of the DS in water. In acetonitrile at the solubility limit there is a small band beginning to appear near 400nm. This second band is also due to a higher oligomer forming. However it is never present in significant amounts. The 400nm band is just beginning to be apparent at the solubility limit in the acetonitrile solutions. The equilibrium constants are included in table 10 with the other multinuclear equilibrium constants determined in the following section.

Determination of  $K_2$ ,  $K_3$  and  $K_4$  Solving of the formation constants was done using the hyperquad suite of programs developed by Gans et. al (48). Using the equilibrium models that were determined from the CV experiments for the hyperquad program resulted in refinement for the stepwise equilibrium constants. The hyperquad program calculates the overall formation constants

$\beta$ 's, but simple algebra is all that is needed to determine the stepwise constants from the overall formation constants. Where

$$\begin{aligned}\beta_1 &= K_1 \\ \beta_2 &= K_1 K_2 \\ \beta_3 &= K_1 K_3\end{aligned}$$

The overall formation constant  $\beta_4$ , is given by three different stepwise formation pathways that all lead to the tetra-nuclear species (29).

$$\begin{aligned}\beta_4 &= K_1 K_2 K_4 \\ \beta_{4'} &= K_1 K_3 K_{4'} \\ \beta_{4''} &= [K_1]^2 K_{4''}\end{aligned}$$

$\beta_4$  is the overall formation constant through the cationic 2,1 trimer.  $\beta_{4'}$  is the overall formation through the anionic 1,2 tri-nuclear species and  $\beta_{4''}$  is the constant through dimerization of the dimer. It will always be true for this equilibrium model that  $\beta_4 = \beta_{4'} = \beta_{4''}$ .  $\beta_2$ ,  $\beta_3$  and  $\beta_4$  were refined with the hyperquad program simultaneously.  $\beta_1$  and thus  $K_1$  were determined in low concentration solutions. Figure 38 shows a pictorial representation of the equilibrium in water for (5) at  $1.0 \times 10^{-3}$ M.

The low concentration data evaluated graphically with eq. 11 was useful to determine if the equilibrium program was fitting the absorption data satisfactorily.  $K_1$  determined graphically and with the hyperquad suite of programs were within 5% of one another. The  $K_1$  determination by hyperquad was the one used in further refinements of the higher constants.

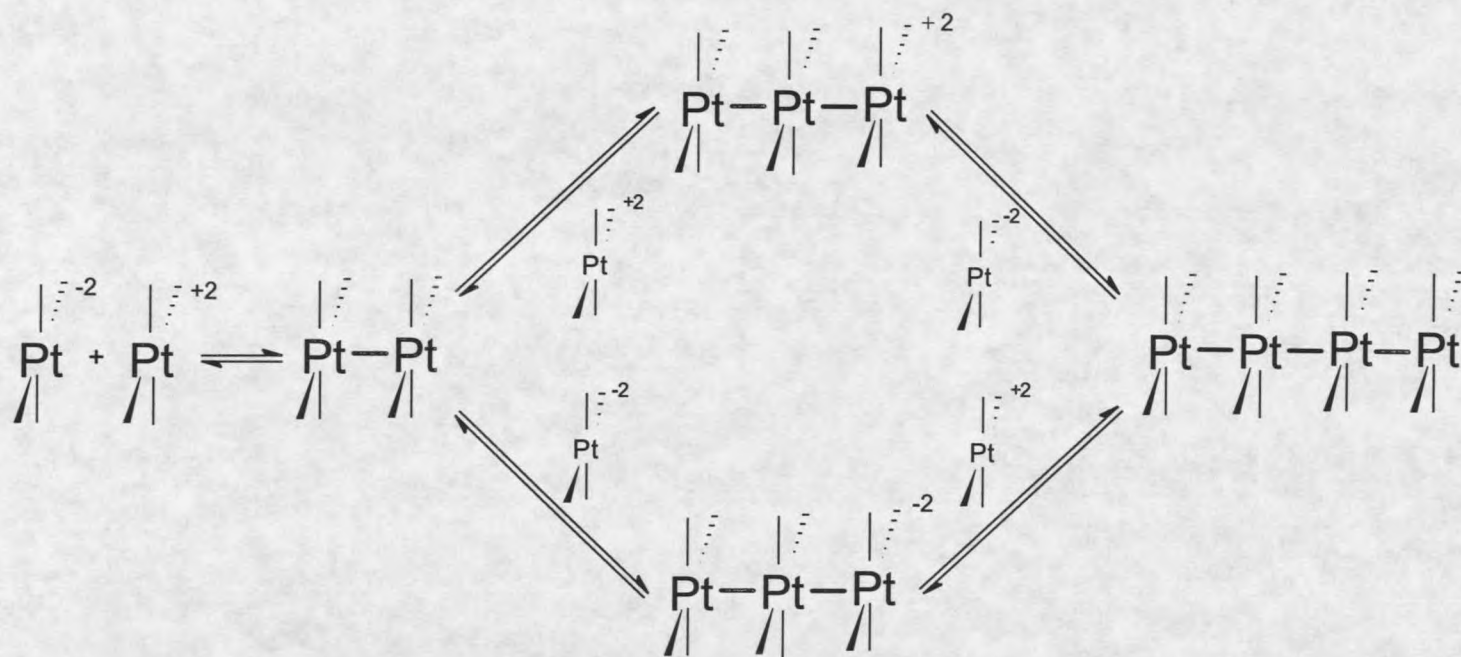


Figure 38. Pictorial representation of the equilibrium of (5).

Further testing of the validity of the computer generated equilibrium constant was done by incorporating data from solutions where the concentrations are higher than  $3.0 \times 10^{-5}M$ . These solutions result in spectra with significant absorption at 363nm due to (28). The resulting unsuccessful refinement indicated the program was able to determine that only a 1,1 dinuclear model was no longer sufficient. Incorporating the 2,1 model into the refinement along with the 1,1 model then resulted in successful refinement. These solutions also contain 1,2 species but at the lower concentrations the combination of the smaller molar absorptivity and the smaller equilibrium constant for the 1,2 species makes its presence nearly negligible to the refinement.

$\beta_2$  was determined from a solution with about a 10 fold increase in concentration of the solutions that were used to determine  $K_1$ . The solution that was used in the CV experiments was also used for the determination of  $\beta_2$ . These solutions were  $1.0 \times 10^{-4}M$  in total platinum complex concentration. It was attempted to solve for  $\beta_2$  and  $\beta_3$  simultaneously however the program would not refine within an acceptable error for the  $\beta_3$ . Attempting to solve for both  $\beta_2$  and  $\beta_3$  was done because both the 2,1 and 1,2 species are assumed to be present in significant amounts at this concentration level. After excluding the  $\beta_3$  model for the 1:2 formation the program would then successfully solve for the  $\beta_2$ . This was not entirely surprising because of the possible smaller value of  $K_3$  (thus smaller  $\beta_3$ ) and the smaller  $\epsilon$  of the 1,2 trimer. These two properties of the 1:2 complex

would cause its resulting spectral contribution to have little significance in the refinement of  $\beta_2$  at  $1.0 \times 10^{-4}\text{M}$ . The error values were considered large for these refinements. The standard deviations were 30% of the value of the formation constants. The errors associated with these formation constants are large but the refinements give good estimates for the values of  $\beta_2$  and  $\beta_3$ . Formation of the tetra-nuclear 2:2 species was also contributing to the error when only the dinuclear and tri-nuclear models are included in the refinement but the 2:2 concentration was low enough that when it was included the formation constant errors did not get any better. Solution concentrations were then increased so the 1,2 and 2,2 formation would be significant in the equilibrium calculations.

Going to concentrations of  $1.0 \times 10^{-3}\text{M}$  results in sufficient concentrations of 1,2 and 2,2 formation for their presence to be significant in the refinement. This resulted in needing to solve the equilibrium problem by refining  $\beta_2$ ,  $\beta_3$  and  $\beta_4$  all at the same time. Like most computer modeling programs good estimations of the answers are needed. The rejected model of the 1,2 and the values refined for the 2,1 at  $1.0 \times 10^{-4}\text{M}$  gave a reasonable approximation of the equilibrium values for the tri-nuclear species. This resulted in successful refinement for all three  $\beta$  values. The equilibrium constants were first obtained at  $22^\circ\text{C}$  then the succeeding equilibrium constants were determined at  $17^\circ\text{C}$ ,  $12^\circ\text{C}$  and  $7^\circ\text{C}$ .

Table 10 shows the multi-nuclear species present in solution at high concentrations and their corresponding overall formation constants at  $22^\circ\text{C}$ ,  $17^\circ\text{C}$ ,  $12^\circ\text{C}$  and  $7^\circ\text{C}$ . Also included is the  $\epsilon$ 's at the corresponding  $\lambda_{\text{max}}$  in the

visible region of the spectrum for each associated species. The multi-nuclear species shown in table 11 represent whose formation is described by the given overall formation constant  $\beta_x$ . The overall log of the formation constants is accurate to within  $\pm .5$ . The accuracy is further described in a later section.

Table 11. Overall formation constants of the association of the DS  $[\text{Pt}(\text{CNC}_2\text{H}_5)_4][\text{Pt}(\text{CN})_4]$  in water refined using the hyperquad suite of programs

|           | Oligomer | $\log\beta$ 22°C | $\log\beta$ 17°C | $\log\beta$ 12°C | $\log\beta$ 7°C | $\epsilon_{\text{max}}$ |
|-----------|----------|------------------|------------------|------------------|-----------------|-------------------------|
| $\beta_1$ | 1,1      | 4.7              | 4.8              | 4.9              | 5.1             | 15000 <sub>319nm</sub>  |
| $\beta_2$ | 2,1      | 7.7              | 7.9              | 8.0              | 8.2             | 57000 <sub>363nm</sub>  |
| $\beta_3$ | 1,2      | 7.6              | 7.8              | 7.9              | 8.2             | 21000 <sub>350nm</sub>  |
| $\beta_4$ | 2,2      | 12.8             | 13.1             | 13.4             | 13.7            | 35000 <sub>420nm</sub>  |

Table 12 shows the absorptivities at all wavelengths that were supplied to the hyperquad suite of programs for refinement. In addition to all the multinuclear species in the solution the absorptivities are given for the parent complexes (8) and (20) in table 13.

Table 12. Molar absorptivities for the four multi-nuclear formed from the dissolution of the DS  $[\text{Pt}(\text{CNC}_2\text{H}_5)_4][\text{Pt}(\text{CN})_4]$  in Water.

| Wavelength(nm) | 1,1   | 2,1   | 1,2   | 2,2   |
|----------------|-------|-------|-------|-------|
| 207            | 22430 | 22280 | 10270 | 6867  |
| 216            | 21180 | 21210 | 36560 | 2340  |
| 231            | 10510 | 13770 | 11680 | 15450 |
| 242            | 5943  | 6982  | 2438  | 9331  |
| 255            | 3899  | 0     | 9600  | 0     |
| 319            | 14880 | 0     | 5307  | 0     |
| 350            | 2500  | 46790 | 20960 | 6600  |
| 363            | 439   | 56640 | 19670 | 17490 |
| 420            | 0     | 0     | 0     | 34750 |
| 440            | 0     | 0     | 0     | 28000 |

The molar absorptivities of the multinuclear species are accurate to  $\pm 5000 \text{ Lmol}^{-1}\text{cm}^{-1}$  except for the 319nm band is accurate to  $\pm 1000 \text{ Lmol}^{-1}\text{cm}^{-1}$  and the molar absorptivities of **(8)** and **(20)** are accurate to within  $\pm 500 \text{ Lmol}^{-1}\text{cm}^{-1}$ .

The absorptivities of the parent complexes were all held constant throughout the refinement since these are known. The absorptivities shown for the multi-nuclear species are averages from the refinements at the different temperatures.

The refinements of the solutions at different temperatures resulted in absorptivities that agreed well with each other. Large variances in absorptivities at the same wavelengths with different temperatures would indicate the equilibrium model is not correct or the data obtained is unsatisfactory. The biggest differences in absorptivity between the different temperatures occurred at the long wavelength region of the spectrum. As the temperature is lowered the subsequent refinement gave higher values for  $\epsilon$  at 420nm. This is the result of higher associated species than the tetra-nuclear species beginning to become more prevalent in solution with decreasing temperatures. The large  $\epsilon$  at 420nm for the cooler temperatures is the result of the refinement contributing the higher associated species such as penta and hexa-nuclear species to the 2,2 complex since it is the model supplied to the computer and is in the region where the further associated species will absorb. Although absorbtivities are solvent dependent they are not temperature dependent and should remain constant in our refinements if our models are correct. The refined  $\epsilon$ 's of the visible bands resulting from the multi-nuclear species never varied by more than 20%.

Table 13. Molar absorptivities for the  $\text{Pt}(\text{CNC}_2\text{H}_5)_4^{2+}$  and the  $\text{Pt}(\text{CN})_4^{2-}$  in Water.

| Wavelength (nm) | $\text{Pt}(\text{CNC}_2\text{H}_5)_4^{2+}$ | $\text{Pt}(\text{CN})_4^{2-}$ |
|-----------------|--|-------------------------------|
| 207             | 20400                                      | 6500                          |
| 216             | 7100                                       | 20000                         |
| 231             | 4300                                       | 700                           |
| 242             | 8400                                       | 2000                          |
| 255             | 7300                                       | 11100                         |
| 273             | 2400                                       | 700                           |
| 280             | 1300                                       | 1600                          |

The molar absorptivities for the 273 nm and 280 nm bands are included in table 13 because in some of the spectra shown these bands are apparent. For the equilibrium constant calculations these wavelengths were not used because the absorbance values were small compared to the other bands from (8) and (20). The magnitude of the change in the absorbance values for these two wavelengths is very small compared with the other bands in the UV region with a change in solution ratio. Since the error in the calculations is inherently larger with increasing wavelengths supplied to the hyperquad suite of programs the bands at 273 nm and 280 nm were the most practical to leave out of the calculations (48).

Table 14 shows the stepwise equilibrium constants that were calculated from the overall formation constants. The stepwise formation constants were all determined from the overall formation constants that were refined using the hyperquad suite of programs. All formation constants are accurate to within a power of ten less than their value.

Table 14. The stepwise equilibrium constants at 7°C, 12°C, 17°C and 22°C.

|           | 7°C    | 12°C   | 17°C   | 22°C   |
|-----------|--------|--------|--------|--------|
| $K_1$     | 1.1E 5 | 8.5E 4 | 6.8E 4 | 5.1E 4 |
| $K_2$     | 1.6E 3 | 1.3E 3 | 1.2E 3 | 9.5E 2 |
| $K_3$     | 1.3E 3 | 1.1E 3 | 9.7E 2 | 8.1E 2 |
| $K_4$     | 3.1E 5 | 2.5E 5 | 1.7E 5 | 1.3E 5 |
| $K_{4'}$  | 3.7E 5 | 3.0E 5 | 2.0E 5 | 1.5E 5 |
| $K_{4''}$ | 4.3E 3 | 3.9E 3 | 2.9E 3 | 2.4E 3 |

Accuracy of the Equilibrium Constants The confidence of the equilibrium values refined by the program was furthered with the results of the equilibrium constant calculations at  $1.0 \times 10^{-3}M$ . The initial  $\beta_2$  value refined at  $1.0 \times 10^{-4}M$  and only the 1,1 and 2,1 models included in the refinement is larger than the  $\beta_2$  value when the other models are included at the higher concentrations. This is evidence that the calculations for  $\beta_2$  are effected by the 1,2 species but at  $1.0 \times 10^{-4}M$  DS the contribution of the 1,2 species to the total absorbance is not significant enough for the program to recognize its effect on the equilibrium. When only the 1,1 and 2,1 model is refined it results in a higher  $\epsilon$  for the 2,1 then when all four models are refined. The program is taking into account the presence of some 1:2 by increasing the absorptivity constant for the 2,1 compared to the value refined when all four models are used.

Changing the known value for  $\beta_1$  also results in worse statistical indicators for this model. The program rejects equilibrium models if the standard deviation of the  $\beta$  value exceeds a predetermined value. The operator can change the limit of acceptability for the model. The error limit was generally set at .20. This

means the model will be rejected if the standard deviation of the  $\beta$  value is 20% of the calculated value of the formation constant. Once the model was accepted at the 20% error level it was attempted to see if the values for the formation constants could be fit at error levels as low as 15% and 10%. The 15% level was always achieved with the standard deviation of the 1,1, 2,1 and 2,2 models. The standard deviation of the 1,2 model was never less than 20% of its calculated value.

Incorporating additional equilibrium models into the program was done for further testing the validity of the equilibrium constants as well as the models chosen at concentrations of  $1.0 \times 10^{-3}M$ . In addition to the four models the refinement was done with additional models indicating penta-nuclear and hexa-nuclear formation. These models are labeled 2:3, 3:2 and 3:3 for the anionic and cationic penta-nuclear species and the 3:3 model indicates the hexa-nuclear species. When these models are included in the calculation in addition to the four correct models the hyperquad program will not refine the additional models. The computer program in turn discards the additional models and refines the initial four correct equilibrium models. The equilibrium models were also tested for their validity by changing the correct models to other legitimate models. This resulted in unsatisfactory refinement of all equilibrium models chosen. For example the penta-nuclear and the hexa-nuclear models were again chosen in place of the tri-nuclear and tetra-nuclear species.

The smaller contribution to the overall stability constant of the 1,2 species was apparent after refinement was achieved for this model. When the 1,2 model is left out of the equilibrium calculations containing all  $\beta_s$ , the hyperquad program will still give a refinement for the other three models. However, all statistical indicators are not as good as when the 1,2 model is included in the refinement. This can be evaluated using the refined values. The actual molar absorptivity of the 1,2 species is 36% of the value of the molar absorptivity for the 2,1 species. The absorption maximum of the 1,2 species occurs at 350nm, which overlaps with the 1,1 and 2,1 bands at 319nm and 363nm. The bands at the two latter wavelengths easily obscure the additional absorbance that results from the 1,2 complex, which results in the 1,2 band not having nearly the influence on the spectrum as the 1,1 and 2,1 species.

#### Thermodynamic Studies of the Oligomers

Thermodynamic data was determined for the multi-nuclear species from the formation constants at 22°C, 17°C, 12°C and 7°C. There is a considerable quantitative shift to **(29)** for the solutions at  $1.0 \times 10^{-3}M$  when they are cooled from 22°C to 7°C. Casual observation of the spectrum will convince one of the large shifts to higher associated metal-metal species upon cooling of the solution. The spectrum at 22°C indicates **(29)** is not a dominating influence in the spectrum because the band has not been shifted out to a  $\lambda_{max}$  at 420nm. Figure

39 shows the visible absorbance bands at the four temperatures. For each of the spectra shown (8) and (20) are in a 1:1 ratio. The maximum for (29) at 420nm is not apparent at 22°C and a concentration of  $1.0 \times 10^{-3}\text{M}$  in total platinum concentration. The lowest energy absorption maximum at 22°C is not lower in energy than 400nm. As the  $1.0 \times 10^{-3}\text{M}$  solution is cooled to 7°C the lower energy band shifts out to an obvious maximum at 420nm. With this shifting to 420nm there is a significant negative deviation from Beers law in the absorbance band at 319nm. This indicates a significant shift in the equilibrium from (5) to (29). There is also an increase in consumption of the monomers with a decrease in the solution temperature.

The thermodynamic parameter  $\Delta H^\circ$  was determined from Van't Hoff plots. From equation 12

$$d\ln K/d(1/T) = -\Delta H^\circ/R \quad (12)$$

the  $\Delta H^\circ$  can be determined for the metal-metal association from the plot of  $-\ln K$  versus  $T^{-1}$  with the resulting slope equal to  $\Delta H^\circ/R$ . As expected the  $\Delta H^\circ$  is negative for the associations due to bond formation. The favorable  $\Delta H$ 's for multi-nuclear formation generally are more predominate than the unfavorable  $\Delta S$  considerations for associating ions. The large negative enthalpies of formation results in polymerization's being thermodynamically favorable because of bond formation.

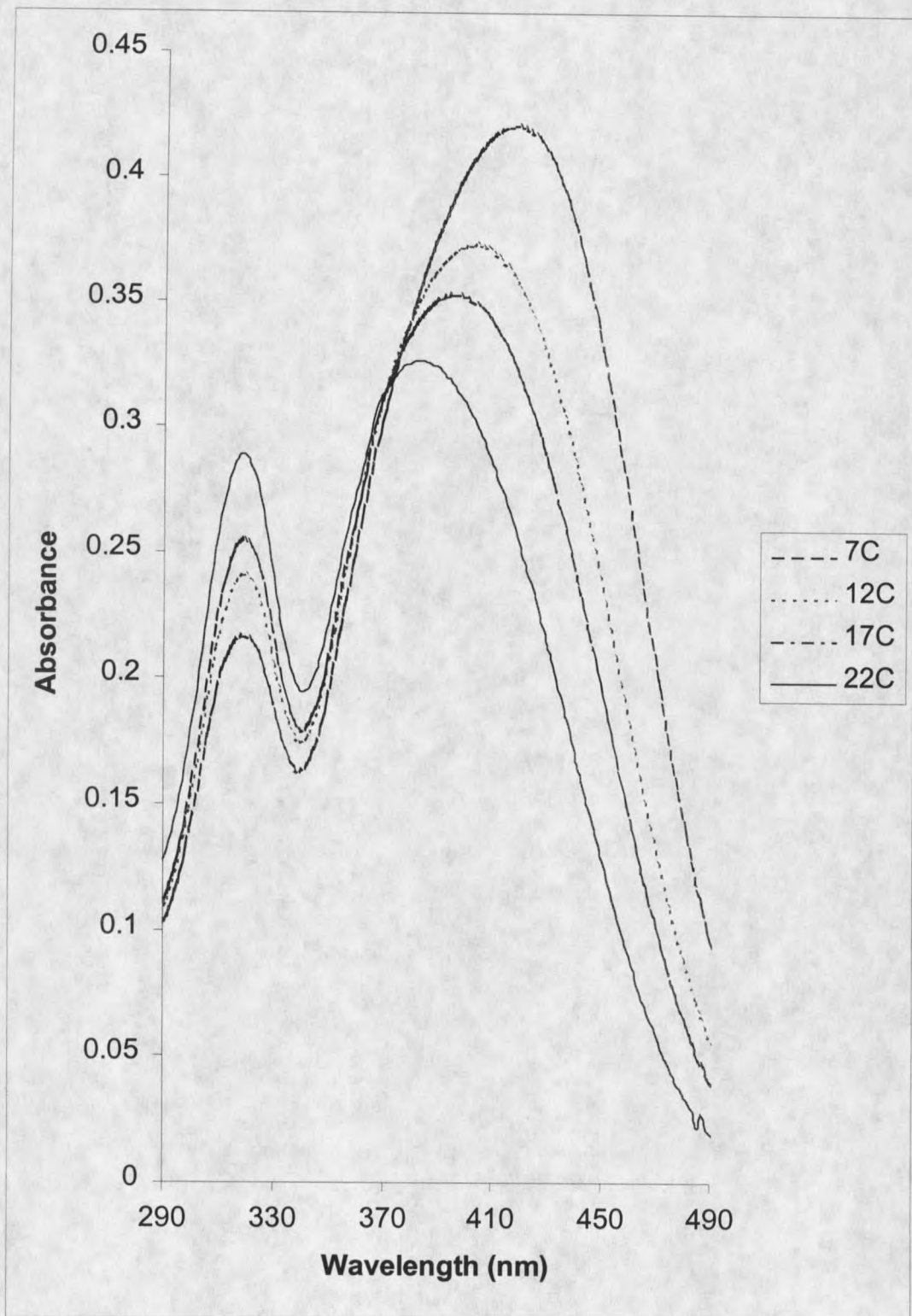


Figure 39. Temperature effect on the equilibrium of the DS (5).

Gibbs free energy ( $\Delta G^0$ ) was determined from the equilibrium constants in equation 13.

$$-\Delta G^0 = RT \ln K \quad (13)$$

As expected from the equilibrium constants the reactions proceed spontaneously.  $\Delta G$  values were checked at each temperature that  $K$  was determined and it produced very similar numbers.

The magnitude of  $\Delta S$  was small for all the reactions done here but there are significant differences between the values. The  $\Delta S$  was calculated by rearranging the Gibbs-Helmholtz equation resulting in equation 14

$$\Delta S = -(\Delta G - \Delta H/T) \quad (14)$$

The three thermodynamic parameters  $\Delta H$ ,  $\Delta G$  and  $\Delta S$  for all the different equilibrium expressions are tabulated in table 15.

Table 15. Thermodynamic Parameters for the Stepwise Formation Constants for the Association of the DS  $[\text{Pt}(\text{CNC}_2\text{H}_5)_4][\text{Pt}(\text{CN})_4]$  in water.

| Stepwise Constant | Model | $\Delta H^0$ kJ/mol | $\Delta G^0$ kJ/mol | $\Delta S^0$ J/molK |
|-------------------|-------|---------------------|---------------------|---------------------|
| $K_1$             | 1,1   | -35                 | -27                 | -30                 |
| $K_2$             | 2,1   | -22                 | -17                 | -18                 |
| $K_3$             | 1,2   | -21                 | -16                 | -15                 |
| $K_4$             | 2,2   | -40                 | -29                 | -36                 |
| $K_{4'}$          | 2,2   | -41                 | -28                 | -44                 |
| $K_{4''}$         | 2,2   | -27                 | -20                 | -26                 |

The thermodynamic parameters listed in table 15 are those determined from the overall formation constants that gave the best statistical indicators in the refinement.

Bonding Interpretation of the Thermodynamic Studies                      The

significance of the thermodynamic data is seen in the less negative values of  $\Delta H$ ,  $\Delta G$ , and  $\Delta S$  for the formation of **(28)** and **(30)** compared to **(5)** and **(29)**. With further association of **(28)** and **(30)** the values become more negative again like the values for the formation of **(5)**. The initial conclusion that can be made from the  $\Delta H$  is that **(28)** and **(30)** are not as stable in solution as **(5)** and **(29)**. The entropy values reveal the greater drive for formation of **(28)** and **(30)** because of the more positive values they have compared to **(5)** and **(29)**. The more positive  $\Delta S$  for **(28)** and **(30)** was not expected because it was assumed that the charged odd numbered species would order solvent to a greater degree than the neutral even numbered species. Further rationalization was needed to explain the values obtained for the thermodynamic parameters.

The thermodynamic values calculated and the evidence that the addition of excess ions to the DS solutions reveals interesting information about the associated complexes. It has generally been the idea that the ionic interactions of the DS complexes were chiefly responsible for the metal-metal interactions. It was initially believed that the addition of excess salts would suppress the metal-metal association and thus the bands at 319nm and 363nm would diminish in the















































































































































